Market-Efficient and Robust Integration of DER in Unbalanced Distribution Systems

Author:
James S. RUSSELL

Supervisory Panel:
Dr. Paul SCOTT
Dr. José IRIA
Assoc. Prof. Patrik HASLUM

A thesis submitted for the degree of
Doctor of Philosophy of
The Australian National University

18/12/2025

SCHOOL OF COMPUTING
COLLEGE OF SYSTEMS & SOCIETY
AUSTRALIAN NATIONAL UNIVERSITY

Declaration of Authorship

I, James S. RUSSELL, declare that the work presented in this thesis is my own original work. I confirm that:

- This work was done wholly or mainly while in candidature for a research degree at this University.
- No part of this thesis has previously been submitted for a degree or any other qualification at this University or any other institution.
- Where I have referenced or quoted the published work of others, this is always clearly attributed.

The following is a list of publications I have produced whilst undertaking this research. The work from these publications is incorporated into this thesis.

- J. S. Russell, P. Scott and A. Attarha, "Stochastic shaping of aggregator energy and reserve bids to ensure network security," *Electric Power Systems Research*, vol. 212, p. 108 418, 2022
- J. S. Russell, P. Scott and J. Iria, "Robust operating envelopes with phase unbalance constraints in unbalanced three-phase networks," in *2023 IEEE PES Innovative Smart Grid Technologies-Asia (ISGT Asia)*, IEEE, 2023, pp. 1–5
- J. S. Russell, P. Scott and J. Iria, "Network-secure aggregator operating regions with flexible dispatch envelopes in unbalanced systems," *Electric Power Systems Research*, vol. 123, p. 123 456, 2024

Both publications in *Electric Power Systems Research* were presented as papers at the *Power Systems Computation Conference*, in 2022 (Porto) and 2024 (Paris).

Signed: James Russell

Date: 18/12/2025

Acknowledgements

This thesis would not have been possible without the support and encouragement from many people.

First, I want to thank my supervisors. I am sincerely grateful to Dr. Paul Scott for his exceptional research guidance, technical expertise, and ongoing support throughout this journey. My thanks also go to Dr. Jose Iria, whose insightful feedback and technical direction were key to many aspects of this work. I am also grateful to Assoc. Prof. Patrik Haslum, my panel chair, for his oversight and for helping me stay on track.

I am also thankful to Dr. Matt Attarha, whose mentorship over the years have been invaluable to my growth as a researcher.

The warm environment created by my colleagues was essential to this work. I give special thanks to Dr. Mark Burgess, Dr. Mahdi Noori, and Dr. Masoume Mahmoodi for their friendship, and for the many discussions that helped me refine my ideas. Our time spent problem-solving together made this process much more enjoyable.

Most importantly, I want to thank my wife, Yangchen. Your love and support have been the foundation of everything I've achieved. You have been there through every high and low, and your belief in me kept me going. I truly could not have reached this milestone without you.

Finally, I want to dedicate this achievement to my parents. Mum, Dad, thank you for teaching me what it means to be truly passionate, and for working tirelessly to give me every opportunity to reach for the stars. We made it.

This work reflects the combined wisdom and kindness of everyone mentioned here. Thank you all.

Abstract

Uptake of distributed energy resources (DER) is accelerating across the globe. There is growing need for coordination frameworks to ensure high volumes of DER can participate effectively in existing market structures at the transmission-scale, while also satisfying technical constraints at the distribution-scale. Dynamic operating envelopes (DOE) have emerged as the leading approach in Australia for enabling effective integration of DER into power systems.

Calculating dynamic operating envelopes in a manner that enables effective DER participation while providing robust guarantees of network-feasible outcomes is a complex computational task. Sources of complexity include non-linear and non-convex formulations of power flow and network operational constraints, the uncertainty of DER dispatch within envelopes due to their flexibility, and the balancing of various objectives (including efficient system operation, maximising assigned flexible capacity and ensuring fair outcomes) arising from the multitude of actors whose interests may not align. As the technical readiness level of dynamic operating envelope frameworks approach wide-spread deployment in industry, there are several aspects to their design which warrant further consideration by the research community. In this thesis we delve into three aspects.

We first develop an operating envelope optimisation framework that maximises the market efficiency of expected wholesale market outcomes, as opposed to existing methods that maximise total import and export capacity or metrics of fairness. Our proposed formulation incorporates projections of wholesale market prices in energy and reserve markets, constituting a novel form of TSO-DSO coordination in envelope calculation. Our objective function maximises expectations of producer and consumer surplus as defined in microeconomics, effectively prioritising the expected value-generating potential of DER, across a range of potential market price outcomes. As a result, our framework navigates a trade-off between allocating capacity to efficient bidders and maximising total allocated capacity as a function of evolving

TSO needs. We employ a stochastic programming formulation to handle price uncertainty, demonstrating robust performance even during periods of significant price volatility.

Our second contribution addresses feasibility considerations in unbalanced three-phase networks by proposing a completion of voltage constraints. We develop a linearised proxy for the voltage unbalance factor by linearising the Line Voltage Unbalance Rate (LVUR) with respect to variables in the LinDistflow power flow model, and using a linearised phase angle recovery. This approach enables efficient large-scale calculations despite introducing conservatism due to the LVUR approximation and the need to ensure constraint satisfaction under improbable dispatch scenarios.

Our final contribution mitigates the conservatism of robust DOE approaches through aggregator coordination. Rather than calculating independent operating envelopes, we develop an approach to partition high-dimensional representations of unused network capacity amongst aggregators using robust polytopic projection. This framework provides aggregators with scalar functions to calculate DER-level envelopes as a function of feeder-scale dispatch outcomes. Results show this approach can significantly increase the aggregate flexible allocations of import and export capacity compared to an alternative robust DOE approach in literature. This is achieved by steering aggregators away from dispatch outcomes that would cause significant variations in network utilisation across phases, thereby mitigating the risk of network constraint violations caused or exacerbated by mutual impedances between electromagnetically-coupled phases.

The methods developed in this thesis provide new avenues for distribution system operators to enhance the effectiveness of DER integration, including into wholesale markets, while ensuring safe operation of distribution networks.

Nomenclature

Abbreviation	Description	Reference
AEMO	Australian Energy Market Operator	
BESS	Battery Energy Storage System	
CPP	Connection Point Power	
DER	Distributed Energy Resources	
DNSP	Distribution Network Service Provider	
DOE	Dynamic Operating Envelope	
DSO	Distribution System Operator	
FCAS	Frequency Control Ancillary Service	
IBR	Inverter Based Resources	
ISO	Independent System Operator	
LP	Linear Programming	
LVUR	Line Voltage Unbalance Rate	
MCP	Market Clearing Price	
NEMA	National Electrical Manufacturers Association	
NEM	Australian National Electricity Market	
PVUR	Phase Voltage Unbalance Rate	
TSO	Transmission System Operator	
VPP	Virtual Power Plant	
VUF	Voltage Unbalance Factor	

Contents

Chapter 1

Introduction

1.1 The Changing Energy Mix

For over a century, fossil fuels — primarily coal and gas — have dominated electricity generation. This has been largely due to the lack of cleaner and cheaper alternatives. However, the 21st century has witnessed a significant shift in this paradigm, driven by multiple converging factors. The environmental impacts of fossil fuel combustion have become increasingly apparent and concerning. Coal-fired and gas-fired power plants are major contributors to greenhouse gas emissions, with the energy sector contributing approximately 40% of global CO_2 emissions [4]. These environmental concerns have spurred research into alternative technologies for electricity generation, in order to push towards a more sustainable energy mix.

Thanks to decades of innovation, renewable energy sources now present themselves as economically viable pillars of decarbonised energy systems. The levelised cost of electricity (LCOE) for utility-scale solar PV decreased by approximately 90% between 2010 and 2023, while onshore and offshore wind LCOE fell by 70% and 63% respectively during the same period [5]. The combination of environmental imperatives and economic advantages has accelerated the global energy transition. In 2023, renewable energy sources accounted for 85.5% of new electricity generation capacity added worldwide [5]. This transition represents not merely a substitution of generation technologies but a fundamental reimagining of electricity systems.

A key feature of this new energy paradigm is its scalability across different system levels. While conventional thermal generation typically operates at utility scale due to economies of scale, solar PV and batteries can be deployed efficiently at residential scale. This shift represents a major departure from the traditional centralised generation model, creating opportunities for consumers to become active participants in the electricity system— "prosumers" who both consume and produce energy. This shift toward distributed energy resources (DER) has the potential to enhance system resilience, reduce transmission losses, and defer network infrastructure investments [6].

However, this transition also introduces new complexities in system operation and coordination. The traditional unidirectional flow of electricity from large generators through transmission networks, then through distribution networks to passive consumers is giving way to bidirectional flows and more complex network interactions. Managing these dynamics effectively requires new approaches to system operation and coordination, particularly at the distribution level where DER are connected.

1.2 Integration of Distributed Energy Resources

1.2.1 Consumer Motivations for DER Adoption

Widespread adoption of DER is fundamentally changing the relationship between consumers and the electricity system. Traditionally passive recipients of electricity services, consumers are increasingly investing in technologies that allow them to generate, store, and manage their own energy. This shift is driven by multiple factors beyond environmental consciousness.

Economic considerations play a significant role in DER adoption decisions. Residential solar PV systems, often combined with battery storage, can reduce electricity bills through self-consumption and, where available, feed-in tariffs for exported energy. [7]. As retail electricity prices have recently increased in many jurisdictions while technology costs have declined, the financial case for DER investment has strengthened [8]. Battery storage systems can further enhance economic benefits by enabling consumers to shift their energy consumption from high-price to low-price periods, effectively performing energy arbitrage at the household level [9].

DER also offer consumers a degree of energy independence and price insulation. By generating and storing their own electricity, households can reduce their exposure to retail price volatility and potential future price increases. In rural and remote areas, where distribution networks may be less reliable or where the cost of network augmentation is prohibitively high, DER can significantly improve energy security and quality of supply [10]. In these contexts, DER may serve not only as economic investments but also as essential infrastructure for reliable electricity access.

Beyond individual consumer benefits, coordinated DER deployment and operation can deliver broader system benefits. When appropriately integrated, the flexibility offered by DER can contribute to peak demand reduction, frequency regulation, voltage support, and other ancillary services that support system stability and reliability [11]. These capabilities become increasingly valuable as power systems incorporate higher shares of variable renewable generation.

1.2.2 Network Implications and Coordination Requirements

The integration of DER into distribution networks presents opportunities, but also challenges for network operators. Distribution networks were traditionally designed for unidirectional power flows from substations to end consumers, with limited monitoring and control capabilities compared to transmission systems [12]. The increase in utilisation and potential for bidirectional power flows introduced by DER can stress network components and create operational challenges.

Voltage regulation represents one of the primary technical challenges. In radial distribution feeders, voltage would traditionally gradually decrease along the feeder in a fairly predictable manner, due to aggregated loads of households and businesses. However, if all residential battery systems in a neighborhood were programmed to charge during the same low price period, they could create a new demand peak that stresses the local network infrastructure [13]. This may cause significant drops in voltage, risking recourse actions form of protection equipment, resulting in network failures. Similarly, distributed generation (mainly solar PV) can cause significant voltage rise during periods of high generation and low local consumption, again risking the tripping of protection equipment [14]. These effects are most pronounced in low-voltage networks with high resistance-to-reactance (R/X) ratios, where active power injections have a stronger influence on voltage than in transmission systems [15]. Increased network utilisation may also risk violating thermal constraints (i.e. current exceeds safe operating limits).

The responsibility of safely operating distribution networks falls to distribution network operators (DNO), also called distribution network service providers (DNSP) in Australia. Traditionally, managing network voltages has been achieved through adjusting network elements such as tap-changing transformers and capacitor banks [16]. However, approaches requiring adding and adjusting network elements may be insufficient to address the rapid voltage fluctuations that can occur with high DER penetration.

Given the limited capacity of networks to directly adjust network elements to accommodate growing DER load flows, network operators are increasingly considering methods to coordinate DER activity. Effective coordination of DER promises to significantly increase the hosting capacity of distribution networks—the amount of DER that can be accommodated without requiring network reinforcement [17]. The challenge is to develop coordination mechanisms that enable efficient network utilisation, while respecting the autonomy of DER owners and the operational constraints of distribution networks. This requires new approaches to distribution network management that go beyond the traditional role of network operators, adopting some responsibilities of *system operators*. We provide further information about the distinction between network operators and system operators in Section 2.

1.3 Coordination Approaches for DER

1.3.1 Challenges Integrating DER Directly in Wholesale Markets

Network-aware coordination of millions of DER was studied in the U.S. Department of Energy's ENERGISE and ARPA-E's NODES program in 2016-2020. These research efforts led to a number of innovations in scalable DER coordination, and centralised coordination of millions of DERs was found to be feasible. Objectives studied in these works include integration into distribution network management systems, and sourcing of synthetic reserves [18].

While these large scale coordination challenges have proven feasible, network-aware integration of millions of DER devices into existing wholesale market structures represents a different challenge, constrained by practicalities that govern existing operations. For example, unbundled power systems typically separate responsibilities among different entities - generators, network operators, retailers and system operators - each with distinct roles and objectives [19]. As such, visibility over the state of distribution networks may not be available to the wholesale market operator.

As a result, there is interest in industry for approaches that enable millions of DER devices to participate in existing wholesale market structures in a manner that respects distribution network constraints.

1.3.2 Operating Envelopes as a Mechanism for Network-Aware Participation Wholesale Markets

Operating envelopes have gained prominence, particularly in Australia, as an approach that respects the division of responsibilities in unbundled power systems while enabling effective DER integration [20].

Operating envelopes define the allowable range of power import and export at each connection point, within which DER can operate freely according to their owners' preferences or market signals. These flexible allocations can adapt to changing network utilisation rates, enabling networks to cater for greater overall DER capacity than rigid, static connection agreements. Traditionally, connection agreements have specified fixed export limits constrained by worst-case network utilisation scenarios, often resulting in conservative constraints that significantly underutilise available network capacity most of the time. Dynamic operating envelopes, by contrast, can adapt to changing network conditions, allowing greater DER utilisation during favourable periods while maintaining secure operation during constrained periods [21].

The implementation of operating envelopes requires several key components: some level of network monitoring to assess current conditions, forecasting of load and generation patterns, power flow analysis to identify constraints, and communication systems to disseminate the calculated envelopes to DER or their aggregators [22]. These components enable the calculation of envelopes that reflect actual network conditions rather than worst-case assumptions.

From a market perspective, operating envelopes facilitate DER participation in wholesale markets by clearly defining the network-secure operating range within which market participants can respond to price signals. This enables aggregators to optimise their DER portfolios against market opportunities while respecting local network constraints.

1.3.3 Technical Challenges Calculating Dynamic Operating Envelopes

The calculation of operating envelopes that effectively balance network security considerations with maximising opportunities for effective DER utilisation presents several technical challenges that warrant further research attention.

In this thesis we delve into three aspects:

1. When distribution network capacity is constrained, how should limited capacity be efficiently allocated among individual DER connections?
2. How can we ensure that an allocation of envelopes will satisfy network constraints in *unbalanced distribution networks*?
3. Should a DSO/DNSP seek robust capacity allocations in unbalanced distribution networks, how can aggregators help to effectively expand an unbalanced distribution network's dynamic hosting capacity by coordinating their customers' dispatch?

Research Question 1: Efficient Allocation of Operating Envelopes using a novel form of TSO-DSO Coordination

Our first contribution considers the question of who should be assigned, or who should be given priority access, to constrained distribution network capacity in the context of congestion. While greater overall capacity can be assigned to DER in voltage-constrained radial networks by prioritising connections closer to the substation, numerous works in the literature have instead proposed *fairer* allocations by crafting objective functions that incentivise a greater spread of curtailment. Instead, we note that DSOs are well-positioned to coordinate redistributions of market benefits to achieve fair outcomes, and should instead seek to maximise the value-generating potential of DER in distribution networks.

Our first contribution therefore proposes to maximise the *market efficiency* of allocations of constrained network capacity, in the context of DER providing valuable arbitrage and reserve services to wholesale markets. Inspired by the concepts of producer surplus and consumer surplus in micro-economics, our proposed framework maximises the total value of arbitrage and reserve services that reach the wholesale market, while subtracting the economic costs borne by aggregators for providing these services on the assumption of cost-reflective bidding. This is equivalent to maximising the value-generating potential of DER. One notable point of difference with respect to literature is that our optimisation objective is a function of aggregator bids *and anticipated wholesale market prices* across energy and various reserve markets. This effectively communicates TSO preferences to the DSO as it assigns constrained distribution network capacity to competing aggregators, constituting a novel form of TSO-DSO coordination unexplored in operating envelope literature.

Research Question 2: Designing Operating Envelopes that Constrain Voltage Unbalance Between Phases in Unbalanced Distribution Networks

Our second contribution aims to derive a more comprehensive set of network feasibility conditions for calculating operating envelopes in unbalanced three-phase networks. In unbalanced three-phase networks, voltage magnitude constraints only represent one part of voltage constraints that must be satisfied. Networks are also required to ensure that voltage unbalance factor (%VUF) remains bounded by an operational limit, and this is generally ignored in literature studying single-phase, or single-phase equivalent networks. From a computational perspective, incorporating this constraint into operating envelope calculations represents a new challenge.

While voltage magnitude constraints have a formulation that is linear with respect to modelled variables (e.g. $v \leq \overline{v}$), the voltage unbalance factor is itself a non-linear function of modelled network state variables. This necessitates either the inclusion of non-linear constraints, or deriving a linear approximation of the voltage unbalance factor that can be bounded above. Inspired by the computational efficiencies of linear power flow formulations when applied at scale, our second contribution therefore proposes a linearised proxy for the voltage unbalance factor by using a linearised form of the Line Voltage Unbalance Rate (LVUR).

Research Question 3: Guidelines for Aggregator's Coordination of Customers to Enable Greater Robust Allocations of Network Capacity in Unbalanced Distribution Systems

Our final contribution studies whether the conservatism of robust DOE approaches for unbalanced networks, particularly with the inclusion of voltage unbalance constraints, can be mitigated by aggregators coordinating their customers in groups. We noticed in our second contribution that the assumption of independent operation of CER caused fully robust DOE frameworks to calculate fairly conservative envelopes. This is due to the possibility that DER on different phases may be dispatched in a fairly unbalanced manner, risking voltage unbalance constraint violations, but also voltage magnitude constraint violations (due to the effects of mutual impedances between phases). In practice, it is common for a smaller number of aggregators to represent larger fleets of CER within distribution networks.

Our final contribution therefore proposes a framework for aggregators to be assigned a higher-dimensional *region* for dispatching their DER fleets, rather than a set of operating envelopes assigned to specific customers, effectively requiring aggregators to limit unbalance in their dispatch, resulting in greater hosting capacity being available for allocation to other aggregators / consumers. We achieve this by partitioning a high-dimensional representation of unused network capacity amongst aggregators, applying robust polytopic projection, then providing aggregators with trivial scalar functions to calculate DER-level envelopes as a function of feeder-scale aggregator dispatch outcomes.

Chapter 2

Background

This background chapter serves as a reference to gain a foundational understanding of concepts which are discussed in the literature review and contribution chapters of this thesis. For this reason, its structure is more akin to a catalogue than the more deliberate progressions in the Literature Review.

2.1 Distributed Energy Resources (DER)

Distributed Energy Resources (DER) are "devices that can generate, store, and be controlled to consume energy at a particular time, to form part of the electricity supply network" [23]. DER have existed for some time in the form of controllable loads such as hot water systems. More recently, solar photovoltaic (PV) systems, grid-connected batteries and electric vehicles are emerging as new opportunities for energy consumers to not only control their utilisation, but also to generate electricity and perform arbitrage. An example of a smart home with each of these technologies is depicted in Figure 2.1.

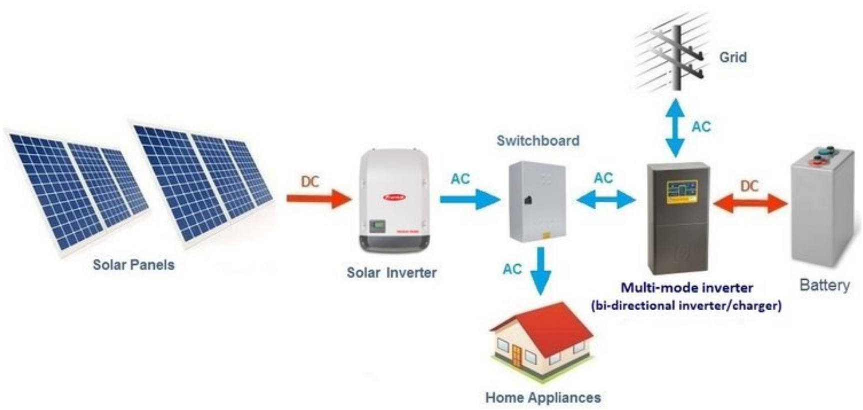

FIGURE 2.1: Example of a smart home with DER including solar PV, a household battery and an EV [24]

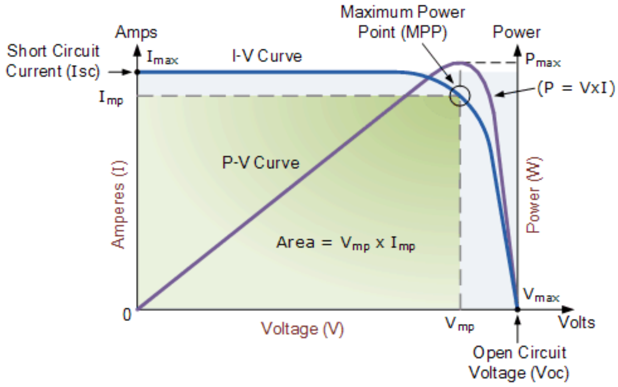

FIGURE 2.2: Example I-V and P-V curves of solar PV systems [25]

- Batteries can be controlled to provide a wide range of system services, including energy arbitrage, frequency and voltage regulation, congestion management, synthetic inertia.
- Solar PV systems generate electricity through exposure to sunlight. The output of solar PV systems can be controlled by adjusting the current flow through panels, away from the Maximum Power Point (MPP) towards positions of lower power output as demonstrated in Figure 2.2. This enables solar PV to be curtailed if required. In practice, some older PV systems may lack the ability to modulate current flow.

Inverters are required to connect generation and storage devices to the network. Solar PV and battery systems produce direct current (DC) power. In order for this power to be used by electricity networks and household appliances, this power must be converted to alternating current (AC) power. Inverters comprise of electronic switching components used to (a) rapidly switch the DC input on and off, and (b) change the voltage sign (+/-). Pulse-width modulation (PWM) is used to create an AC output that closely mimics a sine wave, which is the standard waveform for AC power. This process is represented in Figure 2.3.

Inverters can deliberately induce small phase shifts in their output signals compared to the network's reference signal, and this enables inverters control over their export of real and reactive power. As a result, inverter-based DER are able to act as inductive or capacitive loads as required by the network. This can prove particularly useful on hot days, when inductive loads such as air conditioners cause current to lag voltage within distribution networks, causing a reduction in apparent power delivered per unit of current. The

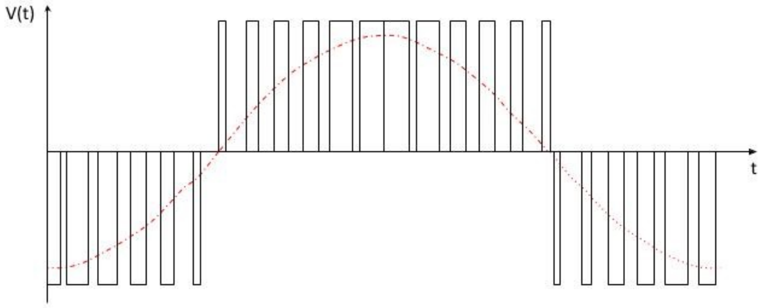

FIGURE 2.3: Demonstration of how inverters use Pulse Width Modulation (PWM) to generate AC signals [26]

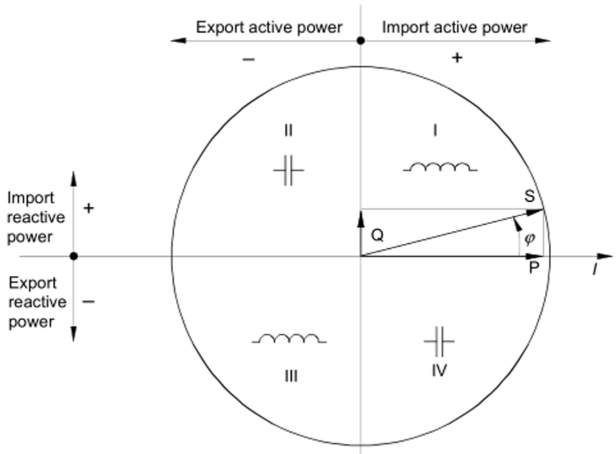

FIGURE 2.4: Relationship of the phase shift of power exports and real / reactive power exported [27]

relationship between phase shift φ and real and reactive power exports is visualised in Figure 2.4.

The concept of *demand response* had once traditionally referred to consumers adjusting their energy consumption to help balance supply and demand measured at the transmission scale. With growing volumes of DER installed within distribution networks, it is increasingly important to ensure their coordination can help to support growing congestion within distribution networks.

2.2 Distribution Networks

Distribution networks form the medium- and low-voltage components of electricity grids. While transmission network infrastructure in Australia spans approximately 44,000 kilometres, distribution network infrastructure extends to over 850,000 kilometres [28], demonstrating the challenge of coordinating DER in a network-robust manner.

2.2.1 Network Structure

Distribution networks generally operate assuming a radial structure, although it is common for redundant branches to stand ready in the event of contingencies. They commence at HV/MV substations that connect to a transmission network (also known as a bulk supply point in Australia), from which the network progressively forks and step down in voltage at various MV/MV and MV/LV transformers. In this thesis, we model an MV and an LV feeder with radial structures.

There are notable differences between the topologies of medium and low voltage (MV-LV) networks around the world. In Europe, low-voltage components of distribution feeders are typically longer than in the United States, where medium voltage networks often extend closer to individual households requiring a larger number of substations stepping down voltage to low levels. This thesis will focus on networks akin to the European context.

2.2.2 Three-Phase Power Delivery

Transmission and distribution of electricity across all voltage levels is generally performed using three phases. Each phase comprises of a wire conducting alternating current, and each phase is shifted by 120 degrees. In a perfectly balanced three-phase system, the instantaneous current across each phase sums to zero.

While phases are often fairly well balanced at the transmission scale, due in part to widespread summation of loads, unbalance between phases may be more pronounced at low voltage levels due to the increased relative impact of single-phase loads. The degree of unbalance between phases is measured by the voltage unbalance factor (VUF), which is defined as the ratio of the negative sequence voltage component to the positive sequence voltage component, given by

$$\text{VUF} = \left| \frac{V_{ab}\angle\theta_{ab} + a^2 V_{bc}\angle\theta_{bc} + a\ V_{ca}\angle\theta_{ca}}{V_{ab}\angle\theta_{ab} + a\ V_{bc}\angle\theta_{bc} + a^2 V_{ca}\angle\theta_{ca}} \right| \tag{2.1}$$

where V_{ab} and θ_{ab} represent line-line voltage magnitudes and phase angles, and $a = -\frac{2\pi i}{3}$. In Australia, the National Electricity Rules Clause S5.1a.7 requires that the 30-minute average maximum negative sequence voltage (as percentage of nominal voltage) remain below 2% [29].

In many distribution networks, a wye-configuration is adopted on the low-voltage side of MV-LV transformers to obtain a four-wire distribution system. This fourth wire represents a neutral wire, serving to conduct sums of unbalanced current phasors back to the substation when the sum of voltages does not equal zero.

In this thesis we study two different three-wire distribution networks. The first is the IEEE 69-bus Medium Voltage network in Chapter 4, and the second is a three-wire representation of the four-wire IEEE European Low Voltage Feeder (Chapters 5 and 6), obtained through Kron's reduction of the impedance data on the assumption that the neutral is perfectly grounded everywhere. While this represents a simplification of the network structure, this approach is often applied when modelling Multiple Earthed Neutral (MEN) networks commonly found in Australia and New Zealand, as the measuring the set of neutral grounding impedance values across customer and feeder locations may be unworkable in practice. Derivations used to define optimisation constraints in Chapters 5 and 6 apply the LinDistFlow model, which implicitly assumes this Kron's reduction to a three-phase feeder.

2.2.3 Impacts of DER on Network Voltages

When PV generation exceeds a household's consumption or when batteries discharge, excess power is exported to the distribution network. This results in a net decrease in power flowing from the transformer, and increases voltage at the customer location. Large loads arising from EV or household battery charging have the opposite effect, causing net reductions in voltage at customer locations and net increases in current flowing from the substation.

As DER uptake continues to accelerate, distribution network operators are increasingly managing risks of voltage and thermal constraint violations. A primary focus of this thesis is developing methods for distribution network operators to coordinate DER in a manner that ensures voltage constraints remain satisfied across the distribution network (some simulations also factor thermal constraints). We consider both voltage magnitude (Chapter 4, 5, 6) and voltage unbalance constraints (Chapter 5, 6), which remain relatively unexplored in DER coordination literature.

2.2.4 Networks Studied in This Thesis

Simulations in this thesis use two IEEE test feeders.

IEEE 69-bus Medium Voltage Test Feeder

Simulations in Chapter 4 use the IEEE 69-bus Medium Voltage test feeder. The network was first proposed in the literature by [30].

This network operates at 12.66 kV, and serves 1,910 in our simulations. We use this network to perform studies into methods of how a simple form of coordination between the DSO and the wholesale market operator, namely sharing expectations of wholesale prices, can help to achieve a more economically efficient allocation of operating envelopes.

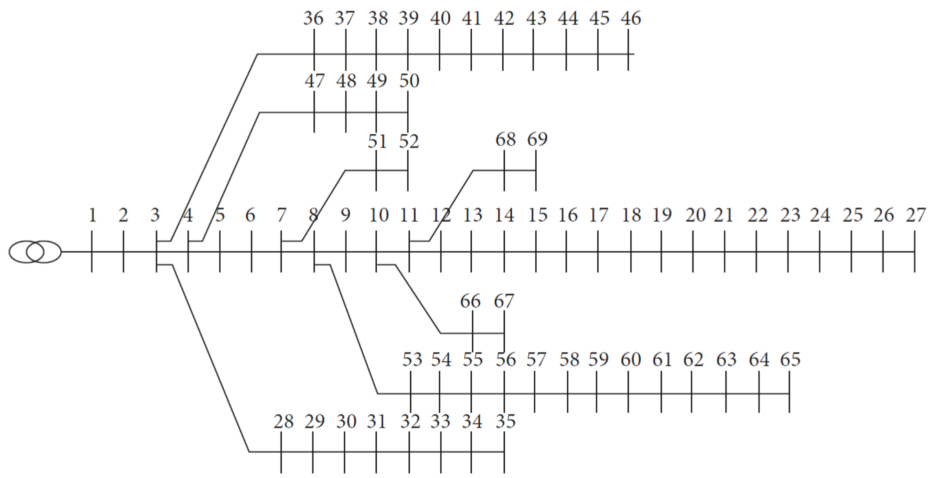

FIGURE 2.5: Representation of the IEEE 69-bus Medium Voltage Test Feeder, with all 69 buses indexed (image copied from [31], network data available at [32])

IEEE 906-bus European Low Voltage Test Feeder

Simulations in Chapters 5 and 6 use a three-wire variant of the IEEE 906-bus European low voltage feeder, obtained by applying Kron's reduction to the impedance data on the assumption that the neutral is perfectly grounded everywhere. The network has 55 customers. This second network will be used in studies of the feasibility of operating envelopes in networks that may experience unbalanced loading.

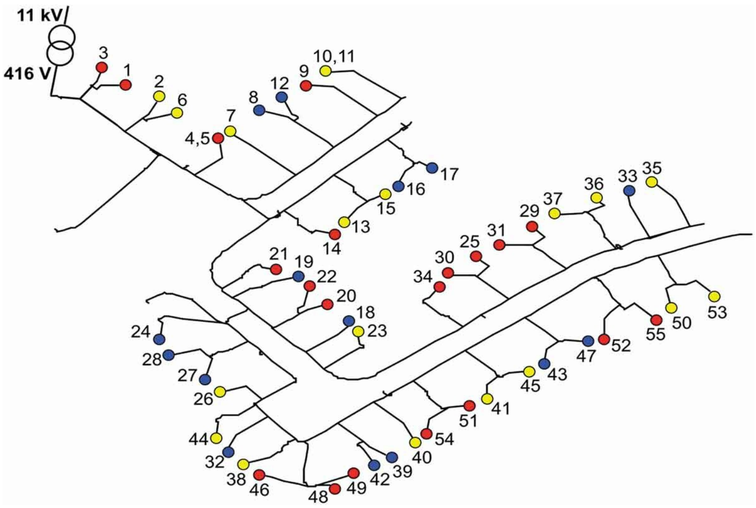

FIGURE 2.6: Representation of the IEEE 906-bus European Low-Voltage Test Feeder, with 55 load locations shown and indexed (image copied from [33], network data available at [32])

2.3 Coordination of Power Systems

Power systems often connect millions of devices, and system operators must coordinate generation, consumption, and arbitrage to ensure supply and demand remain in balance, and networks satisfy their operational constraints.

Throughout the 20th century, power systems around the world were often developed as state-owned assets. Generation, transmission and distribution network infrastructure would be operated by a single entity, and this model of operation by a single entity is referred to as *vertically integrated utilities*. With the rise of privatisation of utilities, many power systems around the world have instead experienced an unbundling of these core functions to separate entities, and this separation is regulated as a means to protect consumers. We now present two of the primary actors in unbundled power systems.

The accelerating uptake of DER is increasingly requiring some adaptations to the conventional responsibilities and interactions between these actors.

2.3.1 Definition of Actors in Unbundled Power Systems

In unbundled power systems, we identify the following actors responsible for safe and effective coordination of energy flows at the distribution scale and ensuring reliable operation of the electricity system with high uptake of DER:

- **Distribution Network Operators**: Network operators are responsible for managing the physical infrastructure of electricity networks, at either the distribution or the transmission scale. At the distribution scale, these entities have historically not engaged in any coordination of power exchanges at connection points, other than establishing fixed import or export restrictions. In Australia, distribution network operators are referred to as distribution network service providers (DNSPs).

  As the volume of DER in distribution networks grows, there is an increasing need for more active coordination approaches within distribution networks to enable greater overall DER participation while managing risks in periods of peak network utilisation.

- **Distribution System Operators**: A DSO represents an evolution of the concept of a distribution network operators (or DNSP), adopting additional coordination functions to ensure reliable network operation. This typically takes the form of applying time-varying restrictions limiting DER participation in electricity markets, or sourcing reserve capacity which may be dispatched according to system needs.

In Australia, distribution network service providers (DNSPs) are increasingly adopting system operator functions through mechanisms such as the Emergency Backstop Mechanism [34], and the increasing field deployment deployment of dynamic operating envelopes (DOE).

- **Independent System Operator**: An ISO (e.g. AEMO in Australia, CAISO in California) is responsible for whole-of-system coordination of energy flows through wholesale markets, and is generally also responsible for coordinating market-responsive DER.

Other key actors not listed above include transmission network operators (or transmission network service providers, i.e. TNSPs) and transmission system operators (TSOs). Where an ISO manages a wholesale market, the transmission network is generally managed by a transmission network operator (or TNSP), whereas the term system operator is considered in literature when the TSO is assumed to conduct additional coordination functions such as operate a wholesale market.

In [35], a designation of market operator (MO) is made in addition to designations of DNSP, DSO and TNSP, indicating who conducts the function of clearing a wholesale market. In different models proposed in [35], the market operator is either the ISO alone, or market clearing functions at the transmission scale may also be complemented by a market operator at the distribution scale. This is done by a DSO, or an independent DSO (IDSO).

We now provide greater detail on each of these functions, providing context for how each is modelled in our simulations.

2.3.2 Independent System Operators

In unbundled power systems, such as Australia, the primary goal for independent system operators is to ensure the transmission-scale system frequency remains with a safe interval. Imbalances between supply and demand across the system cause system frequency to fluctuate[1], therefore a primary responsibility of the independent system operator is to coordinate generators, flexible loads and storage devices to maintain this balance.

[1]This is because spinning inertia effectively acts as an energy storage mechanism for the grid. A shortage in generation is accounted by a reduction in spinning inertia, and surplus generation adds to spinning inertia.

This is generally achieved by operating a wholesale market, in which generators and loads bid to provide market services. The primary market is for the provision or the consumption of energy. Depending on the jurisdiction, this price is calculated on a regional or a nodal basis. Wholesale markets also include reserve markets, accounting for imbalances between cleared supply and demand, and to provide network relief in the event of contingencies.

Market structures vary across jurisdictions. Some wholesale markets enable participants to bid in forward markets with contractual obligations, such as a day ahead market, enabling system operators to reduce uncertainties on the spot market. However, other markets such as the National Electricity Market (NEM) operate a spot market that clears every 5 minutes. Participants do generally submit bids one day in advance, however it is possible to re-bid up to mere minutes before market clearing.

Simulations in Chapter 4 of this thesis model participation of DER-scale batteries in the Australian NEM. To provide some context for the implementation of our solution in Chapter 4, we now provide an overview of bidding formats in the NEM. We note that the principles applied in Chapter 4 can apply to a wide range of electricity market settings, however it is appropriate to provide some background here about the NEM given it is our application setting.

Study of the Australian National Electricity Market (NEM)

The National Electricity Market (NEM) is the wholesale market that operates along the east coast of Australia, servicing 80% of the nation's electricity demand.

The NEM operates the following markets:

- Energy Market: Operates as a spot market for energy
- Regulation Frequency Control Ancillary Service (FCAS) Market: Generators and loads can bid for contracts to provide raise (generation) or lower (load) services to correcting for small deviations in system frequency. These deviations are encountered due to discrepancies between supply and demand.
- Contingency FCAS Market: Generators and loads bid to provide raise and lower services in the event of contingencies that significantly impact system frequency outside of what is expected under normal operating circumstances. At the time of writing, the NEM operates four raise

and four lower markets, in which successful bidders are required to provide responses within 1 second, 6 seconds, 60 seconds and 5 minutes. Simulations in Chapter 4 do not include participation in the 1 second market.

Generators and loads participating in NEM as scheduled assets produce bids in each market in the form of a bid stack, defining bid volumes and prices across 10 different bands, as shown in an example in Table 2.1

Band	Capacity (MW)	Price ($/MWh)
1	100	-950
2	10	0
3	20	23
...	...	...
9	30	300
10	40	15,000

TABLE 2.1: Capacity and Price Bands

This bid stack indicates that the generator is willing to supply the first 100 MW of electricity at $-950, which is common for synchronous generators who do not wished to be curtailed in this portion. The next 10 MW of electricity is made available for spot prices above $0, and this process continues across 10 bands. For storage assets performing arbitrage, including DER, this stratification of capacity can enable a form of opportunity hedging, given the relatively small state of charge of household batteries compared to their maximum rate of charge and discharge.

Scheduled generators and loads active in the NEM are able to bid into multiple markets (energy and reserves) simultaneously by defining bid trapeziums, illustrated in Figure 2.7. These consist of inter-market dispatch constraints, informing the NEM of the technical limits that prevent dispatching their full capacity in two markets simultaneously.

The key parameters defining bid trapeziums are tabulated in Table 2.2

2.3.3 Transition from Distribution Network Service Provider to Distribution System Operator

We will later provide a review of literature on coordination frameworks for distribution systems with high DER uptake in Section 3.2. The purpose of this section in the background chapter is merely to illustrate how DER uptake is forcing a change of roles and responsibilities in the management of distribution networks.

Parameter	Symbol	Description
Enablement Min	E_{min}	The minimum dispatch in the energy market that allows for non-zero dispatch in the ancillary market
Low Breakpoint	B_{low}	The minimum dispatch in the energy market that allows for participation in the ancillary market at the *Max Availability* rate
High Breakpoint	B_{high}	The maximum dispatch in the energy market that allows for participation in the ancillary market at the *Max Availability* rate
Enablement Max	E_{max}	The maximum dispatch in the energy market that allows for non-zero dispatch in the ancillary market

TABLE 2.2: Enablement and Breakpoint Parameters

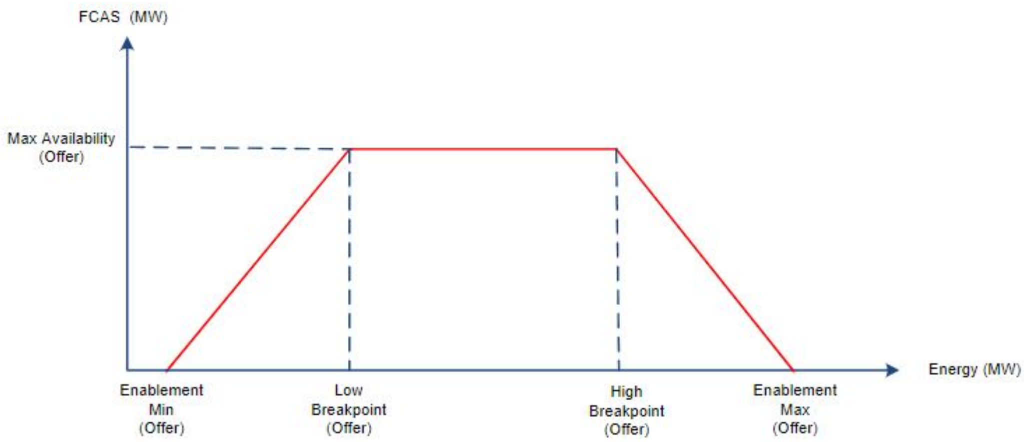

FIGURE 2.7: Bid trapezium structure in NEM, figure sourced from [36]. Note that x axis label 'Energy' refers to power provided in the NEM energy market, as opposed to ancillary markets.

In the context of rising participation of DER, managers of distribution networks face new challenges. Increases in distributed PV generation and dispatchable distributed storage capacity are already driving changes in network utilisation patterns. This can result in networks experiencing more extreme voltage and current values at peak times. These stresses can be mitigated to some extent using devices such as on-load tap changers.

When all levers of control available to distribution network service providers are exhausted, it is expected they will be required to impose temporary restrictions to DER imports and exports. This requires distribution network service providers to conduct a form of coordination of consumers' behaviour not generally considered within their conventional role, and adopt some additional responsibilities akin to a *distribution system operator*, or DSO.

In networks where DER have a relatively small footprint in wholesale markets, the effect of curtailing DER imports and exports is unlikely to have consequences on system coordination at the transmission scale. From a system operator's perspective at the transmission scale, small fluctuations in aggregate rooftop PV generation due to distribution network curtailments would be managed through regulation services, much in the same way that system operators would manage variability of utility-scale solar and wind generation.

As installed DER capacity grows, and its role in coordination of power systems becomes more important, it is expected to play an increasing role in wholesale markets. In this context, it will be subject not only to coordination at the distribution scale for the purposes of safe distribution network operation, but also coordination at the transmission scale to achieve economically efficient dispatch outcomes across the system. In increasingly decentralised power systems, where batteries at distribution scale will likely play an important role ensuring secure power system operation through providing arbitrage of power from intermittent sources, it is likely that greater TSO-DSO coordination will be required to ensure effective and secure system operation at the transmission-scale, and secure network operation at the distribution scale.

In Chapter 4 of this thesis, we will demonstrate that a simple form of DSO-TSO coordination can help to significantly improve the market efficiency of DER participation in wholesale markets, compared to the case where DSOs manage DER challenges without regard to TSO needs (communicated through a price proxy).

2.4 Power Flow Modelling

Market clearing by system operators is an example of an optimal power flow problem. To introduce the concept of an OPF, we first establish the concept of a power flow model, then introduce optimisation in the next Section.

2.4.1 Power Flow Models

Power flow models are sets of equations capturing the physical relationships between voltages, currents, power flows and network impedances. These equations model the steady state of power systems under specific loading conditions. There are two power flow models commonly used in literature: the bus injection model (BIM) and the branch flow model (BFM). Both models are constructed from instances of Ohm's Law for AC power, nodal power balance, and the definition of complex power as a function of complex voltage and line impedance. Both models exist in various variable spaces, including natural current-voltage (IV), power-voltage (SV), and power-lifted voltage (SW, as used in SDP forms), and for different choices of coordinates (polar or rectangular). The primary differences between these models include:

- The bus injection model fundamentally embeds Ohm's law in admittance form, whereas the BFM embeds it in impedance form. This means that zero impedance connections are not representable in BIM.
- The bus injection model only requires complex voltages as variables, whereas the branch flow model requires an explicit variable for series current.

2.4.2 Branch Flow Model

Simulations in this thesis use the branch flow model (BFM). One benefit of the branch flow model is the availability of linearised forms of the model, such as LinDistFlow, which are well suited for application in radial distribution networks. We now define the branch flow model for a single-phase equivalent radial distribution network network [37][2].

[2]Mathematical derivations in this thesis require the network to represented as a tree, i.e. they do not contain loops or parallel lines. More general branch flow model mathematical formulations exist for meshed networks [38] and networks with parallel lines [39]

Consider a network of $N^i \in \mathbb{N}$ nodes[3]. Each node j has exactly one parent node i, but may have 0, 1 or multiple child nodes (which we will generally refer to using the letter k). Let D_j be the set of node j's child nodes. Let s_j be the complex power injected at node j, let S_j be the *sending-end* complex power[4] sent from node i towards node j, and let z_j be the impedance of the branch from parent node i to node j. Let V_i be the phasor representing AC voltage at node i, and let I_j be the current entering node j from its parent node i. The branch flow model is given by

$$s_j = \sum_{k \in D_j} S_k - (S_j - z_j |I_j|^2) \tag{2.2a}$$

$$V_i - V_j = z_j I_j \tag{2.2b}$$

$$S_j = V_i I_j^* \tag{2.2c}$$

2.4.3 DistFlow Relaxation

The branch flow model in this form is not convex, and is therefore unsuitable for direct application in many optimisation problems. This is due to the bi-linear terms in (2.2a) (losses) and (2.2c) (definition of complex power).

The branch flow model can be relaxed to obtain a convex form. Begin by substituting (2.2c) into (2.2b) then taking the squared magnitude of both sides

$$V_j = V_i - z_j (S_j^* / V_i^*) \tag{2.3a}$$

$$(V_j)(V_j)^* = \left(V_i - z_j (S_j^* / V_i^*)\right) \left(V_i - z_j (S_j^* / V_i^*)\right)^* \tag{2.3b}$$

$$(V_j)(V_j^*) = \left(V_i - z_j (S_j^* / V_i^*)\right) \left(V_i^* - z_j^* (S_j / V_i)\right) \tag{2.3c}$$

$$v_j = v_i - V_i z_j^* (S_j / V_i) - z_j (S_j^* / V_i^*) V_i^* + |z_j|^2 \ell_j \tag{2.3d}$$

$$= v_i + |z_j|^2 \ell_j - (z_j^* S_j + z_j S_j^*) \tag{2.3e}$$

[3]When defining a single natural number, a superscript is used as a label. We provide a more detailed notation guide in footnote 3 of Chapter 4.

[4]Our notation seeks to avoid using two letters to designate branches, as we may wish to use a second subscript term to designate phases in three-phase models. Our naming convention designates branches according to the child node as this is unambiguous in radial structures. We acknowledge that this notation choice is different from common practice where the sending and receiving end buses are both identified in subscripting.

Variables for sending-end power along a branch inherit the same naming convention as for branches. It is important to note sending-end power S_j for the branch linking nodes i and j is defined as the product of current I_j^* and voltage V_i *at the parent node* i. This is different to the receiving-end power, which would be equal to $I_j^* V_j$ along the same branch.

$$
\begin{aligned}
&= v_i + |z_j|^2\ell_j - ((z_j^* S_j) + (z_j^* S_j)^*) && \text{(2.3f)}\\
&= v_i + |z_j|^2\ell_j - 2\mathcal{R}(z_j^* S_j) && \text{(2.3g)}\\
&= v_i + |z_j|^2\ell_j - 2\mathcal{R}((r_j - jx_j)(P_j + jQ_j)) && \text{(2.3h)}\\
&= v_i + |z_j|^2\ell_j - 2\mathcal{R}(P_j r_j + Q_j x_j + j(Q_j r_j - P_j x_j)) && \text{(2.3i)}\\
&= v_i + |z_j|^2\ell_j - 2(P_j r_j + Q_j x_j) && \text{(2.3j)}
\end{aligned}
$$

for $v_j = V_j V_j^*$ the squared magnitude of voltage at bus j, and $\ell_j = I_j I_j^*$ the squared magnitude of current flowing from parent node i towards node j. By separating terms in (2.2a) according to their real and reactive components, and squaring magnitudes on both sides of (2.2c), we obtain the DistFlow model

$$
\begin{aligned}
P_j - r_j\ell_j + p_j &= \sum_{k \in D_j} P_k && \text{(2.4a)}\\
Q_j - x_j\ell_j + q_j &= \sum_{k \in D_j} Q_k && \text{(2.4b)}\\
v_i + |z_j|^2\ell_j - 2(P_j r_j + Q_j x_j) &= v_j && \text{(2.4c)}\\
P_j^2 + Q_j^2 &= v_i \ell_i && \text{(2.4d)}
\end{aligned}
$$

This form is relaxed as we no longer model the phase angles of voltages, currents and power transfers, and this represents a loss of information. In mesh networks, solutions to the DistFlow model may violate the cycle condition, which states that the sum of all phase shifts along branches forming closed cycles must be zero. Analysis in [40] shows that in radial networks, where each child node has a unique parent node and no cycles exist, solutions to the DistFlow model generally satisfy the branch flow model conditions, and phase shifts with respect to the reference bus can be easily recovered.

In single-phase radial networks, or single-phase equivalent models of a balanced three-phase system, phase shifts are generally ignored as there is no cycle condition to satisfy. As a result, there is generally little value in knowing the difference in phase angle between two locations. In an unbalanced three-phase network, the phase angle has much more significance due to the need to ensure that voltage unbalance remains within acceptable tolerance.

The DistFlow model is still non-convex due to the equality constraint (2.4d). A convex relaxation of the DistFlow model is obtained by relaxing this constraint to an inequality constraint, i.e.

$$P_j^2 + Q_j^2 \leq v_i \ell_i \tag{2.5}$$

Equations (2.4a), (2.4b), (2.4c) and (2.5) together form a convex power flow model, namely the relaxed DistFlow model.

2.4.4 LinDistFlow Approximation

In time-critical settings, such as clearing markets or allocating constrained network capacity within a distribution network, the benefits of obtaining solutions very quickly using a linear model may outweigh operational risks associated to linearisation error.

The LinDistFlow model is obtained from the DistFlow model by ignoring losses. This has the effect of setting all terms ℓ_i to zero, and removing (2.4d) from the power flow model entirely (instead of applying a convex relaxation). In cases where losses are known to be small, significant computational advantages may be obtained through linearisation.

Notes on approximations and relaxations

The LinDistFlow model is an *approximation* of the DistFlow formulation. A key feature of approximations is that solutions satisfying the physically-accurate branch flow model may not satisfy the approximated LinDistFlow model. This means that optimal operation of a network may not be discoverable to a solver under the approximated power flow formulation. In contrast, the DistFlow formulation was obtained from the branch flow model by *relaxing* individual constraints (cycle condition, with further convex relaxation available through (2.5)), meaning that the optimal solution to the original problem is guaranteed to exist within the search space of the relaxed problem. Further, the solution to a relaxed problem may be verified as the optimal solution of the original problem by checking it satisfies an additional constraint set.

It follows that solutions to relaxed problems provide some information about performance bounds in the original problem, however solutions found using approximations yield no such guarantees.

2.4.5 Multi-Phase DistFlow Relaxation

The branch flow model discussed to this point is modelled on a single-phase equivalent network. This may be used to represent a balanced three-phase network on the condition that all loads and generators are three-phase and balanced [41]. In distribution networks with single-phase connections, loads and branch flows may become unbalanced across phases. This motivates the derivation of power flow models that capture differences in network utilisation across phases.

A three-phase branch flow model is introduced in [42]. Variables for voltage, current and power injections are augmented to 3-vectors, i.e. $V_i, I_i, s_i \in \mathbb{C}^3$, and power flows along branches and line impedances are augmented to 3-by-3 matrices matrices, i.e. $S_i, z_i \in \mathbb{C}^{3\times 3}$. Using the same conventions for subscript identifiers as above[5], the three-phase branch flow model introduced in [42] is expressed as

$$s_j = \sum_{k\in D_j} \mathrm{diag}(S_k) - \mathrm{diag}(S_j - z_j(I_j I_j^H)) \tag{2.6a}$$

$$V_i - V_j = z_j I_j \tag{2.6b}$$

$$S_j = V_i I_j^H \tag{2.6c}$$

A three-phase DistFlow formulation is then obtained using the same principles as applied to the single-phase case. Define $\ell_j = I_j I_j^H \in \mathbb{C}^{3\times 3}$ and substitute into (2.6a) to obtain

$$s_j = \sum_{k\in D_j} \mathrm{diag}(S_k) - \mathrm{diag}(S_j - z_j \ell_j) \tag{2.7}$$

Define $v_j = V_j V_j^H \in \mathbb{C}^{3\times 3}$, and multiply both sides of (2.6b) by its Hermitian transpose to obtain

[5] As a notation guide, use of capitalisation in this Background section is consistent with the original works [40], [42] to assist readers who may wish to learn more from these references. In Chapter 4 we formalise a notation style applied to the contribution chapters in this thesis, which differs slightly from these references to enhance legibility in our studies.

$$v_j = v_i - (S_j z_j^H + z_j S_j^H) + z_j \ell_j z_j^H \tag{2.8}$$

Finally, the definition of complex power is augmented in the three-phase case by applying positive-semidefinite and rank constraints

$$\text{rank}\left(\begin{bmatrix} v_i & S_j \\ S_j^H & \ell_j \end{bmatrix}\right) = 1 \tag{2.9}$$

$$\begin{bmatrix} v_i & S_j \\ S_j^H & \ell_j \end{bmatrix} \succeq 0 \tag{2.10}$$

to capture the fact that

$$\begin{bmatrix} v_i & S_j \\ S_j^H & \ell_j \end{bmatrix} = \begin{bmatrix} V_i V_i^H & V_i I_j^H \\ I_j V_i^H & I_j I_j^H \end{bmatrix} = \begin{bmatrix} V_i \\ I_j \end{bmatrix} \begin{bmatrix} V_i \\ I_j \end{bmatrix}^H \quad \text{with} \quad \begin{bmatrix} V_i \\ I_j \end{bmatrix} \in \mathbb{C}^6 \tag{2.11}$$

The branch flow model for three-phase networks is given by the combination of (2.7), (2.8), (2.9) and (2.10). The rank one condition is non-convex, therefore a convex rank-relaxed formulation can be obtained by combining equations (2.7), (2.8) and (2.10) only.

2.4.6 Multi-Phase LinDistFlow Approximation

The authors of [42] then propose a linearisation of the three-phase branch flow model, taking a similar approach to the single-phase equivalent case. The approximation assumes that losses are small, i.e. $z_j \ell_j \ll S_j$, resulting in losses being neglected. To achieve this, the rank and semidefinite constraints (2.9) and (2.10) are omitted.

One complication that arises from omitting these constraints is that off-diagonal elements of matrices S_j become undefined, as constraint (2.7) only affects diagonal elements of S_j. In the unbalanced three-phase case, off-diagonal elements of S_j impact calculations of the effects of mutual impedances between phases. The three-phase LinDistFlow proposed in [42] instead assumes that phase shifts between phases are approximately 120 degrees, and defines

$$\gamma = \begin{bmatrix} 1 & e^{2\times(-j2\pi/3)} & e^{-j2\pi/3} \\ e^{-j2\pi/3} & 1 & e^{2\times(-j2\pi/3)} \\ e^{2\times(-j2\pi/3)} & e^{-j2\pi/3} & 1 \end{bmatrix} \in \mathbb{C}^{3\times 3} \tag{2.12}$$

and then requires that

$$\Lambda_j = \text{diag}(S_j) \tag{2.13}$$

$$S_j = \gamma \, \text{diag}(\Lambda_j) \tag{2.14}$$

Due to the fact losses are neglected, and due to the radial structure of the network, branch flows can be computed directly as the sum of bus injections *downstream* of a given node.

All in all, the three-phase LinDistFlow formulation in [42] is expressed as

$$\Lambda_j = -\sum_{k\in\text{Down}(j)} \text{diag}(s_k) \tag{2.15}$$

$$S_j = \gamma \, \text{diag}(\Lambda_j) \tag{2.16}$$

$$v_j = v_i - (S_j z_j^H + z_j S_j^H) \tag{2.17}$$

One significant benefit of the multi-phase LinDistFlow model is the ability to express network voltages directly as linear functions of bus injections across the network. For instance, in the event that exported reactive power $q_i = 0$ across all nodes, we can construct real matrix $\boldsymbol{A_v}$ and real vector $\boldsymbol{b_v}$ such that

$$\boldsymbol{v} = \boldsymbol{A_v}\boldsymbol{p} + \boldsymbol{b_v} = \boldsymbol{l_v}(\boldsymbol{p}) \tag{2.18}$$

where $\boldsymbol{v}$ and $\boldsymbol{p}$ in **bold** typesetting are concatenations of all voltage magnitude vectors $v_i \in \mathbb{C}^3$ and real power injection vectors $p_i \in \mathbb{C}^3$.

2.5 Optimisation

2.5.1 Optimisation Fundamentals and Optimal Power Flow

Optimisation problems in computer science are defined by three key attributes: (a) decision variables, (b) an objective function, and (c) constraints. A simple example of an optimisation problem is given by

$$\max_{x} \quad \cos(x) \tag{2.19}$$

$$\text{s.t.} \quad x \geq 0.5 \tag{2.20}$$

$$x \leq 1 \tag{2.21}$$

where the set of decision variables is $\{x\}$, the objective function is $\cos()$, and the constraints placed on the decision variables are $x \geq 0.5$ and $x \leq 1$.

In the context of power systems studies, an optimisation problem is described as an optimal power flow (OPF) problem when equations from power flow models appear in the constraints set. As a simple example, a system operator may seek to minimise costs associated to operating the system.

Let $N^g \in \mathbb{R}$ be the number of dispatchable generators in the system. Let $\boldsymbol{p} \in \mathbb{R}^{N^g}$ be the vector of generator real-power outputs, and let $c : \mathbb{R}^{N^g} \to \mathbb{R}$ be the function that computes system costs as a function of generator outputs. The set of feasible solutions are constrained by constraints from a number of sources, including

- **Unit constraints**: Generator dispatch is constrained by its maximum rated generation capacity, i.e. $0 \leq p_i \leq \overline{p_i}$. Let $\mathcal{S}_{\text{generator}}$ be a set representation of generator constraints.
- **Network constraints**: Across all nodes j in the network, we may require that voltages remain within a safe range, i.e. $\underline{V_i} \leq V_j \leq \overline{V_j}$. Let $\mathcal{S}_{\text{network}}$ be a set representation of generator constraints.
- **Power flow constraints**: The impacts of generator exports p_i on network state variables are captured by power flow constraints. Let $\mathcal{S}_{\text{power flow}}$ be a set representation of generator constraints.

This problem can be described as

$$\min_{p} \quad c(p) \tag{2.22}$$

$$\text{s.t.} \quad \mathcal{S}_{\text{generator}}(p) \quad \text{is satisfied} \tag{2.23}$$

$$\mathcal{S}_{\text{network}}(p) \quad \text{is satisfied} \tag{2.24}$$

$$\mathcal{S}_{\text{power flow}}(p) \quad \text{is satisfied} \tag{2.25}$$

2.5.2 Categorisation of Optimisation Problems

Optimisation problems, including OPF problems, may be simple or challenging to solve depending on their composition. The most influential factor that determines the algorithmic complexity of solving an optimisation problem is whether or not the objective and constraint functions are convex, collectively defining a convex optimisation problem.

Convex Optimisation

Convex optimisation concerns the minimisation of convex functions over convex sets [43]. A problem is convex if its objective function is convex, the inequality constraint functions are convex, and the equality constraints are affine. Mathematically, the standard form can be expressed as:

$$\text{minimise} \quad f_0(x) \tag{2.26}$$

$$\text{subject to} \quad f_i(x) \leq 0, \quad i = 1, \ldots, m \tag{2.27}$$

$$Ax = b \tag{2.28}$$

where $f_0, f_1, \ldots, f_m$ are convex functions[6].

There exist a wide range of solver algorithms for constrained convex optimisation. These include interior point methods, gradient descent variants, proximal algorithms, augmented Lagrangian methods, and active-set approaches. For specific problem structures, the alternating direction method of multipliers (ADMM) and sequential quadratic programming (SQP) are frequently employed. In practice, solvers like CPLEX, Gurobi, and MOSEK

[6]Note that while the equality constraint (2.4d) can be re-arranged to define a convex function in the form $h(P_j, Q_j, v_i, l_i) = 0$, it is non-linear, and this causes the feasible region defined by power flow constraints to be non-convex. Convex relaxations for power flow problems are discussed in [44]

implement sophisticated versions of these algorithms, often with automatic selection of the most appropriate method based on problem characteristics.

Interior point methods (IPMs) are a particular class of solving algorithms for constrained convex optimisation problems. Starting from a strictly feasible point, IPMs generate a sequence of interior points that converge to the optimal solution, remaining within the feasible region at all times. In simulations in this thesis we employ IPOPT, an interior point solver, to solve convex relaxations of power flow equations.

Linear Programming (LP)

Linear programs are optimisation problems defined by a linear objective function and linear constraints. Conceptually, linear constraints collectively define a polyhedron. A linear objective effectively reduces the problem to maximising an inner product, and the solution is found at the vertex (or multiple vertices in a level set) that extends furthest in the direction defined by coefficients in the objective.

The solving speed of linear OPF problems is generally quite fast. The traditional method of solving an LP is using the simplex method. Starting at a vertex, the algorithm determines the most effective edge to follow to reduce the objective, and repeats this process. Convexity of the polyhedron feasible region guarantees that a globally optimal solution will be found. While small-scale linear programs may now be considered trivial to solve, adaptations of solvers have been proposed to solve larger-scale problems more efficiently. For instance, the Harwell Subroutine Library includes solvers such as MA27, which is well suited to solving sparse symmetric systems. Further information about linear solvers in the HSL library can be found at [45].

In the context of optimal power flow studies, linear OPF problems use linearised power flow models such as LinDistFlow or its multi-phase variant. Approximations in these models introduce small linearisation errors, meaning that solutions may not be feasible in practice. This typically manifests as over-estimations of voltage magnitudes. In voltage-constrained distribution networks, one approach to accounting for linearisation error is to introduce a small buffer to voltage bounds when optimising envelopes, yielding a slightly conservative but safe result. We adopt such an approach when optimising operating envelopes in Chapter 5. Monte Carlo simulations performed to validate the network feasibility of our proposed approach apply a non-convex power flow model, employing an iterative solving technique. Results demonstrate that the voltage buffer we introduce only needs to be very small, particularly in comparison to the magnitude of voltage constraint violations which may occur under operating envelopes that assume a balanced network.

Stochastic Optimisation

Stochastic optimisation addresses decision-making problems under uncertainty, where some problem parameters are random variables rather than deterministic values [46]. Unlike deterministic optimisation, which assumes perfect knowledge of all parameters, stochastic optimisation explicitly incorporates the probabilistic nature of uncertain parameters [47]. The general form of a linear stochastic programming problem is:

$$\begin{aligned} \text{minimise} \quad & c^T x + \mathbb{E}_\xi[Q(x,\xi)] && (2.29)\\ \text{subject to} \quad & Ax = b && (2.30)\\ & x \geq 0 && (2.31) \end{aligned}$$

where:

- x represents first-stage decisions made before uncertainty is revealed
- ξ is a random vector representing uncertainty
- $c^T x$ is the cost of first-stage decisions
- $\mathbb{E}_\xi[Q(x,\xi)]$ is the expected cost of the second-stage problem
- $Q(x,\xi)$ is the optimal value of the second-stage problem given by:

$$\begin{aligned} \min_{y} \quad & q(\xi)^T y && (2.32)\\ \text{subject to} \quad & T(\xi)x + W(\xi)y = h(\xi) && (2.33)\\ & y \geq 0 && (2.34) \end{aligned}$$

This formulation is general and applies to both discrete and continuous distributions of the random vector ξ. When ξ has a discrete distribution with a finite number of scenarios $1, 2, \ldots, S$ and corresponding probabilities p_s, the expectation becomes a weighted sum: $\mathbb{E}\xi[Q(x,\xi)] = \sum s = 1^S p_s Q(x,\xi_s)$.

For continuous distributions, the expectation involves integration over the probability space of ξ.

In Chapter 4 of this thesis, we employ stochastic optimisation to determine operating envelopes that maximise the expectation of benefit attained by DER households participating in wholesale markets, under the uncertainty of energy market prices.

Chapter 3

Literature Review

We begin our literature review with a general review of how optimisation has been applied in power systems operation (noting we omit consideration of long-term network planning problems). Many established applications focus on transmission-scale operational challenges, however the recent proliferation of DER has provided consumers and operators of DER new opportunities to optimise their energy usage and aggregate DER at scale. The increased participation of DER in power systems presents new challenges and opportunities for distribution network operators aiming to ensure safe network operation.

We then present a review of network-secure DER coordination strategies, considering both direct control-based approaches (e.g. network-owned assets) and the coordination of consumer-owned DER (e.g. operating envelopes, market-based approaches). The necessity of alignment between a) distribution-scale DER coordination schemes and b) market interactions between prosumers and transmission-scale market interactions requires the adoption of TSO-DSO coordination schemes. We present categorisations of these coordination schemes in literature, and comment on the advantages and limitations of each, paying particular attention to the centralised ancillary services market model.

We then provide an overview of literature that has studied dynamic operating envelopes. We discuss the various objectives considered in calculation (total capacity vs. fairness), computational aspects (centralised vs. distributed), and handling of uncertainty.

3.1 Optimisation in Power Systems

The act of optimising a system relates to maximising or minimising some objective (e.g. cost, reliability) in the presence of constraints (e.g. availability, network capacity). Given the ubiquitous role of electricity in society, its costs of production and transmission/distribution, and its value derived from its scarcity, the operation of power systems has long been governed by large optimisation processes. In this first Section we outline some of the most prominent applications of optimisation in power systems operations, beginning with longstanding transmission-scale challenges, before outlining new consumer-scale opportunities for optimisation made possible by DER.

3.1.1 Transmission-Scale Optimisation Applications

At transmission scale, system operators are responsible for maintaining power balance (i.e. supply matches demand) in order to maintain a stable system frequency. This requires procuring sufficient energy and reserve capacity, determining which units must remain available (unit commitment), factoring differences in generation technologies, and responding to potential environmental threats. Below we outline a selection of the most prominent and enduring applications of optimisation towards the operation of power systems.

System/Network Operations - Market Clearing, Stochastic Unit Commitment, Reserve Dimensioning and Environmental Risks

From a system operators' (SO) perspective, energy market clearing and day-ahead unit commitment represent the most intuitive and well-known applications of optimisation in power systems. The process of operating an energy market optimally from a utility perspective, while respecting approximations of transmission constraints and unit commitment considerations, can be solved through constrained linear programming [48] (although it can become more complex e.g. considering non-convex pricing by generators [49], [50] or non-linear transmission constraint formulations). Dual variables associated with energy balance constraints represent the marginal price of electricity in the system. Stochastic unit commitment was originally studied as a means to factor uncertainties of day-ahead energy utilisation and production [51], [52], and have received additional interest in recent times due to the increasing influence of variable renewable energy [53], [54].

Maintaining a stable system frequency requires procuring sufficient reserve capacity that can be used to regulate differences between supply and demand, or activate in contingency events. Market participants providing reserve services must be compensated, therefore the system operator must weigh the costs of reserve services against their likely need. Changes in power systems' energy mix towards variable renewable generation, and inverter-based resources (reducing total system inertia) have further motivated research on optimally estimating the quantity of reserves required [55], [56]. Due to potentially prohibitive costs of ensuring total robustness (i.e. sufficient reserves in the event of widespread generation failures), chance-constrained approaches are well-suited to reserve dimensioning [57], [58].

System operators must also contend with environmental risks. One such example is wildfire, where optimisation can be applied both before and during a wildfire event. Beforehand, system operators can optimise network disconnections to balance consumer inconvenience and wildfire risk [59], and during/after disruptions the restoration of systems can be optimised using fast heuristics [60].

Generator/Customer Operations - Factoring Uncertainty into Bidding Strategy

In the case of energy market participants, large generators and consumers operating at the transmission network scale may be exposed to volatile wholesale electricity prices, face complex operational costs, and may be constrained by environmental factors. A generalised stochastic optimisation model for the operation of energy systems was proposed in [61]. This has been applied to mitigate financial risks of large energy consumers in [62], [63]. Hydroelectric power systems must also factor projections of future rainfall in [64], and natural gas plants must factor gas storage costs in [65]. The premise of these methods is to account for environmental, price or demand uncertainties in order to formulate a strategy that maximises the *expected* value of an entity's objective, which generally captures its financial return. As these studies consider optimisation from a market participant or consumer's perspective, network constraints are generally ignored.

Historical Emphasis on Transmission-scale Operational Challenges

Before widespread uptake of distributed energy resources and home energy management systems enabling demand response, distribution-scale networks and assets were generally not modelled in great detail in power systems optimisation studies. This was due to:

- Relatively low-controllability of distribution-scale loads.

- Low observability of real-time state of distribution networks
- Relatively minor impacts of distribution-scale disruptions on transmission-scale operation, as energy resources connected to distribution networks were traditionally not responsible for providing significant shares of generation.

The emergence of smaller-scale distributed energy resources and smart home energy management systems have opened many since new opportunities for consumers, or *prosumers* (consumers who also produce energy) to optimise their operations.

3.1.2 Opportunities for Optimisation at the Distribution-Scale

Rapid growth of distributed energy resources (DER) has provided consumers, or *prosumers* (consumers who also produce electricity) new avenues to optimise their energy usage. In this Subsection, we begin by studying approaches to optimise DER utilisation by owners/operators of DER, before discussing the implications of these new arrangements on network and system operators.

Demand Response and Optimal Utilisation of DER

The role of demand-side flexibility to help address system challenges has been studied in literature for many decades [66], [67]. The premise of *demand response* is to incentivise demand-side behaviours that reduce the severity of peak loads, instead shifting energy utilisation to off-peak periods [68], [69], [70]. One common way to achieve this behavioural shift is through effective tariff design, involving time-of-use tariffs [71], dynamic pricing [72], or increasing consumers' exposure to wholesale prices.

The development of controllable and programmable devices such as DER and smart appliances has significantly facilitated consumers' adherence to desired behavioural profiles by responding to varying price signals. Home energy management solutions (HEMS) are increasingly able to schedule and optimise energy utilisation to maximise consumer benefit. The optimal scheduling problem generally takes the form of a receding horizon problem [73], and often involves solving a stochastic optimisation problem (stochastic programming in [74], particle filter modelling in [75]). Constraint programming has also been employed to determine DER schedules [76]. These studies aim to minimise operational costs to households in light of uncertain costs and future utilisation of household appliances.

A recent work [77] has sought to provide a new updated definition of demand response, arguing that existing definitions are either too restrictive (limiting to just load reduction) or too imprecise, creating confusion about what constitutes demand response and undermining its full potential value. The key contribution in [77] is proposing a new, comprehensive definition of DR:

The actions of customer-sited energy resources downstream of metering points to voluntarily, actively, and temporarily adjust their electricity production and/or consumption in response to signals (e.g., commands, prices, measurements).

The authors of [77] also identify technical, regulatory, and social barriers to demand response adoption.

While the optimal operation of a single smart household may now be considered a well-studied problem in literature, new challenges have emerged relating to the coordinated dispatch of DER by aggregators.

Representation of DER Flexibility at Scale

Aggregators have emerged to unlock the flexibility of consumer DER and deferrable loads to wholesale markets [78]. Their role is to manage wholesale market interactions on behalf of large groups of DER customers at scale. This is beneficial for consumers, who would be otherwise unable or unlikely to engage in wholesale markets independently, and is also beneficial for wholesale markets, who would otherwise field market bids from thousands or potentially millions of participants.

Literature that optimises the aggregation and disaggregation of DER generally considers device *flexibility* in terms of (a) the amount of energy traded by each device, and (b) when these energy transfers are scheduled to occur. Aggregators aim to offer wholesale markets (in this case, wholesale markets that include forward markets e.g. clearing with time-coupling constraints) the maximum aggregate flexibility their portfolio allows, while ensuring any potential market dispatch outcome in the form of an aggregated time series can be disaggregated to the device level respecting devices' internal constraints. This may be challenging when individual devices are subject to heterogeneous utilisation constraints over the forward horizon[1].

The authors of [79] propose a generalised conceptual framework for aggregating and disaggregating flexibility objects. This includes formal definitions for

[1]Note this literature does not consider distribution network constraints, as these problems are viewed only from the aggregators' perspective.

flex-objects, *fix-objects*, measures to quantify flexibility, and general frameworks to compute aggregation and disaggregation functions. Their analysis makes particular mention of *compression-flexibility* trade-offs, which becomes greater as DER-scale utilisation constraints become increasingly heterogeneous. The authors of [80] note that calculating the Minkowski sum of polytopes under facet representation is generally NP-hard, and that many approaches rely on polytopic projection approximations of flexibility regions. Linear-algebra-based geometric approaches to calculate aggregate flexibility regions from device-level constraint sets, and device-level disaggregation of aggregate-level dispatch traces, are proposed in [80], [81], [82]. Constraint elimination methods, such as in [83], can also help to reduce computational complexity of aggregation/disaggregation.

Note: We acknowledge that this thesis does not study time-sequential problems. All our case studies and simulations assume the wholesale market clears frequently without time-coupling constraints. Nevertheless, in Chapter 6, we will exploit an alternative definition of aggregators' flexibility, in terms of (a) the *quantity* of power offered to wholesale markets from each participant, and (b) the manner in which an aggregator *disaggregates a single feeder-scale market dispatch outcome* down to the individual DER level. Despite the difference in characterisation of *flexibility*, our approach in Chapter 6 was directly inspired from literature that studied aggregator flexibility as defined in the previous paragraph. Specifically, our contributions will demonstrate that polytopic projection and homothetic transformations, which appear in the aforementioned literature, are well suited to exploit our characterisation of aggregators' flexibility, helping to ensure that device-level dispatch outcomes can respect distribution network constraints.

3.1.3 Need for Coordination with Networks

While aggregation/disaggregation approaches discussed above ensure feasibility with respect to device-level utilisation constraints, literature mentioned to this point has not factored distribution network constraints when assessing the feasibility of dispatch.

Managing distribution network constraints in scenarios of high DER participation can be performed to some extent using devices such as on-load tap changers [84], [85]. However, with increased electrification and DER uptake, grid investment costs are expected to rise [86], [87], [88], and the need for expensive network upgrades such as widespread rollouts of on-load tap changers can be mitigated effectively through DER coordination strategies.

In order to realise the full potential of DER within the contexts of their constrained distribution networks, this thesis will study how DER, aggregators, distribution system operators, and even system operators at the transmission scale, can coordinate to achieve effective integration of DER into existing networks and market structures, in a manner that enables secure operation of distribution networks.

3.2 DER Coordination Strategies Ensuring Feasible Distribution Network Operation

In this Section, we outline strategies in literature for DSOs to coordinate DER in a manner that enables safe network operation and avoids the activation of protection equipment.

3.2.1 Control-Based Strategies for Distribution Network Management

In this first Subsection, we consider the scenario that the distribution network operator has the capacity to directly elicit active or reactive power from DER, either through tailored droop controller design or by directly instructing dispatch. These control policies are also often studied in the context of microgrid design, in which a distribution network may need to operate in islanded mode [89], [90].

Droop-Based Policies for Microgrid Control

Voltage regulation in micro-grids can be achieved using droop control. We will discuss how this concept can be applied in a naive decentralised way, and may be improved through centralised coordination of droop controllers, or information exchanges between neighbouring agents.

The traditional approach to droop control in AC microgrids is $f - P$ and $V - Q$ droop control [90]. In the case of PQ-inverters, DER regulate AC frequency locally by adjusting their real power output as a linear function of frequency tracking error. Similarly, DER regulate voltage locally by varying reactive power output as a linear function of voltage tracking error. This approach is well-suited to LV networks with mainly resistive lines [91]. Unlike externally-fuelled sources, inverter-based DER providing droop control must regulate their state of charge (SoC). This is commonly achieved in literature through SoC-weighted droop control [92], whereby inverters adjust their droop coefficients according to their state of change. This effectively reduces a DER's contribution to network regulation as their state of charge drifts from its target value. These approaches can be applied in a totally distributed manner, in which case target frequency and voltage values are programmed at the device-scale as constant values and no communication is necessary.

Centralised control architectures can build on the droop-control principle to achieve additional network-wide operational objectives. This can be achieved by adjusting each DER's target values for network state variables, according to a centralised calculation to achieve an operational objective. One example to actively balance state of charge between DER in the network, reducing the maximum depth of discharge of individual batteries and therefore increasing battery life [93]. A centralised control layer has also been proposed to regulate voltage unbalance between phases in microgrids [94].

In addition to centralised approaches, potential limitations on communication bandwidth have inspired distributed multi-agent approaches to achieve cooperation between droop controllers, based on communication graphs that are not complete. This is explored in [95], [96].

Real-Time Coordination of DER Dispatch in Grid-Connected Networks for Safe Network Operation

In grid-connected networks (not an islanded microgrid), frequency at the distribution network scale is coupled to frequency at the transmission-scale. Provision of frequency regulation services is carefully managed by a system operator at the transmission scale, meaning that droop control to provide *real power* is generally not employed by DER. These DER are well suited to provide voltage regulation through droop control modulating *reactive power* dispatch, using available inverter capacity to provide network support at negligible cost to consumers as no energy is exchanged.

In addition to the voltage regulation methods presented above, literature has also studied how distribution network operators may directly control DER dispatch, *including real power*, to help alleviate distribution network congestion. We divide these methods into approaches involving consumer-owned DER, and dedicated network-owned DER such as neighbourhood batteries.

In [97], distribution system operators are assumed to have access to consumers' unused inverter capacity (i.e. beyond the consumers' unrestricted utilisation of their assets), enabling the distribution system operator to dispatch both real and reactive power in order to regulate voltages. This constitutes direct and centralised control of DER, leveraging consumers' existing available assets in real-time. In theory this enables a highly efficient utilisation of DER capacity.

In practice, decisions made by the distribution network operator directing a consumer to increase or decrease net exports may not align with consumers' interests. Implementing such an approach would require a framework for valuing and pricing distribution network support services. We will provide greater discussion around local support markets in Section 3.2.3. The integration of this local market into existing market structures introduces a significant degree of complexity.

An alternative that distribution networks are actively pursuing in Australia is to install network-owned DER battery assets to provide voltage and thermal regulation services. These are commonly termed *neighbourhood batteries*, and optimisation of their dispatch is studied in [98], [99], [100], [101], [102]. In Australia, neighbourhood batteries are generally restricted to only provide non-contestable services, requiring an exemption if they wish to participate in wholesale markets [103].

Comparing these two approaches outlined above:

- Direct control of consumers' DER enables efficient utilisation of existing consumer DER but raises challenges related to role separations, whereas
- Neighbourhood batteries require the commissioning of new DER dedicated to network support, with costs generally borne by consumers, but offer a much simpler framework for operation.

Given the anticipated scale of privately-operated DER capacity to be installed within distribution networks, and given that many distribution networks are already experiencing challenges relating to high DER uptake, there is significant interest in developing approaches for network operators to regulate network voltages and currents in a manner that

1. leverages existing consumer DER, and
2. does not require changes to existing wholesale market frameworks.

3.2.2 Simple Rule-Based Curtailment of Consumer-Owned DER To Ease Network Congestion

An alternative to direct control-based approaches is to strategically curtail DER. We now consider the case where privately-owned DER is curtailed according to simple rule-based curtailment policies in order to alleviate voltage and thermal-related challenges. Existing techniques include queue-based curtailments (e.g. in the UK), and fixed export limits (e.g. in Australia).

Direct Curtailment of DER via Time-Invariant Order of Priority

In distribution networks hosting increasingly large DER capacity, a distribution system operator (DSO) may ensure safe network operation through direct curtailment policies. One such example is National Grid in the UK. In response to risks of network constraint violations, Active Network Management (ANM) programs curtail DER in the reverse order of a customer's connection offer acceptance date [104]. The *Last In First Out* (LIFO) queuing model aims to minimise the impacts of new connections on network access for existing connections. It is important to note this curtailment policy is defined by simple pre-determined control logic [104], ignoring all market interactions between DER prosumers and transmission-scale system operators. As a result, aggregators may be unable to reliably offer flexibility services to wholesale markets due to the risk that an asset contracted to dispatch in the wholesale market may be curtailed within a market trading interval.

Fixed Export Limits in Grid-Connected Distribution Networks

Distribution network service providers in Australia have traditionally pursued fixed import and export limits for all DER [20]. This model provides aggregators greater certainty to offer their flexibility to wholesale markets, however these fixed limits may be overly conservative. In South Australia, new DER connections that do not participate in dynamic operating envelope schemes are restricted to 1.5kW exports. Unlike under ANM, which modulates according changes in distribution network utilisation over time, the fixed limits applied in Australia must be sufficiently conservative as to ensure network constraints remain satisfied under potential extreme operating conditions.

A comparison between these two approaches demonstrates that a trade-off is encountered when there is no coordination between distribution network operators and transmission-scale system operators:

1. ANM: The DSO only curtails DER capacity in real time as network constraint violation risks arise, however the extent of curtailments is unknown to the wholesale market when it procures services in advance, risking the reliability of services offered in the wholesale market.
2. Fixed Export Limits: The DNSP adopts fairly conservative fixed import and export limits, enabling aggregators to reliably offer a reduced portion of their DER capacity to wholesale markets.

Ultimately, distribution network operators are mandated to facilitate DER participation in wholesale markets as much as is practically possible. This is achieved most effectively by conducting DER coordination in a manner that aligns with existing frameworks governing DER participation in wholesale markets. This motivates our review of TSO-DSO coordination frameworks to enable widespread integration of DER.

3.2.3 Foundations of TSO-DSO Coordination

Distribution system operators (DSOs) are responsible for ensuring secure operation of distribution networks, and may seek to restrict network access to DER in order to prevent significant faults. However, as DER provide increasing shares of generation, arbitrage and reserve services, moves to restrict their network access by DSOs will increasingly have consequences for transmission-scale system operators. This motivates our brief survey of literature studying DSO-TSO coordination to facilitate efficient outcomes.

One of the most-studied problems in TSO-DSO coordination is the definition of TSO-DSO flexibility regions [105], [106], [107]. In these studies, a distribution system operator (DSO) seeks to quantify real and reactive power support it can provide to the transmission network. This flexibility is represented by regions plotted in the real-reactive PQ plane. In increasingly decentralised systems, PQ flexibility regions are useful for transmission system operators as they describe what resources the distribution network can technically make available to alleviate system challenges. This provides important knowledge from a system security and operability perspective. These offerings are constrained by the condition that DER dispatch should not risk violations of distribution network constraints.

Derivations of TSO-DSO flexibility regions assume that distribution system operators can directly activate associated DER resources when required. This is often not the case in unbundled power systems. Instead, it is common that aggregators, who have no responsibility for secure operation of the distribution network, participate in wholesale markets that operate at the transmission scale. The variety of communication arrangements that may exist between DER, aggregators, DSOs or DNOs and TSOs has led to works categorising various TSO-DSO coordination frameworks in literature. Our categorisation of frameworks is inspired by two prominent works, [108] and [109]. Our analysis of both works will seek to synthesise both categorisations.

While contributions in this thesis are consistent with the Centralised Ancillary Services market model from [108], we begin our analysis of [108] and [109] by discussing the strengths and weakness of alternative approaches. This provides greater context for our discussion of the strengths of the Centralised Ancillary Services market model. An overview of models presented in [108] is provided in Figure 3.1, and an overview of models presented in [109] is provided in Figure 3.2.

Common TSO-DSO Ancillary Services (AS) Market [108], or TSO-Managed Model [109]

Our first category of approaches is characterised by the clearing of a single market across transmission and distribution networks. DER participate directly in this market without prequalification, and there is no sequential process. It is assumed that the entity clearing the market (either a TSO, or an independent system operator) has visibility over the state and constraints of all distribution networks, assuming the DSO provides this visibility to the market clearer. Assuming bidding behaviour is cost-reflective, this concentration of all market interactions and network constraints should enable market-efficient utilisation of DER.

In practice, markets clearing at the transmission scale generally lack visibility over the state of distribution networks. Even if this visibility were available, the computational complexity of incorporating all network constraints (transmission and distribution) into a single optimisation problem may represent a significant challenge, especially within market trading timeframes. Distributed solving approaches could be applied such as using ADMM. This would introduce iterative communication requirements between distribution system operators and transmission-scale operators in order to converge to

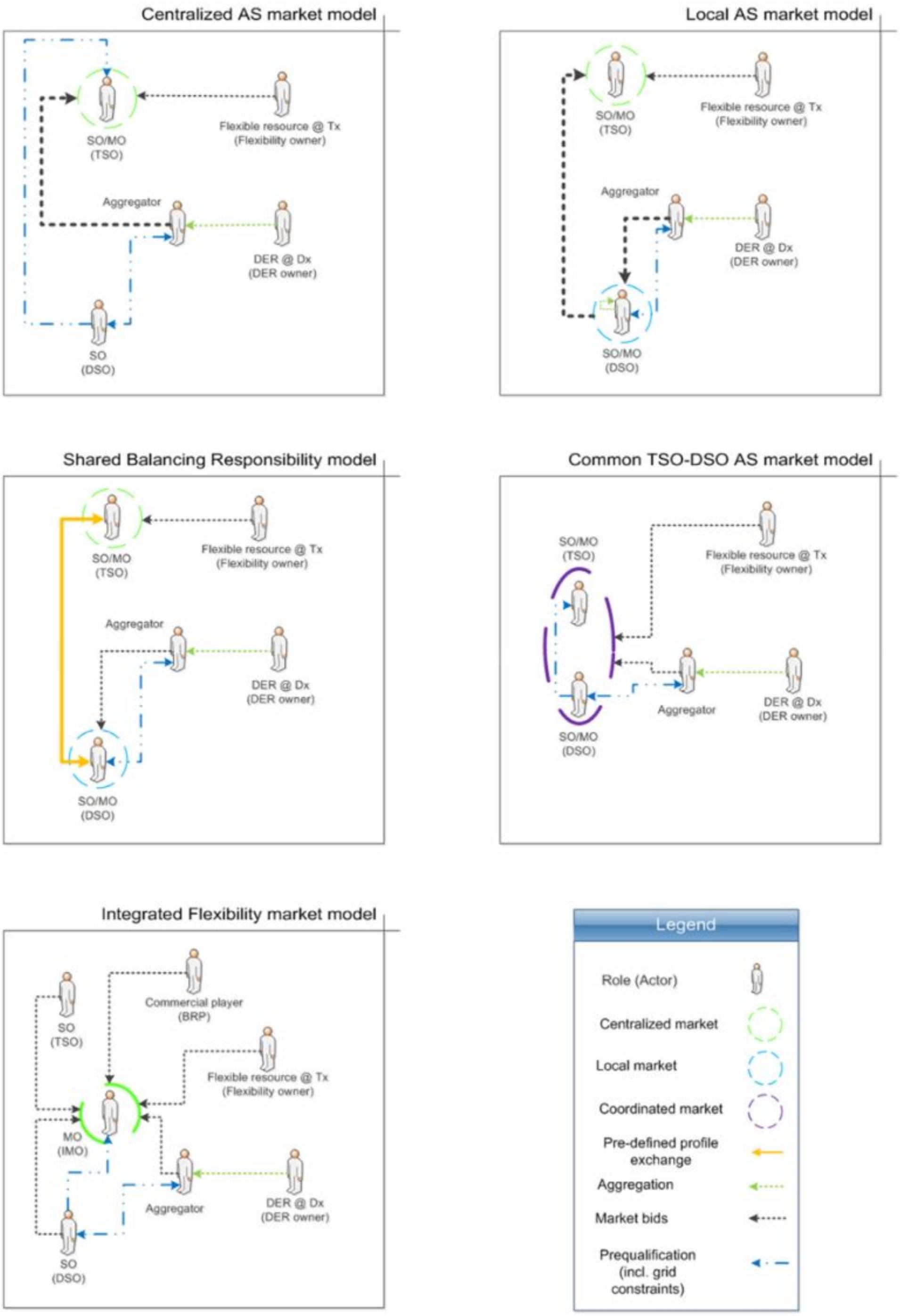

FIGURE 3.1: Categorisation of TSO-DSO coordination frameworks in [108]

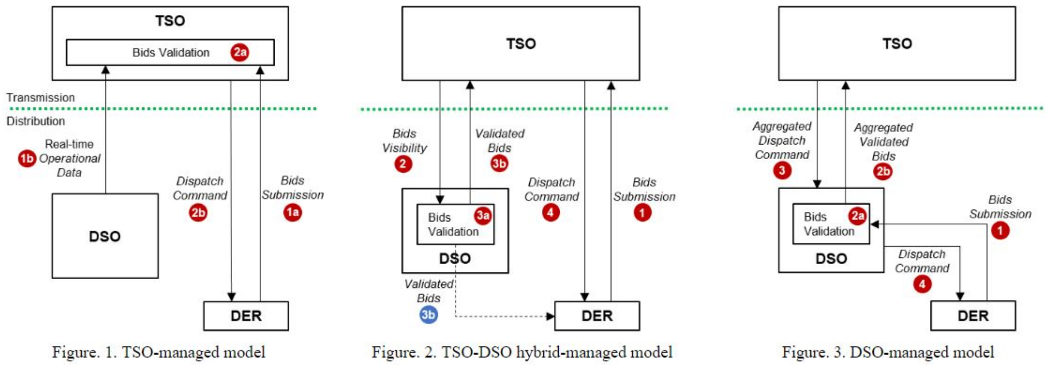

FIGURE 3.2: Categorisation of TSO-DSO coordination frameworks in [109]

economically efficient market clearing results. This distributed and iterative approach does introduce vulnerabilities - compromised communications between any given DSO and the TSO (e.g. communication failure, or nefarious corruption of sent data) can impact the convergence of market clearing with system-wide consequences.

Markets clear on timescales of minutes (each 5 minutes in Australia), and the potential challenges of algorithms requiring iterative communications for convergence may be undesirable in practice.

Local AS Market or Shared Balancing Responsibility Model [108]

Our second category of approaches is defined by the operation of local markets that clear independently of the transmission-scale market. In a sequential manner, secondary markets can then operate on the interface of distribution and transmission networks, either for maintaining energy balance only (Shared Balancing Responsibility Model [108]), or to clear market exchanges between bids that remain after clearing distribution- or transmission-specific markets (Local AS Market Model [108]). The act of initially clearing independent markets at transmission and distribution scales avoids the need to aggregate distribution-scale and transmission-scale network constraints within a single optimisation problem. However, the sequential approach to clearing the market, without any iterative refinement, also has the potential to significantly reduce market efficiency due to price separations between isolated markets.

These first two categorisations of TSO-DSO coordination frameworks represent extreme cases, with (a) fully-centralised handling of information[2], or (b) independent clearing of markets at the distribution scale with subsequent balancing at transmission scale. Many studies aim to strike a balance between the computational feasibility of market clearing and the market efficiency of outcomes. This is generally achieved by continuing to operate a single wholesale market incorporating transmission- and distribution-scale assets, while engaging DSOs through novel approaches to ensure the feasibility of resulting power flows at the distribution scale.

Centralised AS market model [108], TSO-DSO hybrid-managed model and DSO-Managed Model [109]

In our third category of approaches, DER participate in one single market operating at the transmission scale (there is no energy or reserve market operating at the distribution scale), however the DSO plays an integral role to ensure that market interactions of DER do not risk unsafe operation of distribution networks. This occurs through *system prequalification* [108] or *bid validation* [109], whereby the DSO must validate DER bids before they can be cleared in the wholesale market. Variations within this category are defined mainly by varying communications arrangements, and the extent to which a DSO may represent DER in the market. Three variants are proposed between [109] and [108].

Under the TSO-DSO managed model [109] and the DSO-managed model [109], the DSO performs *bid validation* to ensure wholesale market dispatch outcomes respect distribution network constraints. In the first instance, DER submit bids directly to the wholesale market, then the TSO consults the DSO to determine whether some bids must be discarded. In the second instance, DER submit their bids to the DSO for validation, who then represents DER in the wholesale market. In the first case, bid validation can be thought of as a pre-cursor step to market clearing at the TSO-level, whereas in the second case, bid validation is performed by the DSO as a pre-cursor step to bids being submitted to the wholesale market. From an implementation perspective, introducing necessary communications in the short time period between when the wholesale market receives and clears bids may introduce risks that prevent markets clearing in a timely manner. On the other hand, the

[2]In this case, by centralised, we mean that all bid and network constraint data is available to the solving algorithm, even if operators choose to solve the algorith through a distributed technique such as ADMM.

increased influence of DSOs under the DSO-managed model may introduce complications if DSOs are found not to be acting in the best interests of DER and the wholesale market, especially if the influence of DSOs on market bids is not immediately visible to DER prosumers/operators.

The centralised AS market model in [108] proposes an alternative approach to ensuring DER or aggregator bids submitted to wholesale markets do not jeopardise distribution network security. Through a process known as *system prequalification*, DSOs inform DER and aggregators of constraints to their bidding behaviours in advance of a market period. Operators of DER are then permitted to submit any bids complying with these conditions directly to wholesale markets, who can therefore clear bids without consideration of the safety of outcomes from a network perspective. This model has two distinct advantages,

1. aggregators have full visibility over the degree to which their market access may be restricted, and
2. no changes are required to existing bidding protocols between aggregators and wholesale markets, nor to market-clearing processes performed by the TSO.

This thesis focuses on a model for coordination DER that fits within the centralised AS market model.

3.3 Dynamic Operating Envelopes

Managing the issues of over-voltage and over-current associated with high DER uptake through dynamic assessments of hosting capacity has been studied in the literature for some time [110], [111].

Dynamic Operating Envelopes (DOE) have since emerged as the leading approach to ensuring safe integration of DER in Australian distribution networks [112]. Notable trials in industry have included Project EDGE [113], Project Symphony [114], Project Converge [115] and Project Edith [116].

Note that dynamic operating envelopes do not study power system dynamics - the use of the term *dynamic* merely indicates that envelope limits change over time. Operating envelope calculation employs steady state analysis.

3.3.1 Definition of Concept

Dynamic operating envelopes are defined in [20], [21] as time-varying limits applied to DER imports and exports. These traditionally consist of envelopes defined in the PQ plane [117], [118]. The calculation of envelopes aims to ensure that network constraints, such as voltage and thermal constraints, remain satisfied if all DER adhere to their assigned envelopes. The ability to regularly recalculate operating envelopes allows network operators to respond to changes in network utilisation (e.g. reduce exports during peak PV production during the day, reduce imports during periods of peak load in mornings and evenings) [20].

For DER participating in wholesale markets, dynamic operating envelopes are consistent with the Centralised Ancillary Services market model of TSO-DSO coordination in [108]. Operators of DER are required adjust their wholesale market bids to ensure they can satisfy any external wholesale market outcomes while respecting envelopes. It is generally straightforward to apply the necessary adjustments to bids by adjusting the capacity portions of relevant bid stacks, before submitting bids to the wholesale market. Strictly speaking, it is not necessary for there to be coordination between the TSO and the DSO, however in Chapter 4 of this thesis we will demonstrate that such coordination, specifically the TSO communicating expectations of wholesale market conditions to the DSO, can lead to improved outcomes in terms of market efficiency.

The conventional approach to calculating envelopes that ensure safe distribution network operation is to verify that network constraints are satisfied under two extreme operating conditions. These correspond to the scenarios of pre-existing background load plus simultaneous maximum imports across DER, and pre-existing background load plus simultaneous maximum exports across DER.

3.3.2 Simple Rule-Based vs. Optimised Approaches

Allocating constrained distribution network capacity in the form of operating envelopes can be performed using simple rule-based approaches, or through more sophisticated optimisation across DER.

In the simplest case, all DER may be assigned equal operating envelopes, or may be entitled to use equal proportions of their inverter capacity. This effectively reduces the dimensionality of the search space, reducing the problem to determining two scalar values. While this reduces the search space and simplifies the problem, equal allocations of capacity across all connection points may not yield the most desirable outcomes.

For this reason, the most common approach to determining envelope bounds in literature is to solve two optimal power flow (OPF) problems, one for lower limits and one for upper limits [119], [120]. This optimisation problem is defined by sets of power flow constraints, network constraints (e.g. voltage or thermal limits), DER constraints (e.g. max inverter capacity) and the network's choice of objective. Through carefully crafted objectives, or additional constraints, the DSO can tune its optimisation problem to deliver on specific goals from technical and equity perspectives.

In a computational sense, the complexity of envelope calculations is influenced by the choice of power flow model. Linearised power flow models enable OPF problems to be solved by linear solvers, whereas non-linear power flow formulations require non-linear solvers and may converge slower.

3.3.3 Centralised vs. Distributed

Solving OPF problems to calculate upper and lower envelope bounds can be performed centrally (by the DSO) or through distributed approaches. The most common distributed approach discussed in literature is the use of the alternating direction of multipliers method (ADMM) [121], applied to dynamic operating envelope calculation in [122]. The DSO facilitates private iterative bidding by aggregators for constrained capacity, updating locational marginal prices with each iteration. This method is capable of achieving optimal solutions, however the implementation of ADMM in this context can raise challenges in implementation. The coupling of network and aggregator subproblems requires significant amounts of fast communication, and dictates to a large extent how aggregators must represent and solve their sub-problems.

Centralised approaches to calculating operating envelopes by DSOs are much simpler to implement, and these will be the focus of this thesis. While it is true that iterative bid refinement in decentralised approaches allowed the factoring of aggregators' preferences, we will demonstrate in Section 4 how this can also be achieved using centralised approaches if aggregators indicate their upcoming bidding intentions to the DSO.

3.3.4 Choice of Objective

A DSO calculating operating envelopes may seek to maximise the sum of power allocations across connection points, however this does not always lead to the best outcomes in practice. In voltage constrained distribution networks, maximising total capacity will general favour connection points that are close to the substation. This is due to the fact that power exported or consumed at leaf nodes of distribution networks induce gradual voltage rises or falls that span the entire length of the feeder. Power transfers close to the substation may induce similar voltage gradients per unit length of line, however these only span shorter distances.

In order to avoid concentrating all allocated capacity close to the substation, methods to calculate operating envelopes using OPF techniques can choose to factor fairness considerations as constraints, or alternatively, by penalising the l_2 norm of power curtailments [123] across households. This leads to more even distributions of curtailments, as the marginal penalty for curtailments is greater for individuals who are already heavily curtailed. Other objectives studied in literature include cost minimisation, calculated as consumption costs less revenue from generation, and may incorporate tariff information [120]. Trade-offs between the fairness of operating envelopes, and the total capacity that can be allocated across the network, are studied in [124], [125], which considers approaches that use either the optimisation objective or constraints to achieve specific operational goals.

In particular, we note the work of [123] that applied the aforementioned l_2 norm approach to spread the inconvenience of curtailment across nodes of a medium-voltage network, each consisting of several homes, then assign operating envelopes to individual connection points on the basis of the competitiveness of bids between households at the same node. This approach factors prosumers' bid information, which carries the benefit of informing how a household may expect to utilise capacity assigned to it through operating envelopes. This helps to ensure more efficient outcomes, and avoid assigning capacity to households who are unlikely to make use of constrained distribution network capacity. Additionally, this framework incentivises competitive bidding between prosumers. By using bid data destined for the wholesale market, the work of [123] avoids any risk of duplicity between how individuals may bid in a local setting for distribution network access and bid to provide services in the wholesale market. We do however note that allocations at the nodal level ignore this bid information, which caveats the efficiency of allocations overall, as scarce network capacity may be assigned to nodes where households do not intend to make use of the opportunity.

3.3.5 Uncertainty Handling

Numerous uncertainties can influence the efficiency or robustness of dynamic operating envelopes calculated using OPF-based approaches. One major source of uncertainty is the network state, as thermal and voltage constraints are influenced by non-DER demand and generation. In [120], the DSO generates forecasts for generation and demand. It is assumed forecast error follows a Gaussian distribution, enabling the formulation of a chance-constrained optimisation problem. In the event forecast errors do not follow Gaussian distributions, an alternative approach is to regularly perform network state estimation in conjunction with envelope calculation. This has been studied in [124], [126]. Other sources of uncertainty include network characteristics [127].

3.3.6 Alternative Approaches to Operating Envelopes

The dynamic operating envelope concept is similar to the network-wide constraints model proposed in [128]. This framework for safe integration of DER in distribution networks assumes there is a single aggregator, and a common control signal is sent to all DER. In [129] the network-wide constraints and dynamic operating envelope approaches are compared. The primary differences between these formulations lies in the assumptions about the granularity of network data available and the capability to send envelopes to specific nodes.

3.4 Feasibility of Operating Envelopes

3.4.1 Challenges of Using Convex Relaxations in Dynamic Operating Envelope Applications

Operating envelope literature often assumes that envelopes satisfy network constraints if it can be shown that two specific collective DER setpoints satisfy network constraints. These two setpoints correspond to scenarios when (a) all DER maximise their import capacity, and (b) all DER maximise their export capacity.

It is well known that power flow feasibility constraints define a non-convex feasible region [130]. This is because a feasible region defined by a set of constraints containing an equality constraint that is non-linear (e.g. the equality relationship between the square of sending-end power, and the sum of squares of transferred real and reactive power) cannot be a convex region.

Given the distinct computational advantages of using convex optimisation techniques, some studies have calculated dynamic operating envelopes by applying a convex relaxation to the constraint set, namely relaxing the equality constraint to an inequality constraint in order to define a convex feasible region with respect to the convex relaxation. This approach is adopted in [120].

In practice, this has the effect of expanding the feasible set (*with respect to the optimisation problem posed*) to include points that do not satisfy the non-linear power flow equality constraints. This can result in OPF-based methods for calculating DOE to yield envelope bounds that do not satisfy network constraints.

It is true that collective upper and lower envelope bounds can be verified for feasibility by running a simple forward-feed power flow simulation applying the underlying non-convex constraint set. However, it is possible that the 1-dimensional axis between these two collective DER operating points may exit the feasible region of the network, and risk network constraint violations.

3.4.2 Solving in Convex Inner Approximations of Network Feasible Region

The challenges outlined above were mitigated in [131]. Their strategy is to formulate convex inner approximations (CIA) of the feasible region, before then determining two feasible points and constructing operating envelopes. The convex inner approximation was formed by approximating the non-convex terms in power flow equations by a second order Jacobian representation, and bounding the error above and below using convex functions.

This resulted in the calculation of operating envelopes, whose extreme points (maximum import across all nodes, or maximum exports across all nodes) were known to lie within a convex feasible space. This directly implies that any DER operating point that can be represented by a weighted average of these two points - i.e. proportional dispatch of DER as a function of a single scalar in [0, 1] - would be feasible also.

In more intuitive terms, this approach addresses risks that in voltage-constrained networks, scenarios of very high exports may appear to be feasible from a network perspective, but only due to the fact that losses (which increase quadratically with respect to current) become so high that voltage drop from the DER towards the substation is reduced. In these scenarios, it is possible that a reduction in exports causes a disproportionately large decrease in *lost* power, resulting in greater power flow along the feeder and hence a larger voltage rise at the DER connection point compared to the substation.

However, it must be noted that this approach does not strictly guarantee that all points within DER-level operating envelopes defined by these two collective points satisfy network constraints. Because the shape of the network's feasible region for DER is generally *not a hyper-rectangle with edges aligned to the axes of the space.*[3], it follows that operating regions that do take this form, and that comprise both collective maximum import and collective maximum export DER operating points may also contain points that escape the network's feasible operating region. A number of studies have demonstrated that this remains a challenge, particularly in unbalanced three-phase networks, as we discuss below.

3.4.3 Robustness in Unbalanced Three-Phase Distribution Networks

Sensitivity and Robustness of Operating Envelopes in Unbalanced Three-Phase Systems

One notable study was [132], which analysed the conditions in which power flows on a given phase could induce increases or decreases in voltage on adjacent phases. Their method, outlined in Section III of [132], began by stating Ohm's Law in a two-bus system to approximate the change in voltage magnitude on given reference phase (e.g. phase A) as a function of power flows across all phases. Appropriate 120 degree rotational transformations were applied to obtain gradients of this expression with respect to real and

[3]This thesis makes numerous references to orthogonality when describing operating regions assigned to DER within a network, or feasible operating regions for DER with respect to power flow constraints. In a distribution network hosting $n \in \mathbb{N}$ DER assets, we imagine a Cartesian space where each of n basis vectors represents net dispatch of a given DER asset. One point in this n-dimensional space represents a collective DER dispatch setpoint. When we say that a region for collective DER operation is a hyper-rectangle with edges aligned with the axes, this represents the area i which n DER may operate independently subject to individual import and export limits.

reactive components (P, Q) of power flows as defined with respect to each of their reference phases. These derivations resulted in the relationship

$$|V_j^a| - |V_i^a| \approx \frac{r_{aa}P_a + x_{aa}Q_a}{V_a} - \frac{(r_{ab} - \sqrt{3}x_{ab})P_b + (\sqrt{3}r_{ab} + x_{ab})Q_b}{2V_a} - \frac{(r_{ac} + \sqrt{3}x_{ac})P_c + (-\sqrt{3}r_{ac} + x_{ac})Q_c}{2V_a} \tag{3.1}$$

It therefore follows that

$$\frac{\partial|V_j^a|}{\partial P_a} \approx \frac{-r_{aa}}{V_i^a} \qquad \frac{\partial|V_j^a|}{\partial Q_a} \approx \frac{-x_{aa}}{V_i^a} \tag{3.2}$$

$$\frac{\partial|V_j^a|}{\partial P_b} \approx \frac{r_{ab} - \sqrt{3}x_{ab}}{2V_i^a} \qquad \frac{\partial|V_j^a|}{\partial Q_b} \approx \frac{\sqrt{3}r_{ab} + x_{ab}}{2V_i^a} \tag{3.3}$$

$$\frac{\partial|V_j^a|}{\partial P_c} \approx \frac{r_{ac} + \sqrt{3}x_{ac}}{2V_i^a} \qquad \frac{\partial|V_j^a|}{\partial Q_c} \approx \frac{-\sqrt{3}r_{ac} + x_{ac}}{2V_i^a} \tag{3.4}$$

It is common in distribution networks for lines to be mainly resistive. For example, in the 906-bus network, the maximum ratio of imaginary component to real component of off-diagonal entries of impedance matrices is less than $\sqrt{3}$ across all branches. It can therefore be assumed that terms x_{ij} above would not influence the sign of the expression in the context of our studies on the 906-bus network.

We can therefore expect the voltage magnitude on phase A to:

- *decrease* for increasing P_a, Q_a flowing from the parent node on the same phase
- *increase* for increasing P_b, Q_b flowing from the parent node on phase B
- *increase* for increasing P_c but *decrease* for increasing Q_c flowing from the parent node on phase C

It is now clear why operating envelopes calculated by identifying two specific DER operating points will not guarantee feasible voltage magnitudes in unbalanced systems. As an illustrative case study, we can imagine for a moment that DER across all phases maximise their exports, resulting in voltages approaching their allowable upper limits at leaf notes but satisfying network conditions. If DER on one phase then reduce their power exports, this may have the effect of further increasing network voltages on other phases, and therefore causing a voltage constraint violation.

Robust Dynamic Operating Envelopes

In order to account for this phenomena, the authors of [132] have proposed a new method of generating operating envelopes that is robust to the effects of mutual impedances between phases.

Rather than verify network constraint satisfaction at two specific DER operating points, their approach involves deriving the full network feasible region for DER to operate, then defining a hyper-rectangular operating region with edges aligned to the axes of the space, within which DER can operate independently without jeopardising safe operation of the distribution network. In order to represent the network feasible region for DER dispatch, in [133] the authors use a linearised power flow model. The benefit of this choice of power flow model is the ability to express all squared voltage magnitudes as affine functions of DER setpoints through simple matrix manipulation. This means that in voltage-constrained distribution networks, the feasible region takes the shape of a polytope[4].

The work [133] defines network constraints in terms of voltage magnitude and thermal constraints. As maximum and minimum voltage magnitude constraints and thermal constraints are linear with respect to modelled state variables, and these state variables themselves are modelled as linear functions of DER setpoints, network constraints can therefore be expressed as inequality constraints that are linear in DER setpoints. This means that the network feasible region, assuming a linearised power flow model, is defined by a set of hyper-planes in the high-dimensional space representing the setpoints of DER, resulting in a polytopic form.

We note that the work [133] considers voltage magnitude constraints, although voltage unbalance constraints are not considered. In unbalanced distribution

[4]It is important to note that this is a key point of difference with respect to the work of [131]. Under a linearised model, there is no risk that quadratic losses cause unsuitable scenarios of very high exports to appear available for use in calculating operating envelopes. However, linearising power flow equations does of course introduce linearisation error. In Chapters 5 and 6 of this thesis, our proposed methods to calculate operating envelopes adopt linear power flow models as in [133], however all simulations to validate the network feasibility of outcomes are performed by solving the non-convex Distflow model.

In our studies, introducing small safety margins (0.002 p.u.) in voltage constraints had the effect of mitigating all risk of linearisation errors causing network constraint violations. In contrast, the impacts of phase couplings as outlined in the previous subsection risked causing voltage constraint violations which could be an order of magnitude larger.

networks, the level of voltage unbalance must generally be bounded by a measure of the voltage unbalance factor. The work of [134] evaluates the impact of including voltage unbalance constraints when operating envelopes that are calculated according to the general two-point verification approach (validate network safety under maximum imports and maximum exports across all DER), although the work expressly states that envelopes obtained may not satisfy constraints at all collective DER operating points within envelopes due to the impacts of phase couplings and voltage unbalance constraints.

3.4.4 The Need for Contextual Robustness in DOE Solutions

Greater robustness in dynamic operating envelope calculation will generally result in a penalty to the overall capacity that can be allocated to DER. The authors of [135] identify two operational contexts that require different approaches to managing the trade-off between ensuring robustness and increasing capacity:

- In the context of day-ahead forecasted DOEs, a DSO uses forecast data for network loads and distributed generation. These envelopes support planning decisions such as EV charging scheduling, and availability of assigned capacity is important for managing customer expectations. This context calls for a relatively high degree of robustness with respect to forecast network utilisation, as any subsequent reductions in assigned capacity can be detrimental to planning approaches and consumer trust.
- In the context of real-time DOEs, envelope limits are continuously calculated based on near-instantaneous measurements from smart meters or state estimation solutions. When current network state data is available, the associated uncertainty is significantly lower than for a 24-hour forecast. The primary purpose of assigning DOE shifts from guaranteeing minimum capacity for planning purposes, to instead maximising instantaneous utilisation of the network headroom.While the real-time solution must still hedge against measurement noise, communication latency, and potential estimation error, the required safety margin is dramatically smaller, allowing the network to operate closer to its physical limits.

The authors of [135] note that the central design choice for Distribution Network Service Providers (DNSPs) is to determine the acceptable probability of constraint violation, and to apply this value in chance-constrained approaches [5]. This choice directly controls the trade-off between the high capacity (efficiency) offered by less conservative DOEs, and the stringent security (robustness) required to prevent grid constraint violations under uncertainty.

3.5 Open Research Questions

From the literature review outlined above, we identify a number of key opportunities to contribute to the body of knowledge to enable market-efficient and robust integration of DER in unbalanced distribution networks through adaptations to existing dynamic operating envelope calculation methods:

1. While [123] explored the benefits of factoring wholesale bid data when dividing a nodal operating envelope between prosumers co-located a medium-voltage network node, there is potential to utilise bid data in the underlying optimisation objective to devise a more efficient allocation of network capacity that enables the most efficient wholesale market outcomes. We will demonstrate how factoring the value of market services, as well as participant bid data (acting as a proxy for the cost of providing market services) can allow for the calculation of operating envelopes that maximise the value-generating potential for DER collectively in the distribution feeder.

2. While [133] proposed a framework for deriving DOE in the unbalanced three-phase case that ensures voltage magnitude constraints remained respected under any potential envelope utilisation by DER, there remains scope to constrain the level of voltage unbalance between phases through the introduction of new constraints in the optimisation problem. We will explore whether this can be achieved, and whether this rather different type of operational constraint lends itself to the same approach as voltage magnitude constraints.

3. The approach adopted by [133] provides enhanced guarantees for safe network operation in the unbalanced three-phase case. This comes at the expense of reduced network capacity assigned through envelopes.

[5]While these factors represent important consideration for applying robust dynamic operating envelopes in the field, we note that contributions in this thesis consider the hypothetical scenario where loads and PV generation are known exactly. In our studies, the primary source of uncertainty considered in Chapters 5 and 6 is the utilisation of network capacity assigned to other DER, and the impacts of the phasing of other DER within an unbalanced distribution network.

Noting that the conventional approach to calculating dynamic operating envelopes demonstrates there exist safe network operating points outside of the robust envelopes obtained using the framework in [133], but this requires some additional DER communications and control to verify feasibility, can aggregators assist in re-unlocking these potentially quite valuable portions of the network's operating region by adhering to disaggregation guidelines that mitigate, or eliminate, risks of unfavourable levels of unbalance in DER dispatch between phases? The results of Chapter 5 will also provide enhanced motivation to study this question.

These three questions are addressed in Chapters 4, 5 and 6 of this thesis.

Chapter 4

Market-Efficient Operating Envelopes through TSO-DSO Coordination

This first contribution chapter addresses an open challenge relating to how operating envelopes are allocated, particularly in the context of voltage-constrained radial distribution networks.

4.1 Introduction

It has been well established in literature that the allocation of available distribution network capacity between DER is not a zero-sum game, due to location-dependency of a DER's impact on network voltages based on its location in the feeder. While existing approaches to calculating dynamic operating envelopes may choose to maximise either the total sum of capacity allocated through envelopes, or minimise some metric of curtailed capacity inspired by fairness (e.g. l_2 norm), or even constrain outcomes according to fairness criteria through additional constraints, in this Chapter we explore a new objective. We seek to maximise the potential for DER to generate value in the wholesale market, factoring revenue opportunities influenced by wholesale market prices and costs for providing market services captured in cost-reflective bid data.[1]

[1] As this Chapter carries particular focus on the efficiency of allocations of available network capacity, we apply the same network feasibility criteria as is observed in most literature on dynamic operating envelopes, i.e. ensuring network limits are respected under maximum load and maximum export scenarios. Later Chapters of this thesis will explore feasibility in unbalanced three-phase networks in more detail.

In order to achieve efficiency in a market sense, one significant source of novelty in our approach with respect to the literature is that we adopt an additional form of TSO-DSO coordination. In our approach, the DSO factors expectations of wholesale market prices, communicated by the TSO, while optimising operating envelopes to be assigned to market-participating DER. In the context of the Australian NEM, AEMO publishes this information in the form of pre-dispatch prices. Assuming that aggregators have optimised their bidding practices to reflect costs or expected opportunity costs[2], the combination of (a) bid data and (b) projected market value of services can be used to estimate the potential for DER to create value through wholesale market participation.

In our framework, the DSO maximises an objective that (a) sums the total market value of energy or services provided by DER that are expected to clear the wholesale market, while (b) subtracting the costs borne by DER providing these services (including future opportunity costs) reflected in their bid prices. The DSO therefore adopts an objective that maximises the *expected benefit* gained by aggregators from participating in the market. Due to uncertainty of wholesale market prices in the upcoming trading interval, we adopt a scenario-based stochastic program that uses probability distribution data for future market prices.

Compared to applying a central control (i.e. where the DSO directly controls DER dispatch) or distribution locational marginal pricing (DLMP)-based approach to maximise this objective, our approach based on centralised calculation of operating envelopes by the DSO provides the following advantages:

1. Clear role separation between aggregators, DSO and market operators, and the ability to work with existing wholesale market structures. Aggre-

[2] When assuming that bidding practices are cost-reflective, we are primarily referring to opportunity costs associated to a spread of potential future market prices, given that batteries only carry limited state of charge. This is what currently drives bidding practices for utility-scale storage in Australia. Real bidding data from utility scale storage assets demonstrates this cost-reflective bidding approach leads to capacity being spread across a range of price bands, and we apply these real bids in our simulations. We note that devising a similar price-reflective bidding strategy by aggregators in distribution networks may incur additional complexity due to the different setting (e.g. different network tariffs), which may complicate the generation of cost-reflective bids. The main goal in this Chapter is to demonstrate advantages of modulating capacity allocations as a function of wholesale market opportunities, and detailed analysis of what constitutes cost-reflective bidding at the distribution scale is out of scope for this contribution. It is possible that some aggregators may seek to deviate from cost-reflective bidding practices and engage in deceptive bidding practices to gain increased capacity in the network, and this may lead to market inefficiencies. We are not seeking to quantify these potential market inefficiencies under game-theoretic outcomes.

gators have the freedom to develop bids like conventional participants.

2. Greatly simplified constrained optimisation problem compared to distributed optimisation approaches, which avoids iteration back and forth between the DSO and aggregators.

Fairness-based objectives have been employed in [136] and [123], in which operating envelopes are determined at the medium voltage nodal level to minimise the l_2-norm of power curtailments. This achieves a greater spread across nodes than under an l_1-norm, producing a 'fairer' outcome [136]. However, we argue that the primary objective should be maximising the net social welfare across the feeder because the DSO can determine transfers correcting for perceived inequalities when social welfare is maximised[3]. Such redistributions would enable our proposed approach to achieve a desired level of fairness in terms of financial outcomes for households, while momentarily benefiting from more efficient envelope assignments to advantageous locations in the network when this significantly advantages overall DER market outcomes for the feeder.

The approach in [123] improved the social welfare outcome and drove competition among aggregators on a node-by-node basis by applying curtailments to the least competitive bids first. However, this was done in a relatively ad-hoc manner as a second step after nodal curtailments were determined. It does not consider relative competitiveness across nodes in a principled way, nor does it factor the likelihood of different market outcomes and different market values. This misses key opportunities to improve efficiency that smarter allocations of the scarce distribution network capacity can achieve.

To improve the market outcomes, in this chapter, we obtain curtailments by directly factoring in market and bid prices to an optimisation that maximises expected aggregator benefit. This corresponds to maximising social welfare when there is sufficient aggregator competition and their bids are cost-reflective. This bid-shaping process occurs prior to the market clearing, so we formulate our problem as a stochastic program in order to optimise the allocation of curtailment according to likely market outcomes. Moreover, we expand network throughput capacity through real and reactive power co-optimisation.

[3]Specifically, for any fairness-inspired method to assign operating envelopes, there exists a way to increase (or hold constant) every household's benefit gained through market participation by instead applying our approach that maximises social welfare overall, and then performing a redistribution of benefits to ensure no one is worse off than under a given fairness metric.

A benefit of this more principled representation of market value is our ability to consider additional market services, expanding on [123] to include frequency regulation on top of energy and contingency services. This increases the number of simultaneously-dispatchable markets from two to three. In this expanded setting, we move away from the restrictive two-dimensional *trapezium* representation of cross-market dispatch constraints used by the Australian National Energy Market (NEM). Instead, we propose a general representation of feasible dispatch using linear inequality constraints, facilitating application across a wider range of markets.

To summarise, our key contributions are:

- A variation of the nodal operating envelopes concept, that allocates capacity to aggregators based on the market value and bid value of services offered. We demonstrate this can achieve an 8% improvement to the market outcome compared to alternative operating envelope approaches that capture this value using heuristics. Importantly, we do not introduce prohibitive complexity into DSO calculations or aggregator bidding decisions.
- A stochastic programming extension which further increases benefit relative to alternatives. This brings the performance to within less than 1% of what the hypothetical perfect information case obtains in our simulations

4.2 Price-Deterministic Shaping

This section develops an approach to shaping aggregator bids using a confident prediction of market price values $\rho \in \mathbb{R}^{N^m}$, where $N^m \in \mathbb{N}$ is the total number of markets operating concurrently[4]. We call this approach *price-deterministic* in the sense it optimises benefit assuming zero uncertainty in market price. Curtailment results are network-secure for any potential market

[4] As a notation guide,

- Bold font is applied to vectors and matrices only. Scalar entries of vectors/matrices are not bolded, but sub-matrices and sub-vectors remain bolded.
- Matrices and vectors: subscripts are used for indexing entries or sub-matrices, and superscripts are used for labelling variables.
- All other mathematical entities (scalars, functions, sets): subscripts and superscripts are used for labelling. In these cases superscripts help to convey physical meaning, and subscripts identify the instance (often indexed) of node or bid characterised by the variable.

price outcomes, even if the price forecasts are inaccurate.

4.2.1 Problem Setting

Our approach begins with aggregators submitting provisional bids to the DSO, on a node-by-node basis, in advance of the upcoming market trading period. In the context of $N^a \in \mathbb{N}$ aggregators operating in a network of $N^i \in \mathbb{N}$ nodes, there are $N^n \leq N^a \times N^i$ bids submitted to the DSO. These N^n bids can be sorted into N^i subsets, labelled B_i for $i \leq N^i$, containing the indices n of all market bids b_n at node i across all aggregators.

Let tuples $b_n := (\boldsymbol{\pi}^n, \boldsymbol{\chi}^n, c_n^\tau)$ represent aggregator bids. These contain bid price and capacity data in matrices $\boldsymbol{\pi}^n, \boldsymbol{\chi}^n \in \mathbb{R}^{N^b \times N^m}$ respectively, where $N^b \in \mathbb{N}$ is the number of per-market price bands. Let $\boldsymbol{\rho} \in \mathbb{R}^{N^m}$ be the vector of predicted market-clearing prices in each market. Let $\boldsymbol{\mathcal{P}} \in \mathbb{R}^{N^m \times N^n}$ be the matrix of market-cleared dispatch outcomes in each market for each bid. It follows that column vectors $\boldsymbol{\mathcal{P}}_{:,n} \in \mathbb{R}^{N^m}$ represent market-cleared dispatch outcomes across markets for a given bid, and these must satisfy

$$\boldsymbol{\mathcal{P}}_{m,n} \leq \sum_{b=1}^{N^b} \chi_{b,m}^n \tag{4.1}$$

i.e. market-cleared power in a given market is bounded above by the sum of capacities bid across price bands in that market.

Each bid tuple also contains a cross-market dispatch constraint function c_n^τ. This constraint allows aggregators to bid their full capacity into energy, regulation and contingency markets individually without risking market dispatch across all simultaneously, which may be infeasible from the aggregator's perspective. Specifically, $c_n^\tau : \mathbb{R}^{N^m} \to \mathbb{R}^{N^l}$ is a vector-valued affine function that defines the bid's feasible dispatch region, a convex polytope in $\mathbb{R}^{N^m}$. Within the context of the Australian NEM, this takes on the form of the *trapezium regions* that link energy and reserve markets. Dispatch is feasible from the aggregator's perspective for a bid n if and only if

$$c_n^\tau(\boldsymbol{\mathcal{P}}_{:,n}) \leq \mathbf{0} \tag{4.2}$$

4.2.2 Objective Maximising Aggregator Benefit

We define benefit to aggregators as the difference between the market value of traded services and the costs to aggregators of providing those services[5]. We assume that bid prices reflect expected costs to aggregators of delivering capacity. In our objective function, we partition the set of all market indices $M = \{1, \dots, N^m\}$ according to whether aggregators pay or are paid market clearing prices in the associated market. This distinguishes the energy load market, indexed by $m^- \in M$, from the energy generation market and all reserve markets, indexed by values in the set $M^+ = M \backslash \{m^-\}$.

For a single aggregator, at a single node (i.e. a single bid), benefit gained in one trading period is equal to

$$f_n(\boldsymbol{\mathcal{P}}_{:,n}, \boldsymbol{\rho}, b_n) = \Big(\sum_{m \in M^+} \big(\rho_m l \mathcal{P}_{m,n} - \Pi_n^m(\mathcal{P}_{m,n})\big) - \frac{\rho_{m^-}}{l} \mathcal{P}_{m^-,n} + \Pi_n^{m^-}(\mathcal{P}_{m^-,n}) \Big) \times \Delta t \tag{4.3}$$

where

- $\rho_m \in \mathbb{R}$, the m^{th} entry of vector $\boldsymbol{\rho} \in \mathbb{R}^{N^m}$, is the market-clearing price in market m.
- $\Pi_n^m : \mathbb{R} \to \mathbb{R}$ calculates the cost to the aggregator of providing capacity $\mathcal{P}_{m,n}$ in market m according to bid price and capacity data in b_n. It is convex and piece-wise linear with gradients equal to entries of column-vector $\boldsymbol{\pi}^n_{:,m} \in \mathbb{R}^{N^b}$ (the prices in each bid band) as we assume bid prices reflect aggregator costs.
- $l \in \mathbb{R}^+$ is a unitless loss term.
- $\Delta t \in \mathbb{R}$, factored for readability, serves to convert power values to energy values over trading periods.

The loss term l accounts for a DSO's chosen method to allocate the economic costs of line losses, which we leave arbitrary in this general framework. Its derivation can reflect goals including fairness or total loss minimisation. To avoid bilinearity in the objective, the value of l is pre-processed assuming an expected network operating point[6].

[5]This is consistent with producer and consumer surplus in microeconomics.

[6]Note that network feasibility is later verified using a power flow model accurately accounting for losses; l only serves to capture cost distribution in curtailment.

The overall objective is to maximise the sum of aggregator benefit. We can now define an optimisation problem for an ideal, *unconstrained network* case

$$\begin{aligned} \max \quad & \sum_{n=1}^{N^n} f_n(\boldsymbol{\mathcal{P}}_{:,n}, \boldsymbol{\rho}, b_n) \\ \text{s.t.} \quad & (4.1), (4.2) \quad \forall n \leq N^n \end{aligned} \tag{4.4}$$

We will next build on this model to account for network constraints by *shaping* the provisional aggregator bids prior to their submission to the market operator.

4.2.3 Operating Envelope Constraints at Bid and Nodal Levels

We now introduce additional cross-market dispatch constraints on $\boldsymbol{\mathcal{P}}_{:,n}$ in order to restrict bid-level power exchange with the network to be within network-feasible operating envelopes, irrespective of how regulation or contingency services may be activated across the feeder.

When considering possible power transfers, markets interact with each other in non-uniform ways. For example, in the Australian NEM, only one contingency response will be active at a time per participant. However, regulation and contingency response could occur simultaneously, meaning they are additive when considering possible power transfer. All of these reserve responses are additionally relative to an underlying energy market dispatch.

To account for this, we re-partition the set of market indices M from Subsection 4.2.2 according to a new criteria. Let $M^G \subseteq M$ represent the set of markets resulting in power export from the aggregator perspective (generation and raise reserves), and let $M^L \subseteq M$ represent the set of markets resulting in power import (load and lower reserves). We now introduce two sets, $\underline{\Psi} \subseteq 2^{M^L}$ and $\overline{\Psi} \subseteq 2^{M^G}$, containing market combinations that can simultaneously provide response, one for aggregator power import and one for export.

Let variables $\underline{p^\beta}_n, \overline{p^\beta}_n \in \mathbb{R}$, entries of vectors $\underline{\boldsymbol{p^\beta}}, \overline{\boldsymbol{p^\beta}} \in \mathbb{R}^{N^n}$, represent bid-level lower and upper bounds for network-feasible power exchange. These are the key decision variables in our optimisation problem. We restrict power exchange at the bid level to envelopes (intervals) $[\underline{p^\beta}_n, \overline{p^\beta}_n]$ by defining the following constraints for each bid n

$$\sum_{m \in \psi} -\boldsymbol{\mathcal{P}}_{m,n} \geq \underline{p^\beta}_n \qquad \forall \psi \in \underline{\Psi} \tag{4.5}$$

$$\sum_{m \in \psi} \mathcal{P}_{m,n} \leq \overline{p^\beta}_n \qquad \forall \psi \in \overline{\Psi} \tag{4.6}$$

We introduce vectors $\underline{\boldsymbol{p}}, \overline{\boldsymbol{p}} \in \mathbb{R}^{N^i}$ with entries $\underline{p}_i, \overline{p}_i \in \mathbb{R}$ representing nodal-level lower and upper bounds for power exchange. The tightest bounds at a nodal level are obtained through the Minkowski sum, or dilation, of intervals at the bid level. In our framework, we have $0 \in [\underline{p^\beta}_n, \overline{p^\beta}_n]$ by definition. It follows that

$$\underline{p}_i = \sum_{n \in B_i} \underline{p^\beta}_n \tag{4.7}$$

$$\overline{p}_i = \sum_{n \in B_i} \overline{p^\beta}_n \tag{4.8}$$

By directly relating bid-level envelopes to nodal envelopes, (4.7) and (4.8) allow the definition of network feasibility criteria for bid-level envelopes $[\underline{p^\beta}_n, \overline{p^\beta}_n]$.

4.2.4 Network Feasibility Constraints & Reactive Power Co-optimisation

We begin by stating network feasibility criteria for real-power nodal envelopes, and explore the expansion of network capacity through co-optimisation of real and reactive power. We use the DistFlow model for single-phase-equivalent radial distribution networks [40]. Let $p_i, q_i \in \mathbb{R}$, entries of vectors $\boldsymbol{p}, \boldsymbol{q} \in \mathbb{R}^{N^i}$, be the net real and reactive power exchanged at node i across all aggregators. The DistFlow model states that for all nodes $i \leq N^i$ we have

$$P_i - r_i I_i + p_i = \sum_{j \in D_i} P_j \tag{4.9a}$$

$$Q_i - x_i I_i + q_i = \sum_{j \in D_i} Q_j \tag{4.9b}$$

$$V_k - 2(r_i P_i + x_i Q_i) + (r_i^2 + x_i^2) I_i = V_i \tag{4.9c}$$

$$P_i^2 + Q_i^2 = V_j I_i \tag{4.9d}$$

where D_i is the set of i's child nodes; P_i, Q_i and I_i are the real, reactive power and squared current magnitude entering node i from its parent node; r_i and x_i are the resistance and reactance of the branch linking node i to its parent node, and finally V_i is the squared voltage magnitude at node i. The DistFlow model is presented in more detail in [40]. We also constrain squared voltage at each bus by

$$\underline{V_i} \leq V_i \leq \overline{V_i} \tag{4.10}$$

and current along each branch by

$$I_i \leq \overline{I_i} \tag{4.11}$$

to remain within network-feasible bounds $\underline{V}_i, \overline{V}_i, \overline{I}_i \in \mathbb{R}$.

Network-security of operating envelopes $[\underline{p_i}, \overline{p_i}]$ across all nodes i is determined by whether power flow constraints (4.9) and operational constraints (4.10)-(4.11) are collectively feasible at both extreme operating points $\underline{\boldsymbol{p}}$ and $\overline{\boldsymbol{p}}$, each with some jointly-feasible reactive power $\boldsymbol{q}$. In other words, we verify network security in the cases of maximum and minimum net bus injections across all nodes[7].

We now briefly consider real-reactive power co-optimisation. Real and reactive power output at the resource level are typically constrained by a quadratic relationship of the form $p^2 + q^2 \leq \bar{s}^2$. Full real-reactive co-optimisation in our problem, down to the resource level, is incompatible with our chosen framework, in which aggregators provide the DSO with bid data aggregated to medium voltage nodes (i.e., aggregating DER bids across each LV feeder and assigning the aggregate to the high side of the MV/LV transformer). Chapters 5 and 6 model low-voltage distribution constraints in greater detail.

Instead, at the bid level, we approximate this quadratic relationship by defining 4 linear constraints such that

$$|p_n^\beta| + |q_n^\beta| \leq \bar{s}_n^\beta \tag{4.12}$$

[7]Care is needed when calculating operating envelopes using the DistFlow power flow model by evaluating two extreme conditions, namely all DER maximising their exports and all DER maximising their imports. This is due to the fact the feasible region for a network is a non-convex space, due to the non-linear equality constraint (4.9d). As a result, there is potential for the presence of DER operating points that satisfy operating envelope bounds that do not lie within the feasible operating region of the network. This is explained in more detail in Chapter 3.4.1. We note that no voltage or thermal constraint violations were encountered when applying the non-convex DistFlow model to simulation results in Figure 4.2, due to the network operating away from regions of very high voltage rise (where the challenges outlined above are most likely to materialise). Chapters 5 and 6 adopt a different power flow model in derivations of operating envelopes and regions.

for aggregate inverter capacity $\overline{s}_n^{\beta} \in \mathbb{R}$ for bid b_n. Although this conservative approximation of reactive support capacity forgoes some optimality, it provides a lower-bound scalar estimate of the sum of available reactive power capacity from an aggregator's DER fleet connecting to a given MV node, or downstream of an MV/LV transformer at that node.

Expansion of network-feasible real-power envelopes with reactive power co-optimisation requires different reactive responses during periods of peak generation or peak load. The DSO could enforce a functional relationship between real and reactive power exchanges of aggregator-controlled assets. We do not attempt to derive such relationships in this thesis.

4.2.5 Summary of Approach for Forecast Prices

Our approach in the price-deterministic setting is comprehensively defined by

$$\begin{aligned} \max \quad & \sum_{n=1}^{N^n} f_n(\boldsymbol{\mathcal{P}}_{:,n}, \boldsymbol{\rho}, b_n) && (4.13)\\ \text{s.t.} \quad & (4.1), (4.2), (4.5), (4.6), (4.12) && \forall n \leq N^n \\ & (4.7), (4.8), (4.9), (4.10), (4.11) && \forall i \leq N^i \end{aligned}$$

We now provide a high-level overview of the interactions between components of our optimisation.

- The objective in (6.19), for f_n defined in (4.3), represents benefit to aggregators as a function of their bids and predicted market prices.
- Market dispatch outcomes represented by $\boldsymbol{\mathcal{P}}$ in the objective are constrained by bid capacities (4.1) and cross-market dispatch constraint functions c_n^{τ} in (4.2), both contained in provisional bids.
- We introduce additional constraints (4.5), (4.6) applied to $\boldsymbol{\mathcal{P}}$. These constraints are parametrised by bid-level operating envelope bounds $\underline{p^{\beta}}_n, \overline{p^{\beta}}_n$. Their effect is to *shape* or *trim* bid-level feasible regions defined by constraints c_n^{τ} in order to ensure network feasibility of market dispatch outcomes maximising aggregator benefit.
- We ensure network feasibility of bounds $\underline{p^{\beta}}_n, \overline{p^{\beta}}_n$ by relating bid-level envelopes to nodal envelopes in (4.7), (4.8), and applying power flow constraints (4.9) and operational constraints (4.10), (4.11) to both extreme

operating points of the network, specifically $\underline{\boldsymbol{p}}$ and $\overline{\boldsymbol{p}}$.

- Under the influence of the objective, the values of $\underline{p^{\beta}}_{n}$, $\overline{p^{\beta}}_{n}$ in the solution of (6.19) will maximise aggregator benefit.
- Aggregators are informed of their curtailed dispatch regions defined by the combination of constraints (4.2), (4.5), (4.6). They may submit curtailed bids $b_n^{\kappa} = (\boldsymbol{\pi}^n, \boldsymbol{\chi}^n, c_n^{\kappa})$ to the market where

$$c_n^{\kappa}(\boldsymbol{\mathcal{P}}_{:,n}) \leq \mathbf{0} \implies (4.2), (4.5), (4.6) \tag{4.14}$$

  Aggregators would not strictly be required to reduce capacities bid into various bands. This is because new constraint functions c_n^{κ} satisfying (4.14) effectively cap dispatchable capacities to within curtailed envelopes.

This concludes the derivation of our framework in the case of a single price forecast. We note that prices are an influential parameter in the objective, and in Section 4.3 we present an extension to our framework which accounts for estimates of price uncertainty.

4.3 Stochastic Shaping with Price Uncertainty

This section presents a stochastic programming extension of our approach to account for price uncertainty. We motivate this extension by studying the potential impacts of inaccurate price forecasts on benefit using the approach in Section 4.2.

4.3.1 Motivating Case Studies

We consider the extreme scenario in which the projected energy market price $\rho_E \to \infty$. It follows that projected returns from generation are much larger than supply costs for all N^n bids across the network, i.e. $\rho_E \mathcal{P}_{G,n} \gg \Pi_n^G(\mathcal{P}_{G,n})$ for all $n \leq N^n$ where G indicates the energy generation market. This results in all generation capacity becoming approximately equally beneficial to aggregators. In this context, our framework will naturally seek to maximise network throughput without regard to bid prices. Due to restrictive voltage constraints in radial distribution networks, our proposed approach will naturally prioritise market access to nodes close to the transmission network, and consequently constrain market access at far leaf nodes. If this price prediction is inaccurate, and the energy price falls within its usual range, many competitive bids at leaf nodes will be curtailed inefficiently.

This example demonstrates that our framework's flexibility to adapt to changing prices risks becoming a weakness if price assumptions are inaccurate. We mitigate this risk by proposing a price-probabilistic extension to our framework.

4.3.2 Two-Stage Stochastic Programming Formulation

Our stochastic approach is a two-stage stochastic program. Bid operating envelope bounds $\underline{p^{\beta}}_n, \overline{p^{\beta}}_n$ are first-stage decision variables optimised under price uncertainty. Expectations of market outcomes are second-stage decisions, maximising aggregator benefit, constrained by shaped cross-market dispatch constraints c_n^{κ} satisfying envelopes $[\underline{p^{\beta}}_n, \overline{p^{\beta}}_n]$, and made in accordance with realised market prices.

We consider the case of $N^s \in \mathbb{N}$ discrete possible scenarios for market prices, each with probability $\mu_s \in \mathbb{R}$ stored in vector $\boldsymbol{\mu} \in \mathbb{R}^{N^s}$. It follows that $\sum_{s=1}^{N^s} \mu_s = 1$. We construct the matrix $\boldsymbol{\rho} \in \mathbb{R}^{N^m \times N^s}$ consisting of the anticipated prices for each market in each scenario, i.e. $\rho_{m,s}$ is the price in market $m \leq N^m$ in scenario $s \leq N^s$. The deterministic equivalent program of our two-stage stochastic program is given by

$$
\begin{aligned}
\max \quad & \sum_{s=1}^{N_s} \mu_s \sum_{n=1}^{N_n} f_n(\boldsymbol{\mathcal{P}}^s_{:,n}, \boldsymbol{\rho}_{:,s}, b_n) && (4.15)\\
\text{s.t.} \quad & (4.1), (4.2), (4.5), (4.6) && \forall s \leq N^s,\ \forall n \leq N^n\\
& (4.7), (4.8), (4.9), (4.10), (4.11) && \forall i \leq N^i
\end{aligned}
$$

This stochastic approach models different outcomes for market-cleared power $\boldsymbol{\mathcal{P}}^s$ for each price scenario $s \leq N^s$. Each instance of $\boldsymbol{\mathcal{P}}^s$ across all N^s scenarios must satisfy the same curtailed cross-market dispatch constraints, i.e. (4.2) and (4.5)-(4.6). It follows that only two network operating points, $\underline{\boldsymbol{p}}$ and $\overline{\boldsymbol{p}}$, need to be verified for network security for any number of scenarios N^s.

Scenario generation in stochastic programming is commonly performed using Monte Carlo sampling from continuous probability distributions. Although this is efficient in the context of linear problems, our power flow model is non-linear and we seek solutions over short time periods. Our framework therefore requires the DSO to generate a considered selection of scenarios. In Subsection 4.4.1 we briefly discuss our chosen approach in the context of the Australian NEM.

This completes the derivation of our stochastic approach to shaping aggregator bids for maximum expected benefit.

4.4 Simulations

In this section we demonstrate the advantages of our benefit-maximisation framework over methods in existing literature through simulations on a standard test network. Data for market prices and forecasts, customer bids and inflexible load/PV are sourced from real datasets. We demonstrate increases in aggregator benefit available through real-reactive power co-optimisation. We present our approach to price scenario generation in the Australian NEM context allowing our stochastic implementation to achieve increased benefit for aggregators.

4.4.1 Implementation Details

Setup and Data

We use the IEEE 69-bus medium-voltage (12.66 kV) network in its standard single-phase-equivalent radial configuration. Voltages are constrained to be within 0.95 p.u. and 1.05 p.u., and currents are also constrained. Branch data is available in [137].

A total of 1,910 customers populate the network, distributed proportionally to the real-power load configuration studied in [137]. We model significant uptake of DER with 50% prosumers operating 5kW or 10kW inverters (40% and 10% respectively)[8]. All customer inflexible load and prosumer PV generation are sampled from a dataset of 30 households over 5 days obtained during a trial in Tasmania, Australia [138].

Aggregators bid according to historical data from the Hornsdale Power Reserve (HPR), Lake Bonney Battery (LBB) and Ballarat Battery (BAL) grid-

[8]Our generous modelling of DER uptake compensates for our use of a medium-voltage network, requiring greater throughput to incur constraint violations than low-voltage equivalents. Our formulation in this paper is suitable for single-phase-equivalent networks. We plan to extend to unbalanced three-phase networks in future work, where increased computational challenges may require modifications to our stochastic approach.

scale batteries as of 12 March 2021[9]. Capacities and trapeziums (bid feasible dispatch regions) are scaled proportionally to summed aggregator inverter capacity at each node[10]. As a result, we do not model battery state of charge. We use contemporary market price and forecast data from the South Australia 1 region of the NEM. The market clears every 5 minutes, and we use forecast data spanning a half-hour window, updated every 30 minutes. We choose 12 March 2021 as this date presents a wide range of market events. This includes a phase of usual price stability (before 17:00) and significant price volatility (after 17:00), which we analyse separately.

Loss Factor Approach

Our simulations assume the DSO distributes the economic costs of line losses proportionally to total aggregator exchange in the energy market. Market clearing prices reflect power value at the feeder top. Let L, G and X represent projected network-wide total load, generation and net import from the transmission network. We determine l by solving the quadratic relation $Gl + \frac{L}{l} + X = 0$. We pre-process the value of l using modelled network-feasible L, G, X on the basis of expected market prices. This requires a precursor iteration of shaping initially using $l = 1$.

Scenario Generation

We generate scenarios for energy prices using data published by AEMO every half hour, and use forecast reserve market prices across all scenarios. To obtain energy prices, we multiply through 1) pre-dispatch price forecasts, 2) NEM pre-dispatch price sensitivity with respect to changes in demand across regions, and 3) probabilistic forecasts of demand across regions. We condense the total number of scenarios obtained through this method to 8, tailored to capture central tendency and potential extreme events. We add market cap

[9]The purpose of this chapter is to highlight that the chosen objective for allocating constrained network capacity can significantly impact the potential for overall value creation by DER on a voltage-constrained radial distribution network. Studies of exactly how aggregators determine optimal bidding strategies, and studies of how aggregators may engage in bidding practices that depart from cost-reflective bidding, lie outside our intended scope for this chapter.

[10]We do not assume the aggregator has access to grid models. Our selected case study models hypothetical aggregators participating in the Australian National Electricity Market (NEM), in which one market participant (e.g. an aggregator) is only able to bid 10 distinct price and volume bands, meaning that per-node pricing cannot effectively scale. We have modelled aggregators with the same price bands across all assets in their fleet, with capacities in each bid band determined proportionally to the sum of DER inverter capacity at the node, to mimic cost-reflective bidding strategies observed historically by utility-scale storage.

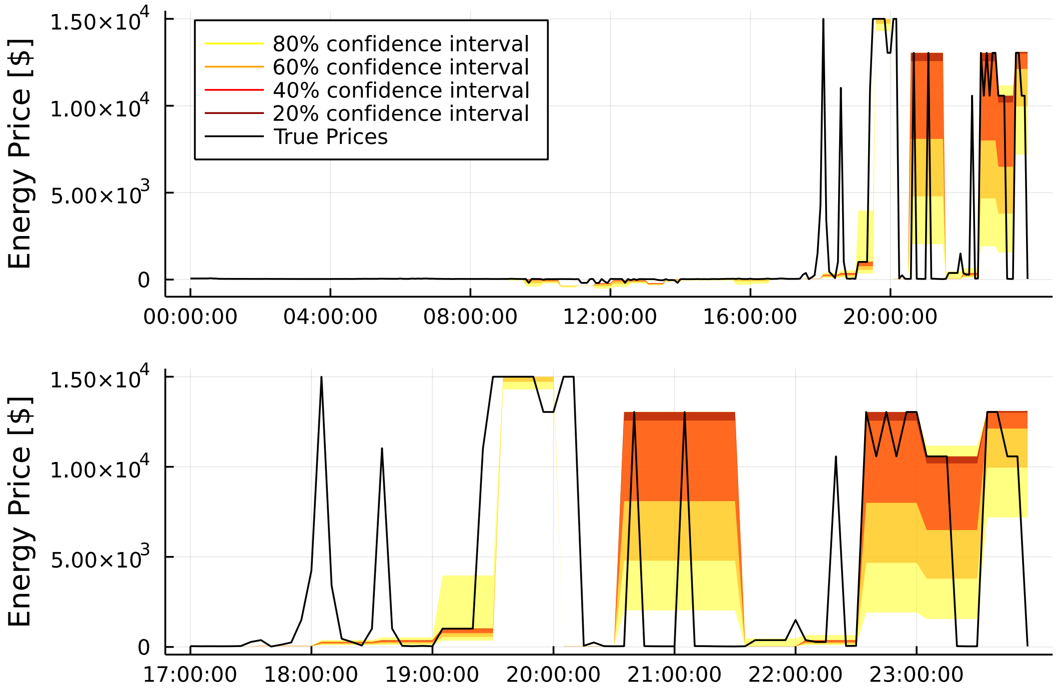

FIGURE 4.1: Confidence intervals for energy price on 12 March 2021 in NEM SA1 region, derived from generated price scenarios

and market floor scenarios, each with probability $\mu = 10^{-5}$, to account for extreme market events unrelated to demand. We display confidence intervals for energy price using this method in Figure 4.1. Data used for scenario generation is of same age and same source as forecasts used in the single forecast case, providing a fair comparison of approaches.

4.4.2 Voltage and Current Analysis

We validate the network-security of our stochastic approach by simulating market dispatch over 24 hours. We plot leaf node voltages for the market dispatch cases of energy-only, energy with maximum raise and with maximum lower in Figure 4.2. Results reveal no instances of voltage constraint violation using our *Proposed* approach. Current analysis also revealed no instances of constraint violation. Our simulations in the *No Curtailment* case do not model the responses of inverters or protective equipment to keep voltages in their safe operating range. We aim to avoid reliance on these recourse actions, which incur energy wastage, inconvenience and failures to meet market obligations.

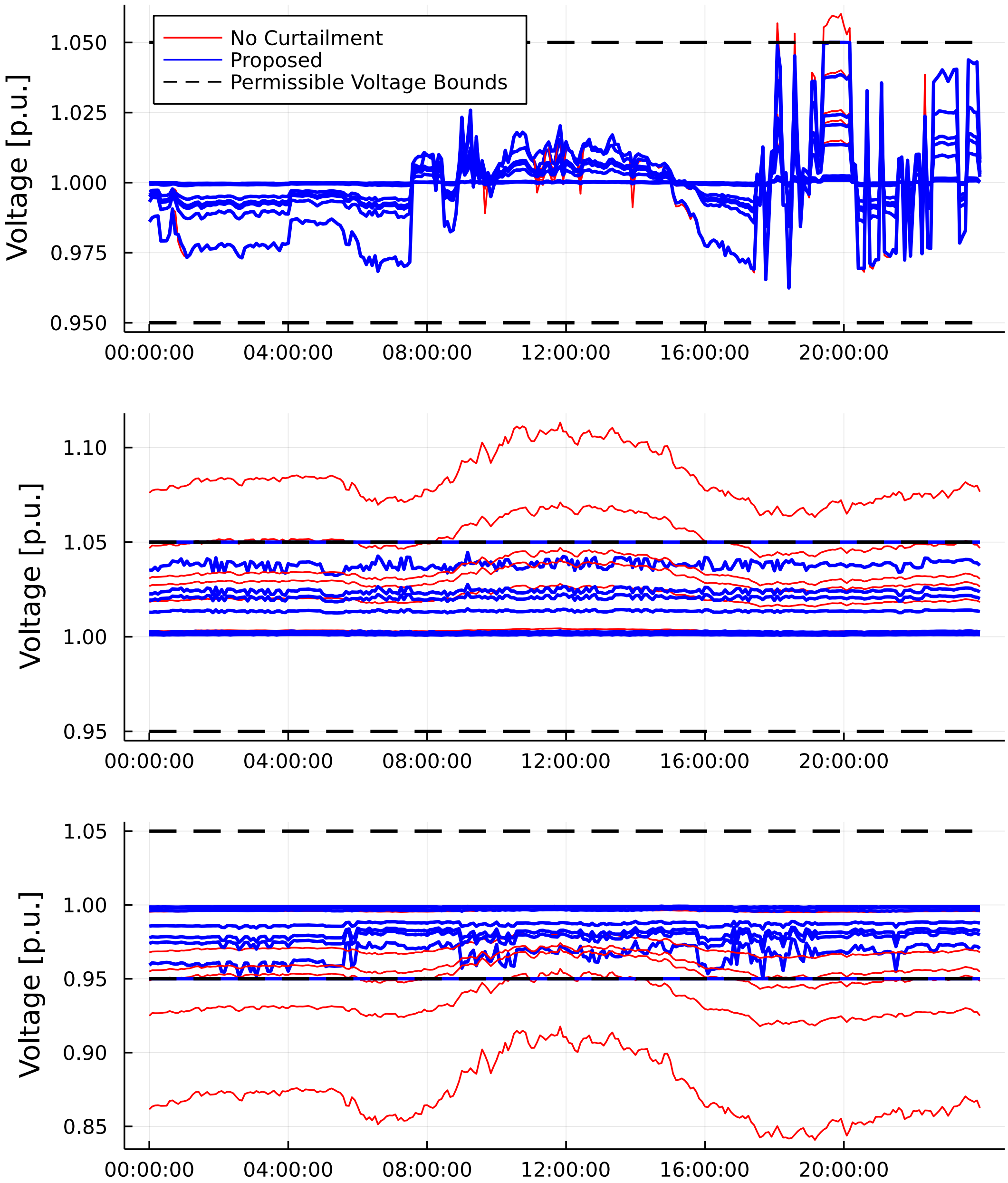

FIGURE 4.2: Leaf node voltages under expected market dispatch using stochastic approach, in the cases of energy-only with no reserve activation (top), energy and maximum potential raise activation (middle) and energy with maximum potential lower activation (bottom)

4.4.3 Advantage of Factoring Prices into Objective

Table 4.3 reports total simulated aggregator benefit using a range of curtailment policies. We apply our price-deterministic approach using true and forecast prices, and our stochastic approach using generated price scenarios, in each case with and without reactive power co-optimisation. We also simulate aggregator benefit in the no-curtailment case (Ideal), an adaptation of closely related work [136] and [123] for this problem setting (Literature) and optimally calculated fixed real-power envelopes (Basecase). We present results for the whole day, before 17:00 and after 17:00 to compare performance in both usual and extreme market conditions. This partitions 288 market trading periods into 204 and 83 periods.

Each result is benchmarked in rows entitled "Rel. to PI" to the perfect information (PI) case using our framework, either with or without reactive power co-optimisation. This choice of benchmark removes the effects of implementation-specific price forecast inaccuracies. We also compare the ideal case to the real-power perfect information case.

SIMULATED AGGREGATOR BENEFIT - RESULTS AND COMPARISONS TO BENCHMARKS

		Ideal	Real Power					Reactive Power Co-Optimisation Benefit Shaping (Proposed)		
			Benefit Shaping (Proposed)			Literature	Basecase			
		No Curtailment	Perfect Information	Stochastic Approach	Forecast Prices	Power l_2-norm	Fixed Envelopes	Perfect Information	Stochastic Approach	Forecast Prices
Full Day	Benefit	$105,207	$103,781	$103,611	$101,825	$94,817	$66,200	$105,032	$104,980	$102,721
	Rel. to PI	+1.4%	-	-0.2%	-1.8%	-9.7%	-37%	-	-0.0%	-2.2%
	Reac. Gain							+1.2%	+1.3%	+0.9%
Before 17:00	Benefit	$6,072	$5,928	$5,911	$5,894	$4,461	$1,412	$6,061	$6,052	$6,041
	Rel. to PI	+2.6%	-	-0.3%	-0.6%	-26%	-77%	-	-0.1%	-0.3%
	Reac. Gain							+2.2%	+2.3%	+2.5%
After 17:00	Benefit	$99,135	$97,853	$97,700	$95,931	$90,355	$64,788	$98,971	$98,929	$96,680
	Rel. to PI	+1.3%	-	-0.1%	-2.0%	-8.7%	-35%	-	-0.0%	-2.3%
	Reac. Gain							+1.1%	+1.3%	+0.8%

FIGURE 4.3: Simulated Aggregator Benefit - Results and Comparisons to Benchmarks

Comparisons reveal that our framework can attain a significantly greater portion of the no-curtailment aggregator benefit than [136] and [123]. This demonstrates the gains to aggregator benefit available when directly including price information into the objective, rather than curtailing for power at nodes then assigning curtailments to aggregators using prices in consecutive steps. Our approach demonstrates advantage in calm and volatile price conditions.

4.4.4 Advantage of Stochastic Approach

Our stochastic approach significantly closes the optimality gap between the perfect information case and the use of forecast prices. The stochastic approach was advantageous throughout the 24-hour period, particularly during the period of high price volatility in which benefit is similar to the perfect information case. Further analysis revealed that trading intervals of greatest stochastic advantage were characterised by the combination of extreme energy market prices, forecasts in the usual range, and probabilistic price scenarios indicating a wider than usual spread. This was observed for a low energy market price at 9:40 and a high energy market price at 19:30.

Our relatively simple implementation of price scenario generation in the NEM context does not use iterative parameter tuning, nor does it use any historical data prior to the most recent forecast. Its strong performance demonstrates the clear benefits in accounting for price uncertainty.

4.4.5 Advantage of Real-Reactive Power Co-optimisation

Reactive power co-optimisation allows our framework to reach almost 100% of the ideal no-constraint benefit in the cases of perfect information and our stochastic approach. Improvements reported in Figure 4.3 may be limited by proximity to the unconstrained case. In any case, this demonstrates tangible improvements are available to aggregator benefit by employing real-reactive power co-optimisation. Greater benefits may be attainable with more sophisticated co-optimisation approaches.

The potential increase in overall value creation enabled by the procurement of dispatchable reactive power from curtailed households warrants consideration of how these reactive power distribution network support services may be remunerated by a DSO. The value of remuneration should consider the dual variables associated to constraints (4.12), reflecting the increased expected benefit to households overall from market participation as a function of availability of reactive power support at each network node (modelled at medium voltage in this study), however the DSO would need to recover the cost of procuring reactive power support, and likely do so from households assigned favourable operating envelopes. This opens new interesting local market design research questions for future work.

4.4.6 Computational Aspects

Average solve time ratio between the stochastic approach with 8 scenarios and the price-deterministic approach was 7.63, with average solve times of 37.3 seconds and 6.8 seconds using each approach. As discussed in Subsection 4.3.2, additional scenarios add cross-market linear inequality constraint instances but to not add further non-linear power flow constraints. An approximately linear increase in solve time is consistent with expectation. The real-reactive power co-optimisation extended solve time in the stochastic case by a factor of 1.5 on average, to 53.2 seconds on average. Solve time values are consistently within 5 minute settlement periods used in the NEM.

Simulations were performed in Julia using IPOPT solver on an Intel®Core™i7-9700 3.00GHz processor with 16GB RAM.

4.5 Discussion

In this Chapter, we have assumed that aggregators may follow similar bidding practices to grid-scale storage, hence our use of real bid data from grid-scale storage assets in our simulations. In particular, we model the various contributions to an aggregators' price and volume bands on a per-customer basis, resulting in trapeziums defined at the customer level as performed in previous literature [123]. For trapeziums defined exclusively on the basis of maximum inverter capacity (ramp rate constraints defined on significantly shorter timescales than 5-minute market trading intervals, therefore do not impact bidding), the aggregation of shaped trapeziums at the feeder-scale conserves trapezium shape.

In effect, this implicitly assumes that the increasing marginal costs of providing increasing levels of market services, based on the perceived opportunity cost of capitalising on future elevate market prices, are experienced at individual customer granularity. This is consistent with the full benefit pass-through model for aggregators, where households participating in an aggregator program are rewarded as a function of their metered contributions. In practice, this represents only one of several options for aggregators to distribute the benefits of wholesale market participation amongst participants. Some aggregator business models may provide fixed benefit payments across all customers, in which case bid costs may not be directly traceable to individual households and should instead by considered on aggregate. In those scenarios, aggregators may have preferences to dispatch their portfolio according to an operational objective, such as distributing the cycling of batteries while factoring different levels of self-consumption use by customers. In future sections, we will consider a range of methods by which an aggregator may dispatch its fleet for a given whole-of-feeder dispatch outcome, and the impacts of this choice on the potential for network constraint violations in unbalanced three-phase networks.

This framework does carry some risks. Most notably, incorrect predictions of the future value of market services provided by the TSO may result in a failure to prioritise the most valuable exchanges. In the case that moderate energy prices were expected but very high prices were realised, our formulation will make less capacity available to the wholesale market than under the perfect information scenario. This may be particularly unfortunate for system operators as high energy prices indicate of a shortage of generation. An additional risk is the potential for aggregators to engage in deceptive bidding strategies. It may become in the interest of aggregators to stray from cost-reflective bidding in order to gain better market access. Manipulation of electricity markets is explored in [139]. These risks would need to be considered carefully before implementation on a real system.

An important feature of the price-stochastic approach is to ensure that all latent capacity in the network is assigned a non-zero market value. By considering the generally highly-improbable scenarios of prices reaching market cap and market floor, the upper and lower bounds of envelopes will always correspond to scenarios where one or more network constraints will be binding (unless there is insufficient DER capacity in the network to dispatch and violate network constraints, in which case envelopes would not be binding). As it is possible for these extreme scenarios to occur in practice, it is important to ensure that network constraints are satisfied in any potential extreme outcome. Simulations in this Chapter study the IEEE 69-bus MV test feeder, which is a single phase network representing a balanced three-phase system that ignores the LV component of the network. Many distribution feeders are unbalanced three-phase networks, and unbalance can be more prevalent at the low-voltage level due the increased impact of individual households on network state variables.

An interesting avenue for extension of this work is to compare network upgrade costs to associated increases in our chosen optimisation objective. This would effectively communicate the potential increase in value-creation potential for DER as a function of network upgrades. This would also extend [140], which studies a closely related problem applying a more straightforward optimisation objective.

In future chapters in this thesis, we will examine whether the conventional conditions for envelope robustness in single-phase-equivalent networks are sufficient to ensure robustness in unbalanced three-phase networks. Studies in these later chapters will employ a simpler objective, namely capacity maximisation, however the insights obtained are equally relevant for the application of our proposed objective in this Chapter, which will always benefit from greater allocations of network capacity in a robust manner.

4.6 Conclusion

In this Chapter we proposed a novel bid curtailment approach, suitable for energy and reserve bids with multiple price bands and feasible dispatch regions, which aims to directly maximise benefit gained by aggregators through market participation. Our results demonstrate that directly factoring bid prices and expected market prices into the curtailment objective function can produce advantageous results for aggregators. In this context, market prices are influential on curtailment outcomes, and we demonstrate in simulations that incorporating knowledge of expected price probability distributions through a two-stage stochastic programming approach can yield greater aggregator benefit than using a single estimate of market prices. We demonstrate that reactive power co-optimisation can attain greater aggregator benefit.

Chapter 5

Constraining Voltage Unbalance Through Envelopes

This Chapter analyses the necessary conditions for operating envelopes to ensure network security in unbalanced distribution systems. This Chapter therefore carries a different focus from Chapter 4, which sought to select the most market-efficient allocation of capacity (emphasis on the optimisation objective) while satisfying a set of network constraints that were sufficient in a single-phase network. Instead, in this Chapter, we will assess how ensuring network security of operating envelopes (emphasis on constraints in optimisation problem) in unbalanced systems requires a more sophisticated approach due to the impacts of mutual impedances and requirements for phase balance.

5.1 Introduction

The premise of operating envelopes is to apply limits to DER customers' capacity to import and export electricity for network security. Specifically, under the conventional definition of operating envelopes, these envelopes are calculated such that network operators can expect network state variables to remain within operational limits for any potential DER actions within their assigned envelopes. It is common in the literature to check for satisfaction of network constraints under two extreme loading conditions - specifically when all DER maximise their net exports, and when all DER maximise their net imports. The justification for this approach in single-phase networks is fairly clear - increases in real power exports increase current flow from DER to the top of the feeder, which causes voltage rise due to Ohm's law. Similarly, decreases in real power exports (e.g. increases in power imports) have an opposite effect, causing voltage drop along the feeder with respect to the reference bus. In [131], the authors identify that non-convexity of the feasible region risks identifying export limits that are not safe in practice. This can be interpreted as when exports have become sufficiently high that the rate of change of voltage is primary influenced by changes in line losses rather than the effects of Ohm's law through the line. Their convex inner approximation approach eliminates this risk, and approach yields safe operating envelopes in the single-phase or balanced three-phase network case.

In practice, DER often connects to unbalanced three-phase networks. In this context, evaluation of network constraints under two extreme loading conditions may not be sufficient to ascertain if envelopes satisfy the conventional network security conditions expected of dynamic operating envelopes - namely to ensure robust satisfaction of network constraints under any potential utilisation of envelopes by DER. The authors of [132] have demonstrated that it is possible for a single-phase DER customer's real power export to induce a reduction in voltage magnitude on other phases. This phenomena is due to electromagnetic phase couplings, resulting in current flows on one phase inducing electric and magnetic fields affecting current on adjacent phases, and this ultimately impacts voltage rise and fall along feeders.

5.1.1 Robust Dynamic Operating Envelopes [133]

In order to account for these risks, the authors of [133] proposed a new method of generating operating envelopes that is robust to the effects of mutual impedances between phases. Rather than verify network constraint satisfaction at two specific DER operating points, their approach involves deriving the full network *feasible region*[1] for DER to operate, then deriving a subset of this region within which DER can operate independently without potentially jeopardising safe operation of the distribution network.

In order to represent the network feasible region for DER dispatch, in [133] the authors use a linearised power flow model. The benefit of this choice of power flow model is the ability to express network state variables as affine functions of DER setpoints through simple matrix manipulation. In [133], network constraints include voltage magnitude constraints and thermal constraints. As maximum and minimum voltage magnitude constraints (e.g. $v \leq \overline{v}$) are approximated linearly with respect to DER setpoints, network constraints are

[1] In this paper, we reserve the term *envelope* for an individual DER, and use the term *region* to designate a set of setpoints of multiple DER

expressed as linear functions of DER setpoints. The network feasible region, under a linearised power flow model, is therefore a polytope.

The DSO then determines DER-level *robust dynamic operating envelopes* such that all combinations of (assumed) independently-operated DER setpoints remain bounded within the aforementioned network-feasible region. Geometrically, these robust dynamic operating envelopes form a hyper-rectangular *operating region* for DER when plotted in high-dimensional spaces representing collective DER setpoints. This approach delivers envelopes, calculated at DER-scale granularity, such that network voltage magnitudes are expected to remain within operational bounds for any arbitrary DER imports or exports satisfying individual envelopes.

While the authors of [133] correctly identified the risk of voltage magnitude constraint violation in unbalanced three-phase networks, their approach does not mitigate risks of voltage unbalance levels exceeding operational constraints. Voltage unbalance constraints are specific to three-phase unbalanced networks, and have therefore been largely ignored by literature that assumes single-phase networks.

5.1.2 Impacts of Unbalanced Network Loading and Impedance Unbalance

Many households and businesses have equipment that connects to all three phases in a distribution system. This machinery is designed on the assumption that an equal quantity of power (specifically, with equal voltage and current) is delivered through each phase with an equal phase shift magnitude of 120 degrees between each phase. If the power delivered through phases becomes unbalanced, through differences between voltage magnitudes or phase shifts between phases, machines will be less efficient at harnessing this delivered power, and this may result in serious damage and danger. Additionally, some distribution networks are characterised by unbalanced impedances when lines and cables have not been adequately transposed, and this can result in unbalanced load flows across phases even when loads across the network are relatively balanced across phases.

A common method of characterising the extent of unbalance in the system is to decompose three-phase voltages as a sum of two balanced components and a vector. These are called the positive sequence component, the negative sequence component and the zero sequence component. The positive sequence component shares the same phase ordering as the underlying three-phase power flow, while the negative sequence voltage has the inverse phase ordering.

Negative sequence voltages represent dangers to three-phase components. Induction motors have different resistances for negative and positive sequence voltage components, and phase shifts between the positive and negative components may cause double-frequency currents through the motor. These motors generally have lower impedance to negative sequence currents than positive sequence currents, meaning that small voltage unbalance can lead to significant negative sequence current.

5.1.3 Application of Voltage Unbalance Constraints in Envelope Construction

In this Chapter we will propose a method to develop robust dynamic operating envelopes that constrains voltage unbalance between phases to within specified tolerances, for any potential utilisation of assigned DER capacity across the feeder.

Our contribution is most similar to [134]. Their study sought to explore the impact of different technical constraints on the values calculated for dynamic operating envelopes calculated in the conventional manner for single-phase networks (ensuring constraint satisfaction in cases of all DER maximising (a) net imports and (b) net exports of real power). When the scenarios of maximum generation and maximum load were required to satisfy voltage unbalance constraints (applied using non-linear constraints), the overall production from distributed generators was found to decrease. This demonstrates that the envelopes calculated in their study without consideration of voltage unbalance constraints could result in voltage unbalance constraint violations when DER either maximised or minimised their net real power exports.

While this study demonstrated the potential for voltage unbalance constraint violations in these extreme cases, their manner of constructing envelopes that factored risks of unbalance does not specifically preclude the possibility that voltage unbalance constraints may be violated in scenarios where not all DER operate at either their maximum or minimum real power net exports. It is likely for this reason that the authors note they do not design DOE calculation procedures in their work, but instead focus on exploring the application of technical limits that influence import/export values derived by such approaches in an LV context.

5.1.4 Research Question

In this chapter, we aim to bring together and extend the contributions of [133] and [134]. Specifically, we aim to achieve robustness of envelopes in terms of voltage constraints with respect to all potential DER behaviours complying with DOE as achieved in [133], while augmenting the set of voltage constraints to include voltage unbalance constraints, as this represents a form of completion of voltage constraint handling in the unbalanced three-phase case.

The focus of our contribution is adherence to network voltage constraints. As such, our derivations and simulations in this Chapter omit consideration of thermal constraints. We advise the reader to consult [133] for handling of thermal constraints in LV networks.

5.2 Problem Formulation

Our aim in this Chapter is to calculate operating envelopes for real power $[\underline{p}, \overline{p}] \subset \mathbb{R}$ for each DER customer within a set of $N_d \in \mathbb{N}$ DER customers (a subset of all $N_c \geq N_d \in \mathbb{N}$ customers) in a low-voltage (LV) radial distribution network. We model an individual DER setpoint as $p_i \in [\underline{p}_i, \overline{p}_i]$ (we model customer background load separately), and aggregate these into a collective DER setpoint variable[2] $\boldsymbol{p} \in \mathbb{R}^{N_d}$ Given that we model network state variables on a phase-by-phase basis, we model customers at node-phase granularity. Three-phase customers are easily modelled as three individual customers with minor additional constraints. We assume a maximum of one customer at a given node-phase site.

Let $N_b \in \mathbb{R}$ be the number of unique nodes where voltage unbalance must be constrained. We require voltage unbalance to be constrained at all nodes with at least one customer, so $N_b \leq N_c \leq 3N_b$. At each of N_b nodes, we require that the ratio of negative sequence voltage to positive sequence voltage (Voltage Unbalance Factor, VUF [141]) must not exceed 2%. Explicitly, let

[2] In terms of typesetting, un-bolded variables, parameters and functions are used when discussing a single bus/phase/instance, whereas bolded variables, parameters and functions form the whole-of-system model. This is important to note in Section 5.3.3, where many derivations are made for a single instance but vectorised to form a whole-of-system expression.

$V_{ab}\angle\theta_{ab}, V_{bc}\angle\theta_{bc}, V_{ca}\angle\theta_{ca}$ represent line-line voltages at a given node and $a = 1\angle\frac{2\pi}{3}$, then

$$VUF = \left|\frac{V_{ab}\angle\theta_{ab} + a^2 V_{bc}\angle\theta_{bc} + a\ V_{ca}\angle\theta_{ca}}{V_{ab}\angle\theta_{ab} + a\ V_{bc}\angle\theta_{bc} + a^2 V_{ca}\angle\theta_{ca}}\right| \leq 0.02 \tag{5.1}$$

We assume all three phases exist at nodes requiring voltage balance, even if they lack customers. There may exist some unbalance at the LV side of the MV-LV transformer originating from unbalance in the MV network.

We also require phase voltage magnitudes $V_i \in \mathbb{R}$ at each of the N_c customer sites remain within operational limits. We omit thermal limits as they do not constrain the optimisation problem in our case study, however they can be modelled.

In this chapter, we will demonstrate how operating envelopes can be constructed in a manner that ensures VUF remains bounded to within specified limits. In doing so, we will highlight the limitations of only being able to approximate the VUF using the line voltage unbalance rate (LVUR), as will be defined in Section 5.3.2.

5.3 Method

Our method consists of expressing network state variables as a function of DER setpoints $\boldsymbol{p}$, then deriving feasible regions for $\boldsymbol{p}$ such that voltage unbalance and magnitude constraints hold. We then use a robust optimisation formulation to calculate envelopes for arbitrary objectives.

5.3.1 Linearised Three-Phase Power Flow Model

In order to derive the network-feasible operating region for DER, we begin by deriving direct expressions for network state variables as a function of $\boldsymbol{p}$. We use the linear approximation for power flow in multiphase radial networks in [42][3], and we introduce variables $\theta_i \in [-\pi, \pi]$ for phase angle of line-neutral voltages. The complex form of line-neutral voltages is therefore given by

$$\sqrt{v_i}\angle\theta_i = V_i\angle\theta_i$$

[3] Linearisation assumes that voltages are nearly balanced. Our results validate this assumption in the operating region where VUF is constrained.

and linearised phase angle constraints are derived using small angle approximation $\sin(x) = x$ for $x \approx 0$ and assuming voltage magnitudes are approximately $1p.u.$ We aggregate constraints in matrix form, assume some voltages at the transformer, and perform matrix manipulation to generate expressions for squared voltage magnitudes $\boldsymbol{v} \in \mathbb{R}^{3N_b}$ and phase angles $\boldsymbol{\theta} \in \mathbb{R}^{3N_b}$ for all phases at nodes with customers as a function of DER setpoints $\boldsymbol{p}$

$$\boldsymbol{v} = \boldsymbol{A}_v \boldsymbol{p} + \boldsymbol{b}_v = \boldsymbol{l}_v(\boldsymbol{p}) \tag{5.2}$$

$$\boldsymbol{\theta} = \boldsymbol{A}_{\boldsymbol{\theta}} \boldsymbol{p} + \boldsymbol{b}_{\boldsymbol{\theta}} = \boldsymbol{l}_{\boldsymbol{\theta}}(\boldsymbol{p}) \tag{5.3}$$

where $\boldsymbol{A_v}, \boldsymbol{A_\theta} \in \mathbb{R}^{3N_b \times 3N_b}$, $\boldsymbol{b_v}, \boldsymbol{b_\theta} \in \mathbb{R}^{3N_b}$ and $\boldsymbol{l}(.)$ represents a linear/affine function. The small impacts of linearisation error will be discussed in Section IV, in which we apply exact power flow models to evaluate our results.

5.3.2 Selection of Proxy for VUF for Envelope Calculation

There are three definitions used for voltage unbalance [142]. Following the notation in [142] in this brief sub-section, we let $\boldsymbol{V} = V\angle\theta$ where $\boldsymbol{V} \in \mathbb{C}$ is the voltage phasor, $V \in \mathbb{R}$ is the voltage magnitude and $\angle\theta$ is the phase angle.

IEC Definition (VUF)

The IEC (International Electrotechnical Commission) defines the voltage unbalance factor (VUF) as the ratio of the magnitudes of the negative sequence voltage component to the positive sequence voltage component. It is calculated as

$$VUF[\%] = \frac{|\boldsymbol{V}_n|}{|\boldsymbol{V}_p|} \times 100 \tag{5.4}$$

with negative and positive sequence components defined as

$$\boldsymbol{V}_n = \frac{\boldsymbol{V}_a + \boldsymbol{a}^2.\boldsymbol{V}_b + \boldsymbol{a}.\boldsymbol{V}_c}{3} \tag{5.5}$$

$$\boldsymbol{V}_p = \frac{\boldsymbol{V}_a + \boldsymbol{a}.\boldsymbol{V}_b + \boldsymbol{a}^2.\boldsymbol{V}_c}{3} \tag{5.6}$$

By measuring the negative sequence voltage, this metric for voltage unbalance directly measures the component that causes greatest risk/harm in unbalance three-phase systems. It is also more sensitive to small unbalances that can still have an effect on the system.

NEMA Definition (LVUR)

The NEMA (National Electrical Manufacturers Association) definition of voltage unbalance is simpler than the IEC method. It calculates the maximum deviation from the average line voltage magnitude across the three phases. It is calculated as

$$LVUR[\%] = \frac{\Delta V_L^{max}}{V_L^{avg}} \times 100 \tag{5.7}$$

where V_{ab}, V_{bc}, V_{ca} represent line-line voltages, and

$$V_L^{avg} = \frac{V_{ab} + V_{bc} + V_{ca}}{3} \tag{5.8}$$

$$V_L^{max} = \max\left\{|V_{ab} - V_L^{avg}|, |V_{bc} - V_L^{avg}|, |V_{ca} - V_L^{avg}|\right\} \tag{5.9}$$

Although it is easier to compute, this definition cannot calculate negative sequence voltage as it does not consider phase angle information. Nevertheless, it has at times been used in standards such as NEMA MG-1 and ANSI C84.1, stating that LVUR must be restricted to less than 3% in power systems.

IEEE Definition (PVUR)

The IEEE definition is similar to the NEMA definition, however instead of measuring differences in line-line voltage magnitudes, it measures differences in line-neutral voltage magnitudes. It is therefore calculated as

$$PVUR[\%] = \frac{\Delta V_P^{max}}{V_P^{avg}} \times 100 \tag{5.10}$$

where V_a, V_b, V_c represent line-neutral voltages, and

$$V_P^{avg} = \frac{V_a + V_b + V_c}{3} \tag{5.11}$$

$$V_P^{max} = \max\left\{|V_a - V_P^{avg}|, |V_b - V_P^{avg}|, |V_c - V_P^{avg}|\right\} \tag{5.12}$$

Typically DNSPs do not have good visibility of phase unbalance across the network. Where a DNSP relies of measurements from smart meters of LV customers, these generally measure line-to-neutral voltages, and therefore only the PVUR can be established in post processing historical data. However, as will be discussed below, VUR and PVUR represent fundamentally different quantities, and this must be considered when choosing a proxy for voltage unbalance.

Comparison of Definitions

While the VUF (IEC definition) is ultimately the most meaningful definition in terms of impact on machinery, it may not be easy to constrain in optimisation given the non-linearity in its definition (norm, division). Analysis in [142] shows that different metrics are more or less suitable, depending on the nature of the unbalance in the system:

- In the event of voltage magnitude unbalance on one phase only (phase shifts remain at 120 degrees), we have

  $$LVUR \approx VUF = PVUR/2 \tag{5.13}$$

  Generally, we are not in a position to know that two phases out of three will remain balanced.

- In the event of voltage magnitude unbalance on two phases (i.e. all three phases of different magnitude, phase shifts remain at 120 degrees), we have

  $$PVUR/2 \leq VUF \leq PVUR/\sqrt{3} \tag{5.14}$$

  This introduces a margin of error of up to 15% of the value of VUF.

  In practice, voltage unbalance will generally be accompanied by a phase shift. This may be due to reactive power flows through mainly-resistive low-voltage lines due to inductive loads such as air conditioners, or may be due to unbalanced real-power load flows through more inductive medium voltage branches of MV-LV networks.

- In the event of phase angle unbalance, PVUR is not a suitable measure of the underlying voltage unbalance. This is because it is possible to obtain a PVUR of 0% (guaranteed when all voltage phase magnitudes are equal) in highly-unbalanced scenarios. For example, if phase shifts on phases A, B and C are 0, 220 and 140 degrees (in place of 240 and 120 degrees) but phase voltage magnitudes remain approximately equal, then $VUF = 22.67\%$ while $PVUR = 0\%$. It is more appropriate to use an approximation using the $LVUR$, for which [142] find that

$$LVUR \lesssim VUF \lesssim (2/\sqrt{3})LVUR \tag{5.15}$$

The authors of [142] conclude that for reasonable ranges of voltage magnitude and angle derivations (0.8 to 1.2 p.u. voltage magnitude and -20° to 20° voltage angle), violations of (5.15) are less than 5%. For this reason, we use the approximation (5.15) in this chapter.

It is worth noting that there exist papers on data-driven approaches to estimating unbalance metrics in the context of incomplete information [143]. The premise is to predict unbalance by training a support vector regression model using historical data. In this Chapter we are primarily motivated to derive robust approaches to ensuring voltage unbalance remains bounded, however we note the results of data-driven solutions may be suitable in contexts where some degree of constraint violation is permitted such as chance-constrained optimisation.

5.3.3 Feasible Region for Phase Unbalance Constraints

Our aim is to derive a feasible operating region for DER setpoints $\boldsymbol{p}$ such that (5.1) holds at each of N_b nodes admitting one or more customers. While the denominator in (5.1) can be approximated assuming approximately balanced voltage phases, the numerator is more challenging to linearise effectively as a function of modelled phase voltage magnitudes and angles. Instead, we note the derivations and empirical findings in [142] suggesting to bound the voltage unbalance factor by bounding the line voltage unbalance rate (LVUR), also referred to as the NEMA (National Equipment Manufacturer's Association) definition of voltage unbalance. At a given node, the LVUR is calulated as

$$\text{LVUR} = \max_{ij \in \{ab,bc,ca\}} \frac{|V_{ij} - \hat{V}_l|}{\hat{V}_l} \tag{5.16}$$

for line-line voltage magnitudes $V_{ab}, V_{bc}, V_{ca} \in \mathbb{R}$ with $\hat{V}_l$ the average line-line voltage magnitude. The results of [142] show

$$\text{LVUR} \lesssim \text{VUF} \lesssim \frac{2}{\sqrt{3}}\text{LVUR} \tag{5.17}$$

and therefore by defining $\mu = \frac{\sqrt{3}}{2}\lambda$ for some VUF target value λ, it follows that

$$\text{LVUR} \leq \mu \iff \text{LVUR} \leq \tfrac{\sqrt{3}}{2}\lambda \tag{5.18}$$

$$\iff \text{VUF} \lesssim \tfrac{2}{\sqrt{3}}\text{LVUR} \leq \tfrac{2}{\sqrt{3}}\left(\tfrac{\sqrt{3}}{2}\right)\lambda = \lambda \tag{5.19}$$

Our aim is now to construct a feasible region, defined by a set of inequality constraints on $\boldsymbol{p}$, restricting LVUR at each of N_b customer nodes to less than μ. To achieve this, we will firstly express the constraint

$$\text{LVUR} \leq \mu$$

as a set of linear inequalities in terms of line-line voltage magnitudes, then derive linear approximations for line-line voltage magnitudes as a function of DER setpoints.

Remaining in the case study of a single node, we note that

$$\frac{|V_{ij} - \hat{V}_l|}{\hat{V}_l} \leq \mu \iff \begin{cases} \frac{V_{ij} - \hat{V}_l}{\hat{V}_l} \leq \mu \\ \frac{\hat{V}_l - V_{ij}}{\hat{V}_l} \leq \mu \end{cases} \tag{5.20}$$

$$\iff \begin{cases} V_{ij} - (1+\mu)(\frac{1}{3}V_{ab} + \frac{1}{3}V_{bc} + \frac{1}{3}V_{ca}) \leq 0 \\ (1-\mu)(\frac{1}{3}V_{ab} + \frac{1}{3}V_{bc} + \frac{1}{3}V_{ca}) - V_{ij} \leq 0 \end{cases} \tag{5.21}$$

To apply constraint (5.21) for all $V_{ij} \in \{V_{ab}, V_{bc}, V_{ca}\}$, we can define matrix M_μ as follows

$$M_\mu = \begin{bmatrix} (\frac{2-\mu}{3}) & -(\frac{1+\mu}{3}) & -(\frac{1+\mu}{3}) \\ -(\frac{1+\mu}{3}) & (\frac{2-\mu}{3}) & -(\frac{1+\mu}{3}) \\ -(\frac{1+\mu}{3}) & -(\frac{1+\mu}{3}) & (\frac{2-\mu}{3}) \\ (\frac{-2-\mu}{3}) & (\frac{1-\mu}{3}) & (\frac{1-\mu}{3}) \\ (\frac{1-\mu}{3}) & (\frac{-2-\mu}{3}) & (\frac{1-\mu}{3}) \\ (\frac{1-\mu}{3}) & (\frac{1-\mu}{3}) & +(\frac{-2-\mu}{3}) \end{bmatrix} \tag{5.22}$$

Such that

$$M_\mu \left[V_{ab}\, V_{bc}\, V_{ca}\right]^\top \leq \mathbf{0} \qquad \Longleftrightarrow \qquad \text{LVUR} \leq \mu \tag{5.23}$$

In order to impose these constraints at a single given node in our model, we first require some approximation for $[V_{ab}, V_{bc}, V_{ca}]$ as a function of modelled state variables $[v_a, v_b, v_c]$ and $[\theta_a, \theta_b, \theta_c]$ at that node. Begin by approximating line-neutral (phase) voltage magnitudes $[\widetilde{V}_a, \widetilde{V}_b, \widetilde{V}_c]$ at a single node as a linear function of their modelled squared values

$$\widetilde{V}_i = \alpha_n \times v + \beta_n = l_n(v_i) \tag{5.24}$$

for $\alpha_{ph} \approx 0.5$, $\beta_{ph} \approx 0.5$, and $l_n(.)$ a scalar linear function. We now establish a linear approximation for line-line voltage magnitudes, which we denote $[\widetilde{V}_{ab}, \widetilde{V}_{bc}, \widetilde{V}_{ca}]$, as a function of $[\widetilde{V}_a, \widetilde{V}_b, \widetilde{V}_c]$ and $[\theta_a, \theta_b, \theta_c]$. Explicitly, we seek to establish the linear function $l_l : \mathbb{R}^4 \to \mathbb{R}$ such that

$$\widetilde{V_{ij}} = l_l(\theta_i, \theta_j, v_i, v_j) \approx V_{ij} \qquad \text{for } ij \in \{ab, bc, ca\} \tag{5.25}$$

In order to achieve this, we define $\Delta\theta_{ab} = \theta_b - \theta_a$ and $\Delta V_i = V_1 - 1$ and derive values for

$$\frac{\partial V_{ij}}{\partial \Delta\theta_{ij}} = \alpha_l \qquad \text{and} \qquad \frac{\partial V_{ij}}{\partial V_i} = \frac{\partial V_{ij}}{\partial V_j} = \beta_l \tag{5.26}$$

for $\Delta V_i \approx 0$ and $\Delta\theta_{ij} \approx \frac{-2\pi}{3}$. Note that $\Delta\theta_{ij} + \frac{2\pi}{3} \approx 0$.

Begin by noting invariance of norms under rotation

$$V_{ij} = |V_j \angle\theta_j - V_i \angle\theta_i| \tag{5.27}$$

$$= |V_j \angle(\theta_j - \theta_i) - V_i| \tag{5.28}$$

$$= |V_j\angle(\Delta\theta_{ij}) - V_i| \tag{5.29}$$

Expanding V_i to obtain $V_i + V_j - V_j$

$$V_{ij} = |V_j\angle(\Delta\theta_{ij}) - (V_i + V_j - V_j)| \tag{5.30}$$
$$= |V_j\angle(\Delta\theta_{ij}) - (2 + \Delta V_i + \Delta V_j) + V_j| \tag{5.31}$$
$$= |V_j\angle(\Delta\theta_{ij}) + V_j - 2 - (\Delta V_i + \Delta V_j)| \tag{5.32}$$
$$\approx |1\angle(\Delta\theta_{ij}) - 1 - (\Delta V_i + \Delta V_j)| \tag{5.33}$$

Noting that $1\angle(x+y) \approx \left(1\angle x + y\angle(x+\frac{\pi}{2})\right)$ for $x, y \in \mathbb{R}$ and $y \approx 0$, we re-express $1\angle(\Delta\theta_{ij})$ as follows:

$$1\angle(\Delta\theta_{ij}) \approx 1\angle\left(\tfrac{-2\pi}{3}\right) + \left(\Delta\theta_{ij} + \tfrac{2\pi}{3}\right)\angle\left(\tfrac{-\pi}{6}\right) \tag{5.34}$$

Substituting into (5.33), we obtain

$$V_{ij} = \Big|\sqrt{3}\angle\left(\tfrac{-5\pi}{6}\right) + \left(\Delta\theta_{ij} + \tfrac{2\pi}{3}\right)\angle\left(\tfrac{-\pi}{6}\right) \tag{5.35}$$
$$- (\Delta V_i + \Delta V_j)\Big| \tag{5.36}$$

Differentiating with respect to $\Delta\theta_{ij}, \Delta V_i, \Delta V_j$, we can calculate gradients $\alpha_l, \beta_l \in \mathbb{R}$. We can therefore establish a linearised expression for line-line voltage magnitudes $\widetilde{V_{ij}}$ using modelled state variables

$$\widetilde{V_{ij}} = \alpha_l \times (\theta_j - \theta_i) + \beta_l \times (\widetilde{V_i} + \widetilde{V_j}) + \gamma_l \tag{5.37}$$
$$= \alpha_l \times (\theta_j - \theta_i) + \beta_l \times \left(l_n(v_i), l_n(v_j)\right) + \gamma_l \tag{5.38}$$
$$= l_l\left(\theta_i, \theta_j, v_i, v_j\right) \tag{5.39}$$

We now vectorise the linear function $l_l : \mathbb{R}^4 \to \mathbb{R}$ to generate $\boldsymbol{l_l} : \mathbb{R}^{3N_b} \times \mathbb{R}^{3N_b} \to \mathbb{R}^{3N_b}$. This function computes $\widetilde{\boldsymbol{V_{ij}}} \in \mathbb{R}^{3N_b}$, approximating line-line voltage magnitudes across all nodes with customers. Substituting expressions of state variables as a function of DER, we obtain

$$\widetilde{\boldsymbol{V_{ij}}} = \boldsymbol{l_l}(\boldsymbol{v}, \boldsymbol{\theta}) \tag{5.40}$$
$$= \boldsymbol{l_l}(\boldsymbol{l_v}(\boldsymbol{p}), \boldsymbol{l_\theta}(\boldsymbol{p})) \tag{5.41}$$
$$= \boldsymbol{A_l}\,\boldsymbol{p} + \boldsymbol{b_l} \tag{5.42}$$

for some $\boldsymbol{A_l} \in \mathbb{R}^{3N_b \times 3N_b}$, $\boldsymbol{b_l} \in \mathbb{R}^{3N_b}$. We now formalise our approximation for LVUR, which we call linLVUR, and define our voltage unbalance constraints with respect to some target value μ' for linLVUR as

$$\text{linLVUR} = \max_{ij \in \{ab,bc,ca\}} \frac{|\widetilde{V_{ij}} - (\hat{\widetilde{V}}_l)|}{(\hat{\widetilde{V}}_l)} \leq \mu' \tag{5.43}$$

We determine μ' by evaluating error between LVUR and linLVUR, as discussed in Section IV. We derive the feasible region defined by constraints linLVUR $\leq$ μ' at all nodes by defining the block-diagonal matrix $\boldsymbol{M_\mu} \in \mathbb{R}^{6N_b \times 3N_b}$ as follows

$$\boldsymbol{M_{\mu'}} = \begin{bmatrix} M_{\mu'} & 0 & \dots \\ 0 & M_{\mu'} & \dots \\ \vdots & \vdots & \ddots \end{bmatrix} \tag{5.44}$$

and constraining

$$\boldsymbol{M_{\mu'}} \, \widetilde{\boldsymbol{V_{ij}}} \leq \boldsymbol{0} \tag{5.45}$$

$$\boldsymbol{M_{\mu'}} \, (\boldsymbol{A_l} \, \boldsymbol{p} + \boldsymbol{b_l}) \leq \boldsymbol{0} \tag{5.46}$$

Let

$$\boldsymbol{E} = \boldsymbol{M_{\mu'}} \boldsymbol{A_l} \in \mathbb{R}^{6N_b \times N_d}$$

and

$$\boldsymbol{f} = \boldsymbol{M_{\mu'}} \boldsymbol{b_l} \in \mathbb{R}^{6N_b}$$

The feasible region for collective DER setpoints $\boldsymbol{p}$ with respect to constraints on linLVUR (5.43) is expressed as

$$\boldsymbol{E} \, \boldsymbol{p} + \boldsymbol{f} \leq \boldsymbol{0} \tag{5.47}$$

5.3.4 Feasible Region for Voltage Magnitude Constraints

For a relatively simple objective (e.g. maximising the Minkowski sum of real-power operating envelopes), defining envelope feasibility criteria with respect to voltage magnitude constraints is relatively straightforward. We return to studying a single customer (node-phase pair). Determine $\underline{v}, \overline{v} \in \mathbb{R}$ such that $\underline{V} \leq V_i \leq \overline{V} \iff \underline{v} \leq v_i \leq \overline{v}$. Define matrix M_v and vector k_v such that

$$M_v \, v_i + k_v = \begin{bmatrix} 1 \\ -1 \end{bmatrix} v_i + \begin{bmatrix} \overline{v} \\ -\underline{v} \end{bmatrix} \leq \boldsymbol{0} \tag{5.48}$$

Defining block-diagonal matrix $\boldsymbol{M_v} \in \mathbb{R}^{2N_c \times 3N_b}$ and block vector $\boldsymbol{k_v}$ as follows

$$\boldsymbol{M_v} = \begin{bmatrix} M_v & 0 & ... \\ 0 & M_v & ... \\ \vdots & \vdots & \ddots \end{bmatrix} \qquad \boldsymbol{k_v} = \begin{bmatrix} k_v \\ k_v \\ \vdots \end{bmatrix} \tag{5.49}$$

We can express voltage magnitude feasibility criteria for a given DER operating point $\boldsymbol{p}$ as

$$\boldsymbol{M_v}\,\boldsymbol{v} + \boldsymbol{k_v} \leq \boldsymbol{0} \tag{5.50}$$

$$\boldsymbol{M_v}\,(\boldsymbol{A_v}\,\boldsymbol{p} + \boldsymbol{k_v}) + \boldsymbol{k_v} \leq \boldsymbol{0} \tag{5.51}$$

Let

$$\boldsymbol{G} = \boldsymbol{M_v}\boldsymbol{A_v} \in \mathbb{R}^{2N_c \times N_c}$$

and

$$\boldsymbol{h} = \boldsymbol{M_v}\boldsymbol{k_v} + \boldsymbol{k_v} \in \mathbb{R}^{2N_c}$$

The feasible region for collective DER setpoints $\boldsymbol{p}$ with respect to voltage magnitude constraints is expressed as

$$\boldsymbol{G}\,\boldsymbol{p} + \boldsymbol{h} \leq \boldsymbol{0} \tag{5.52}$$

This formulation results in the same level of voltage magnitude constraint robustness as in [133], in the sense that all DER setpoints satisfying individual envelopes lie within a polytope, the edges of which are defined by voltage magnitude constraints throughout the network under a linearised power flow model. While the method presented in [133] was more elaborate and enabled application of a non-linear proportional-fairness objective, our goal in this Chapter is simply to demonstrate envelope feasibility with respect to a new class of constraints (voltage unbalance constraints) and assess the resulting impacts on network capacity available for allocation to DER.

5.3.5 Robust Optimisation Formulation

We now wish to generate envelopes $[\underline{\boldsymbol{p}}, \overline{\boldsymbol{p}}]$ such that all DER operating points $\boldsymbol{p}$ satisfying envelopes are within the network's feasible region.

Consider a hypothetical scalar constraint $ax + b \leq 0$, for x bounded by bounds $[\underline{x}, \overline{x}]$ and parameters a, b.

$$\max_{x \in [\underline{x}, \overline{x}]} (ax + b) = \begin{cases} a\overline{x} + b & \text{for } a \geq 0 \\ a\underline{x} + b & \text{for } a \leq 0 \end{cases} \tag{5.53}$$

Defining $(a^+) = \max(0, a)$ and $(a^-) = \min(a, 0)$, we can provide a direct expression for a constraint on (5.53) as follows

$$\max_{x \in [\underline{x}, \overline{x}]} (ax + b) \leq 0 \iff (a^+)\overline{x} + (a^-)\underline{x} + b \leq 0 \tag{5.54}$$

Applying this same principle to matrix inequalities constraints (5.47) and (5.52), we define matrices $\boldsymbol{E}^+, \boldsymbol{E}^-, \boldsymbol{G}^+, \boldsymbol{G}^-$ with entries $E_{ij}^+ = \max\left(0, E_{ij}\right)$ and $E_{ij}^- = \min\left(0, E_{ij}\right)$, and similarly for G_{ij}^+, G_{ij}^-. Envelopes $\underline{\boldsymbol{p}}, \overline{\boldsymbol{p}}$ are robust with respect to voltage unbalance and magnitude constraints if

$$(\boldsymbol{E}^+)\overline{\boldsymbol{p}} + (\boldsymbol{E}^-)\underline{\boldsymbol{p}} + \boldsymbol{f} \leq \boldsymbol{0} \tag{5.55}$$

$$(\boldsymbol{G}^+)\overline{\boldsymbol{p}} + (\boldsymbol{G}^-)\underline{\boldsymbol{p}} + \boldsymbol{h} \leq \boldsymbol{0} \tag{5.56}$$

We use a simple objective maximising the sum of customer imports and exports, however other objectives can be easily adopted. Each DER is modelled with a 5 kW inverter[4], and we assume that the idle position $p = 0kW$ must lie within each envelope. The complete formulation for our robust problem is

$$\max_{\underline{\boldsymbol{p}}, \overline{\boldsymbol{p}}} \sum_{i}^{N_d} \left(\overline{p}_i - \underline{p}_i\right) \tag{5.57}$$

subject to	(5.55), (5.56)	Voltage constraints
	$-5kW \leq \underline{p}_i \leq 0$	DER constraints
	$0 \leq \overline{p}_i \leq 5kW$	

[4]Derivations throughout Section 5.3 can be extended to derive envelopes for both real and reactive power using the same approach, imposing a restriction on reactive power availability according to inverter constraints. It was observed in simulations that reactive power envelopes were always driven to $[0kW]$, and this is due to the requirement for robustness assuming uncoordinated use of real and reactive power. Functional relationships between real and reactive power utilisation by DER could expand envelopes. This is future work.

5.4 Simulations

Our simulations consider a three-wire Kron's reduction of the IEEE 906-bus European Low-Voltage Feeder (where the neutral is assumed to be grounded everywhere) in Figure 5.1. We assign $N_d = 19$ customers with DER of a total of $N_b = N_c = 55$ single-phase customers, distributed across phases as tabulated in Table 5.1. We apply background load from the network's dataset at 6:00pm assuming a power factor of 0.95.

In our simulations we also introduce degrees of voltage unbalance between phases at the top-of-feeder substation. We have done this to engineer a scenario in which voltage unbalance levels (%VUF) across the network

1. Satisfy operational requirements under background loads only, but
2. Risk exceeding safe thresholds due to uncoordinated DER dispatch.

We have sought to apply our methodology to the IEEE 906-bus network due to its familiarity in the research community. However, its relatively small scale makes it challenging to induce voltage unbalance constraint violations without adjusting feeder-top settings. By priming the network through changing feeder-top-settings, we can demonstrate the utility of our approach when applied to real distribution networks in which voltage unbalance does represent a challenge to operators.

We consider two top-of-feeder settings for phase unbalance, namely:

- **Case A**: $V_a\angle\theta_a = 1.03\angle 0.1^\circ$, $V_b\angle\theta_b = 1.00\angle 0^\circ$ and $V_c\angle\theta_c = 0.97\angle -0.1^\circ$
- **Case B**: $V_a\angle\theta_a = 1.01\angle 1.5^\circ$, $V_b\angle\theta_b = 1.00\angle 0^\circ$ and $V_c\angle\theta_c = 0.99\angle -1.5^\circ$

Note phase angle offsets reported above indicate offsets with respect to balanced phase angles, which are each separated by 120 degrees.

The reason we pick two different top-of-feeder settings for unbalance is that changes to voltage magnitudes and phase angles will not always happen proportionately. In lossless networks, variation of squared voltage magnitude and phase angle over a branch is approximated by

$$\Delta \boldsymbol{v} = \boldsymbol{R}\boldsymbol{P} + \boldsymbol{X}\boldsymbol{Q} \tag{5.58}$$

$$\Delta \boldsymbol{\theta} = \boldsymbol{X}\boldsymbol{P} - \boldsymbol{R}\boldsymbol{Q} \tag{5.59}$$

for $\Delta \boldsymbol{v}, \Delta \boldsymbol{\theta} \in \mathbb{R}^3$ representing variations of squared voltage magnitudes and phase angles along a branch for each phase, $\boldsymbol{P}, \boldsymbol{Q} \in \mathbb{R}^3$ representing real and

TABLE 5.1: Customers with DER

Phase A	1, 4, 22, 25, 31, 34, 52, 55	(8 of 21 customers)
Phase B	7, 10, 13, 37, 40, 45	(6 of 19 customers)
Phase C	16, 19, 28, 42, 43	(5 of 15 customers)

reactive power flowing along the branch, and $\boldsymbol{R}, \boldsymbol{X} \in \mathbb{R}^{3\times 3}$ representing the resistance and reactance matrices of the branch. The impacts of unbalanced load flows on voltage magnitudes and phase angles therefore depend on the line characteristics where unbalanced flows occur, and the power factor of the unbalanced loads. Where unbalanced loads have a power factor close to 1, and occur in low-voltage feeders where lines are mainly resistive, phase angles are more likely to remain 120 degrees from each other. On the other hand, where unbalanced loads have a significant reactive component (inductive loads such as HVAC), of when unbalanced loads occur in medium-voltage portions of networks (where lines have greater reactance), phase angles are more likely to become unbalanced.

We will demonstrate how our optimisation-based approach handles instances of voltage unbalance with varying degrees of phase angle unbalance differently. We conduct two types of studies:

- We begin by assessing the accuracy of linLVUR as a proxy for the LVUR. This analysis seeks to quantify the impacts of linearisation error on our approach.
- We then seek to demonstrate the utility of voltage unbalance constraints in practice. We calculate operating envelopes under the conventional approach suitable for single-phase networks, the RDOE approach and our proposed RDOE+VUF approach, at each stage commenting on the increase in envelope robustness and the associated decrease in capacity allocated to DER.

5.4.1 Accuracy of linLVUR as proxy for LVUR

Our first study investigates whether linLVUR can provide a suitable approximation for LVUR in order to bound VUF according to (5.17). The accuracy of linLVUR with respect to LVUR may be affected by approximations in our model, both inherited from [42] and caused by linearisations in our derivations.

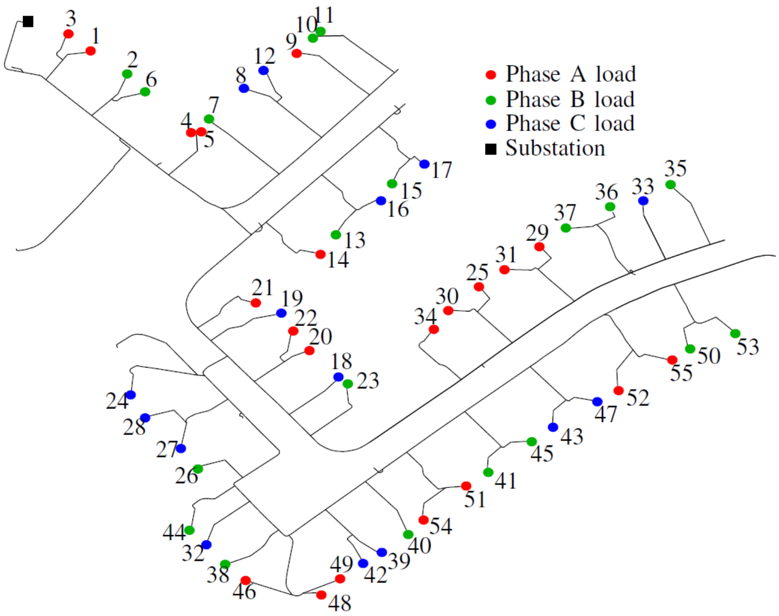

FIGURE 5.1: IEEE 906-bus LV feeder with customers [144]

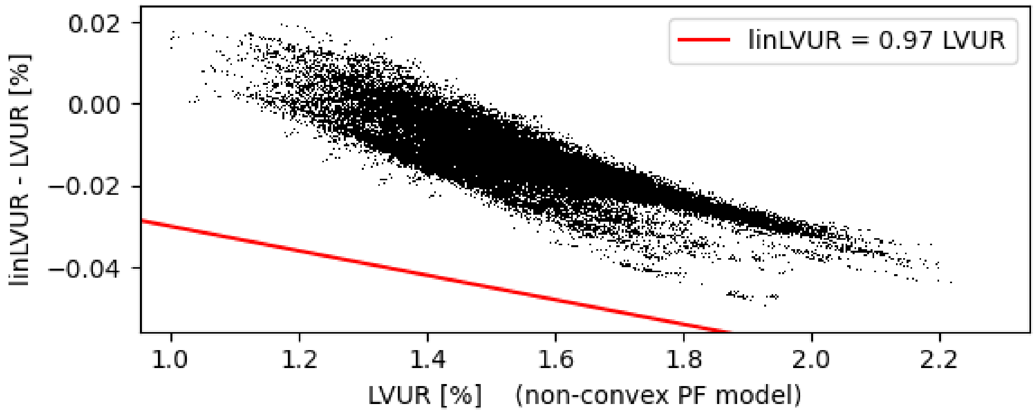

FIGURE 5.2: Error of linLVUR with respect to LVUR

We begin by calculating operating envelopes satisfying voltage magnitude constraints, and generating 1000 scenarios in which each DER is dispatched within its assigned operating envelope. For each scenario, we use a non-convex power flow model to evaluate the true value of LVUR at all 55 customer nodes (producing 55,000 datapoints). We also calculate linLVUR, the approximation of these LVUR values, as a function of DER operating points, and we plot the errors of linLVUR values with respect to their LVUR targets in Figure 5.2.

We observe that

$$0.97\text{LVUR} \leq \text{linLVUR} \leq \text{LVUR}$$

in all modelled cases. This tight error distribution indicates linLVUR represents a suitable tool for estimating LVUR. It follows that by setting

$$\mu' = 0.97\frac{\sqrt{3}}{2}\lambda = 0.840\lambda$$

then we have

$$\text{linLVUR} \leq \mu' \implies \text{VUF} \lesssim \lambda$$

according to (5.16). Voltage magnitude constraints were satisfied in all cases evaluating power flows using the non-convex power flow model.

5.4.2 Rectification of Inherited Unbalance

Having demonstrated that linLVUR represents a suitable proxy for the LVUR, we now use linLVUR to calculate operating envelopes that constrain voltage unbalance for any collective DER setpoint satisfying individual consumer envelopes.

To benchmark, we first calculate envelopes using the conventional approach taken in single-phase networks (verification of network feasibility for two extreme operating points). Simulations showed that all network constraints were satisfied in the case that all DER maximised their exports, and also when all DER maximised their imports, meaning that all DER were assigned their full inverter capacity.

We then re-calculate envelopes using the robust dynamic operating envelopes (RDOE) approach without unbalance constraints, and finally with the inclusion of phase unbalance constraints ($\mu' = 1.68\%$ for $\lambda = 2\%$). We repeat this experiment for two instances of feeder-top unbalance (cases A and B), in order to demonstrate differences in remedial action when voltage unbalance is primarily due to unbalance in voltage magnitude or phase angle.

Case A: Unbalance Due Primarily to Voltage Magnitudes

In Case A, voltage unbalance is primarily due to differences in voltage magnitudes between phases. Envelopes obtained without and with unbalance constraints are plotted in 5.3. When factoring risks of voltage magnitude constraint violations due to mutual impedances (RDOE), average export capacity assigned to DER customers is curtailed by 0.19 kW (from 5 kW to 4.81 kW), and average import capacity is curtailed by 1.94 kW (from 5 kW to 3.06 kW). This results in average envelope size of 7.87 kW.

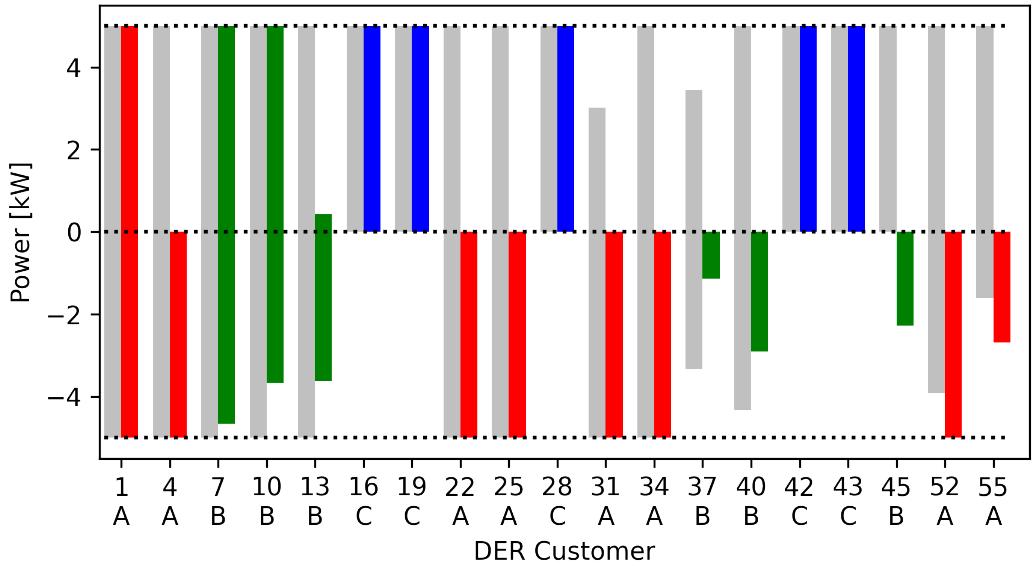

FIGURE 5.3: Case A: Robust Dynamic Operating Envelopes without (grey) & with (phase colour) unbalance constraints

When voltage unbalance constraints are added to envelope construction, the reduction in overall envelope size is more drastic, with average envelopes reducing from 7.87 kW to 5.44 kW. Envelope construction is clearly steering the network towards rectifying unbalance between phases:

- Phase A: Most export capacity assigned by the RDOE approach is curtailed, and customers 52 and 55 are assigned even greater load capacity than using RDOE. This is expected as reducing voltage on phase A would reduce unbalance in the system.
- Phase B: Both imports and exports are additionally curtailed with respect to RDOE.
- Phase C: All load capacity was already curtailed, and it retains all export capacity assigned by RDOE.

These outcomes are consistent with trying to bring voltages back towards 1p.u., which is the feeder-top setting for phase B.

Case B: Unbalance Due to Significant Phase Angle Differences

In Case B, voltage unbalance is primarily due to significant differences in phase angle with respect to the reference value for each phase. Envelopes obtained without and with unbalance constraints are plotted in 5.4. When factoring risks of voltage magnitude constraint violations due to mutual impedances (RDOE), average export capacity assigned to DER customers is

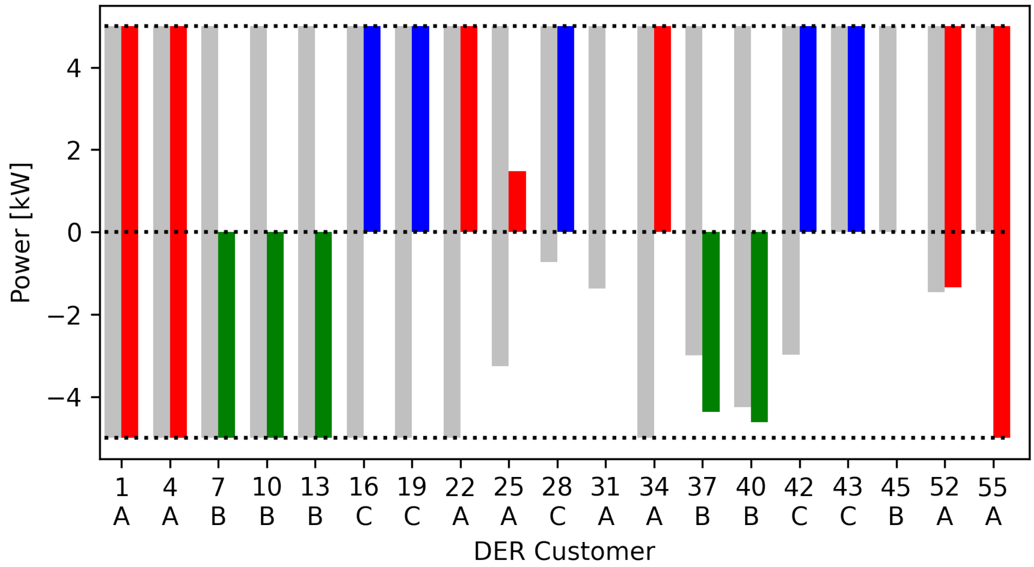

FIGURE 5.4: Robust Dynamic Operating Envelopes without (grey) & with (phase colour) unbalance constraints in Case B (voltage unbalance is primarily due to phase angle differences)

the full 5 kW per customer, and average import capacity is curtailed by 1.74 kW (from 5 kW to 3.26 kW). This results in average envelope size of 8.26 kW.

When voltage unbalance constraints are added to envelope construction, average envelope size reduces from 8.26 kW to 5.10 kW. Although the top-of-feeder settings were intended to be consistent with Case A (in the sense that phase A has a leading phase shift due to exports, phase B is given its reference value, and phase C has a lagging phase shift due to load), the outcomes in terms of envelopes obtained have led to different impacts across feeders:

- Phase A: Only one customer had export capacity curtailed, and only one customer was assigned additional import capacity.
- Phase B: While the feeder-top settings for Phase B bisected the equivalent settings for Phases A and C, the envelopes obtained for customers on Phase B are very asymmetric. All generation capacity is curtailed on Phase B, and customers 37 and 40 are granted additional load capacity.
- Phase C: Full generation capacity is retained, and all load capacity is curtailed.

These results demonstrate that even though the feeder-top voltage settings in Cases A and B both have similar symmetry (Phase B given reference values, and Phases A and C given opposite variations), our formulation applies different strategies on a per-phase basis depending on the extent to which

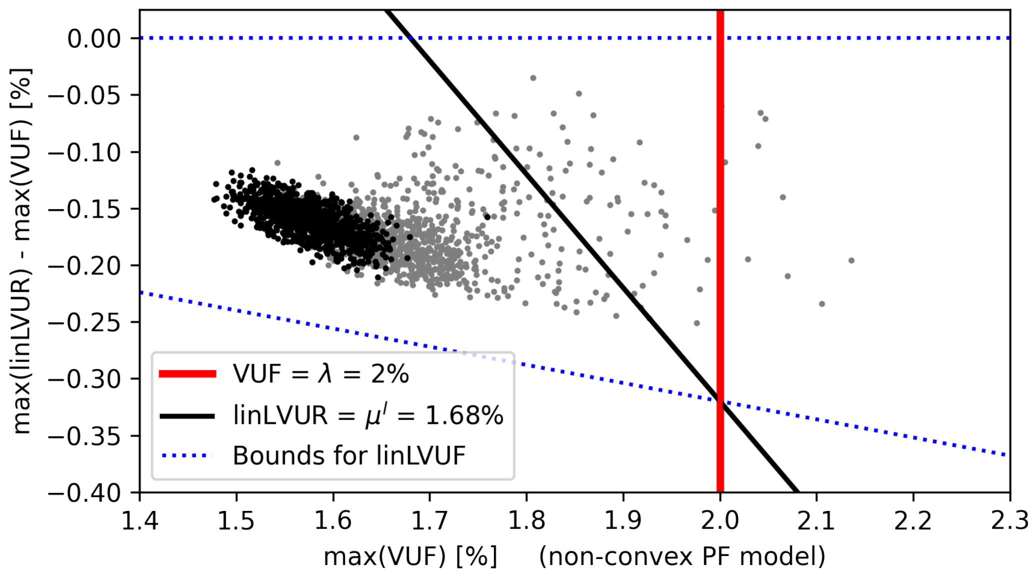

FIGURE 5.5: Maximum VUF observed and linLVUR calculated in Monte Carlo simulations using envelopes without (grey) and with (black) unbalance constraints.

voltage unbalance is caused by voltage or phase angle variations.

Conservatism

The introduction of phase unbalance constraints significantly curtails envelope size, so it worth considering whether there are unnecessary sources for conservatism of results. To analyse this, for the first instance of top-of-feeder unbalance, we have randomly generated 1000 potential collective DER setpoints satisfying RDOE envelopes (only voltage magnitudes) and RDOE+VUF envelopes (satisfying voltage magnitude and voltage unbalance constraints). In each case, we evaluate power flows in the network using a non-convex power flow model, and plot the maximum value for (a) voltage unbalance factor, and (b) our linLVUR proxy.

We plot our results in Figure 5.5. While the VUF value exceeds the 2% threshold when voltage unbalance constraints are not applied in envelope construction, the VUF value is limited to $\approx$ 1.6% when constraints are applied. One source for this conservatism is the fact the linLVUR metric can vary from the value of VUF by up to $\approx$ 15%. This is illustrated by the slope of the black constraint boundary representing linLVUR $= \mu'$. Increasing μ' to values closer to 2% may have the effect of increasing overall capacity allocations, however this would result in a less robust approach. Increasing μ' would have the effect of translating the black line in Figure 5.5 to the right, and would in theory enable VUF in simulation outcomes to be exceeded in scenarios where there is significant error between linLVUR and VUF.

Another significant source of this conservatism is due to the requirement that envelopes ensure secure network operation for any arbitrary combinations of inputs, even highly implausible cases. To illustrate this, we consider the collective DER operating point obtained when

- All DER on Phase A operate at their assigned export limit
- All DER on Phase B operate at their assigned export limit
- All DER on Phase C operate at their assigned export limit

We construct this operating point for envelopes in Case A calculated by applying our phase unbalance constraints (i.e. coloured bars in Figure 5.3), apply the same background loads as previous experiments, and use a non-convex power flow model to evaluate the voltage unbalance factor at all customer locations.

Doing so, we found that the highest value for voltage unbalance factor (true value) reached 1.88% (the value of the linLVUR was equal to $\mu' = 1.68\%$ corresponding the constraint being binding), which is significantly higher than what was recorded across almost all outcomes obtained through randomised dispatch. This demonstrates that ensuring robustness in cases of implausibly unbalanced utilisation of envelopes may result in significant penalties in terms of capacity available for allocation, for relatively little practical benefit - in these simulations only 9 constraint violations were observed our of 1000 scenarios, and the highest observed VUF measurement in simulations reached only 2.1%.

5.5 Discussion

In practice, data-driven solutions could be used to determine if there exists some threshold of unbalance in DER actions which should be accounted for in envelope construction, as a means to build a more appropriate level of robustness in the system. Unfortunately, such an approach would need to be tailored to observations made in a particular feeder, and differences in structure between feeders may cause these results to not be very generalisable. In this thesis we are motivated to determine whether an analytical approach can be developed to ensure robust outcomes without being prohibitively conservative in capacity allocations.

In the case of the RDOE paper, which focused on the magnitude component of voltage constraints, the authors of [133] calculate envelopes under the preconditions that the status of each DER is known as either importing or exporting, and this would mitigate our challenges to a degree. We note that many DER participate in reserve markets that procure both raise and lower services as discussed in Chapter 4. As a result, it is at least in theory possible for some batteries to charge due to low wholesale prices, then a contingency event causes a subset of DER (e.g. one aggregator bidding in a competitive manner) to suddenly provide raise services. Battery storage at the distribution scale may also be tailored to different consumers' behaviours, for instance some DER may provide market services while others decide to charge in expectation of significant power usage by the consumer. For this reason, we are motivated to explore whether there is potential for a robust solution to ensure both voltage magnitude and unbalance constraint satisfaction without explicit conditions on whether a connection point will import or export.

Conservatism in this approach is largely driven by our desire to "hard-wire" robustness with respect to unbalance constraints for any dispatch outcome. This appears to be overly conservative, and alternative approaches should be considered. One alternative approach is to manage network-operated equipment such as a parallel converter at the top of the feeder, to perform current balancing between phases and power factor correction as discussed in [145]. Another alternative approach, which we will study in Chapter 6, is to exploit existing opportunities for DER coordination to expand network-feasible capacity allocations. In particular, we will explore whether aggregators can be assigned more complex forms of capacity allocations, rather than individual envelopes defined on a per-DER basis, allowing for more effective robust partitioning of a network's feasible operating region accounting for all forms of voltage constraints.

5.6 Conclusion

Simulations have demonstrated that our formulation achieves its intended goal. We have demonstrated that in networks susceptible to voltage unbalance constraint violations caused by DER dispatch, the *robust dynamic operating envelope* formulation in literature may not prevent voltage unbalance constraint violation. Our proposed approach in this chapter expands the voltage feasibility criteria considered in the RDOE approach to include voltage unbalance constraints, and simulations show that our proposal prevents voltage unbalance constraint violations. Results demonstrate that including voltage unbalance constraints in envelope construction steers DER towards rectifying unbalance in the network through envelopes biased according to their phasing.

However, the bar charts of operating envelopes obtained in our case studies indicate that the robustness we seek imposes a significant penalty on the total capacity that can be made available. Specifically, we note that simulations applying our approach result in voltage unbalance values that consistently remain significantly less than the threshold set in our constraints, and overall capacity allocated to DER is significantly reduced.

This makes sense when recognising that the most 'at risk' scenarios for DER dispatch occur when all DER on a given phase maximise their real power exports, all DER on a different phase maximise their real power imports, and the third phase takes one of these two extreme positions. While this is technically possible, our formulation ensures robustness to an *extremely* unlikely scenario in practice. This motivates our approach in the next chapter, which exploits an existing opportunity for DER coordination that enables us to deliberately exclude such scenarios when formulating robust methods of allocating network capacity. We do so using an existing opportunity to coordinate DER dispatch carefully within operating envelopes in the form of aggregators.

Chapter 6

Robust Aggregator Operating Regions & Flexible Dispatch Envelopes

This Chapter extends existing literature on operating envelopes in unbalanced systems by considering the opportunity for aggregators to expand network-secure allocations of capacity through coordination of their customers.

6.1 Introduction

Calculating operating envelopes through an optimisation process requires defining and optimisation objective, and setting constraints to ensure these envelopes satisfy network feasibility criteria. Chapters 4 and 5 have studied these two aspects respectively.

- Chapter 4 demonstrated the potential benefits of including market valuations of energy and reserve services into the optimisation objective in order to maximise the market efficiency of outcomes, and
- Chapter 5 proposed adaptations to optimisation constraints when calculating envelopes in three-phase unbalanced networks in order to ensure envelopes continue to satisfy the conventional network security criteria of DOE.

It was noted in the results of simulations in Chapter 5 that attaining envelope robustness in the unbalanced three-phase context, protecting from highly improbable combinations of DER setpoints in practice, could severely penalise the optimisation objective. Motivated by this challenge, we now consider opportunities for additional coordination that may enable network operators to safely unlock greater distribution network capacity while maintaining robust network security guarantees in the unbalanced three-phase case.

In this Chapter, we explore whether aggregators can provide such a mechanism through their ability to coordinate their customers in groups[1]. It is often the case that large fleets of dispatchable storage in distribution systems are controlled by a smaller number of aggregators. In the simplest case, some academic studies assume the DSO performs the role of an aggregator for all DER in a network, providing a single agent with full network visibility the freedom to disaggregate market dispatch outcomes in an optimal manner.

In practice, as observed in Australia, multiple aggregators (including companies such as battery manufacturers, utility-scale asset operators to small tech startups) offer to fulfil the role acting as intermediaries between customers and wholesale markets. These entities are separate from the network operators, and therefore these aggregators may be subjected to forms of curtailment during peak periods. Operating envelopes specific to individual consumers at the DER-scale represent one possible way of curtailing DER participation in markets, and aggregators' capability to coordinate subsets of their DER fleets may enable more flexible partitions of network capacity, resulting in better coverage of the feasible collective operating region for DER in the network.

To begin this Chapter, we present a case study which extends what exists in the literature. While [133] and our prior work have established the theoretical potential for constraint violations in unbalanced three-phase networks when assigning envelopes that are only validated at two extreme setpoints, it remains to be seen whether there is any likelihood of this occurring in a scenario of plausible unbalance in loads across phases when

- most DER are operated by aggregators
- each aggregator's market dispatch outcome at the feeder scale is disaggregated to the DER-scale according to a simple method
- each aggregator's fleet is fairly evenly split between all available phases.

[1]Our approach to modelling aggregators' coordination of DER is different to what we studied in Chapter 4. In Chapter 4 we assumed the need to model each asset's economic costs (reflected in bid prices) down to DER-specific granularity. This results in bid stacks defined for each DER. It is also possible that in practice aggregators may instead choose to have greater flexibility in how they dispatch DER to meet market obligations, and instead pool economic benefits between their customers then redistribute these according to a different business model.

This chapter extends literature on robust coordination of DER by considering the role of aggregators. Without performing this study, we may be ignoring the possibility that conventional approaches undertaken by aggregators operating DER fleets naturally reduce risks of voltage magnitude and unbalance constraint violations specific to the unbalanced three-phase case. For this reason, we ask ourselves the question:

If a small group of aggregators represent a large number of DER participating in the wholesale market, and if aggregators disaggregate market dispatch outcomes to DER according to simple dispatch disaggregation techniques, does there remain a material risk of network constraint violation if operating envelopes are calculated by verifying network feasibility of only two extreme points (e.g. method from Chapter 4), for a plausible scenario[2] of unbalanced loading across phases?

We will study the impacts of aggregators' methods of disaggregating feeder-scale market dispatch outcomes (to individual consumers) on network constraint violations, under envelopes calculated using the conventional approach from Chapter 4 (suitable for single-phase networks).

6.1.1 Motivating Case Study

Experimental Setup

We study the three-wire Kron's reduction of the IEEE 906-bus European Low-Voltage Feeder (where the neutral is assumed to be grounded everywhere), which operates at a voltage of 240V (compared to 11.6 kV for the MV network used in Chapter 4), requiring that customer voltages remain within $[0.94, 1.1]$ per unit. In this study, we expand DER participation to 49% uptake (27 of 55 customers), with each DER customer assigned a 5 kW home battery, and a 5 kW solar PV system (which we consider to be uncurtailable). In this Chapter, we source background load and solar generation data from anonymised smart meter data from Canberra ACT, Australia, plotted in Figure 6.1. All traces used for household load were sourced from the same study and are contemporaneous in time. All simulations in this Chapter assume the same load trace per household, and all simulations conducted in Section 6.1.1 study the network under loads at 7pm.

[2]Load scenario defined in Section 6.1.1

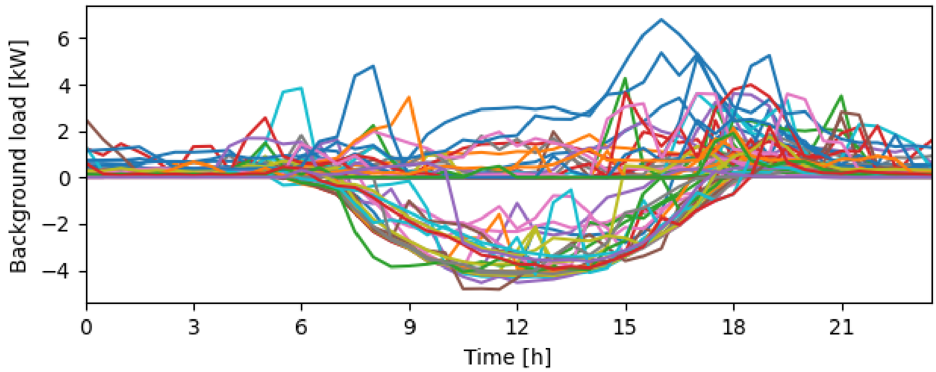

FIGURE 6.1: Real residential background load and solar PV data (summed) for 55 customers at half-hour granularity from smart-meter data in Canberra ACT, Australia

At 7pm, most customer loads in our study can be categorised as "light" (less than 1kW), representing:

- Phase A: 12/21 customers (57%)
- Phase B: 15/19 customers (79%)
- Phase C: 11/15 customers (73%)

The remaining households have the following average loads at 7pm:

- Phase A: 9 customers with average load of 2.63 kW
- Phase B: 4 customers with average load of 2.65 kW
- Phase C: 4 customers with average load of 1.37 kW

The average customer loads per phase are 1.453 kW for phase A, 0.863 kW for phase B and 0.664 kW for phase C.

Distribution system operators are responsible for managing network constraints under any plausible network utilisation scenario. Given the sporadic nature of electricity consumption in small samples (less than 21 dwellings per phase), and the relatively low overall electricity consumption, it is our view that the scenario defined above represents a plausible level of unbalance in loading across phases. For some context, it was noted in [146] that a study conducted by the University of Bath found that of 800 data-rich LV substations in the UK with measurements at 15-minute granularity, more than 50% suffer from serious phase unbalance, where the peak current of the "heaviest" phase exceeds that of the "lightest" phase by a minimum of 50%.

TABLE 6.1: Aggregator DER Customers

	Agg. 1	Agg. 2	Agg. 3	
Phase A	1, 5, 48	3, 9, 54	14, 49, 55	(9 of 21 customers)
Phase B	10, 15, 38	23, 36, 40	7, 26, 50	(9 of 19 customers)
Phase C	8, 17, 32	12, 27, 43	16, 19, 39	(9 of 15 customers)

The market participation of DER customers is managed by three aggregators. We choose to assign each aggregator an *equal aggregate DER capacity* before any curtailment, and in each case, this capacity is distributed *evenly* between all three phases. Explicitly, each aggregator is assigned 15 kW (3 customers with $[-5kW, 5kW]$ dispatchable capacity each) of dispatchable DER capacity on each phase, making $[-45kW, 45kW]$ dispatchable capacity per aggregator, and also corresponding to a total of $[-45kW, 45kW]$ dispatchable capacity on each phase across all aggregators. The breakdown of each aggregator's portfolio is outlined in Table 6.1, and customer locations are shown in Figure 5.1.

Operating Envelopes Defined By Two Feasible Operating Points

We begin by calculating operating envelopes in the conventional manner (suitable for a single-phase network), as performed in Chapter 4, maximising the sum of envelope size. The operating envelopes we obtain, tabulated in Table 6.2, result in aggregators 2 and 3 commanding less dispatchable load capacity on phase A than on phase C. In total, DER load capacity across all aggregators is reduced by 14% on phase A and 5% on phase B.

When verified using a non-convex power flow model, network constraints were satisfied in the cases where all DER operated at setpoints $\underline{p}$ and $\overline{p}$.

Demonstration of Network Constraint Violation

Respecting these envelopes, we generate 1,000 potential scenarios of wholesale market dispatch outcomes at the aggregator scale (i.e. each market dispatch outcome is represented by only three scalars), simulating the potential variability between outcomes in the wholesale market between different aggregators. We maintain the same background loads across all scenarios for consistency, to highlight the impact of the manner of disaggregation on the feasibility of results.

In our first study we assume that aggregators then disaggregate their market dispatch outcomes to their customers *proportionally* to customer envelope sizes (i.e. if 20% of an aggregator's total capacity is dispatched in the market, each

TABLE 6.2: DER Operating Points $\underline{p}$ & $\overline{p}$ Collectively Satisfying Network Constraints

Phase A			Phase B			Phase C		
Cust.	$\underline{p}$ $[kW]$	$\overline{p}$ $[kW]$	Cust.	$\underline{p}$ $[kW]$	$\overline{p}$ $[kW]$	Cust.	$\underline{p}$ $[kW]$	$\overline{p}$ $[kW]$
1	−5	5	10	−5	5	8	−5	5
5	−5	5	15	−5	5	17	−5	5
48	−5	5	38	−5	5	32	−5	5
Agg1	−15	15	Agg1	−15	15	Agg1	−15	15
3	−5	5	23	−5	5	12	−5	5
9	−5	5	36	−5	5	27	−5	5
54	−0.8	5	40	−5	5	43	−5	5
Agg2	−10.8	15	Agg2	−15	15	Agg2	−15	15
14	−5	5	7	−5	5	16	−5	5
49	−4.8	5	26	−5	5	19	−5	5
55	−3	5	50	−2.7	5	39	−5	5
Agg3	−12.8	15	Agg3	−12.7	15	Agg3	−15	15
Total	−38.6	45	Total	−42.7	45	Total	−45	45

DER will be dispatched to 20% of its import or export envelope size). For each dispatch scenario, we record the lowest voltage observed across customer locations, and plot these as a function of total dispatch summed across all aggregators.

We observe in Figure 6.2 that in the event aggregators disaggregate their dispatch proportionally to their individual DER envelope sizes, in 10 instances (1%) there is a voltage magnitude constraint violation. Albeit small, these constraint violations may trigger recourse actions in the network incurring costs and inconvenience.

This result has some significance for the network-wide constraint framework proposed in [129]. In their formulation, it is assumed that only one aggregator operates all DER in the network, and this aggregator dispatches DER proportionally to allocated envelope size (called a *u*-function). Our results here demonstrate that when multiple aggregators co-exist in a network (i.e. in the case the aggregator is a private entity different to the DSO), network constraint violations may occur even if aggregators dispatch DER within curtailed envelopes *proportionally* to their envelope size.

In practice, aggregators may also choose to disaggregate their market dispatch outcomes in arbitrary manners. While voltage magnitude constraint violations were small in the case study above, we now demonstrate the potential

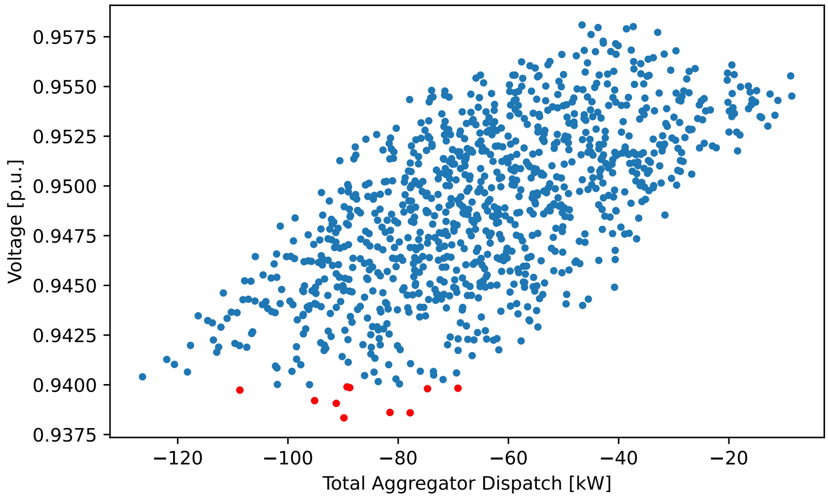

FIGURE 6.2: Minimum recorded voltage magnitudes at customer locations as a function of total aggregator dispatch for *proportional disaggregation*

for much greater voltage magnitude constraint violations under alternative disaggregation strategies, namely

- **Randomised**: Aggregators disaggregate their wholesale market dispatch outcomes randomly between DER customers, ensuring each satisfies individual envelopes. Under this policy aggregators may only deploy a subset of their DER if their wholesale market dispatch result is small.
- **Merit order**: Aggregators privately compute DER-specific dispatch costs (capturing projected needs of customers with self-consumption preferences, or distribution of battery cycling). These variable costs produce a dynamic merit order hidden from the DSO. Aggregators minimise their dispatch costs by maximising dispatch of their cheapest DER first within their respective operating envelopes.

For both disaggregation strategies listed above, we enable a meaningful comparison to the proportional dispatch case by re-using the same 1000 hypothetical cases of aggregators' aggregated (sum) dispatch in the wholesale market.

In the case of randomised disaggregation of market dispatch outcomes, 121 voltage constraint violations were recorded (12.1% of cases), and the lowest voltage magnitude was recorded as 0.9289 p.u. This occurred in a scenario when overall aggregator dispatch was only 60 kW (less than half of the 126 kW made available to the wholesale market). In the case of disaggregation of market dispatch outcomes based on a merit order approach, 215 voltage constraint violations were recorded (21.5% of cases), and the lowest voltage

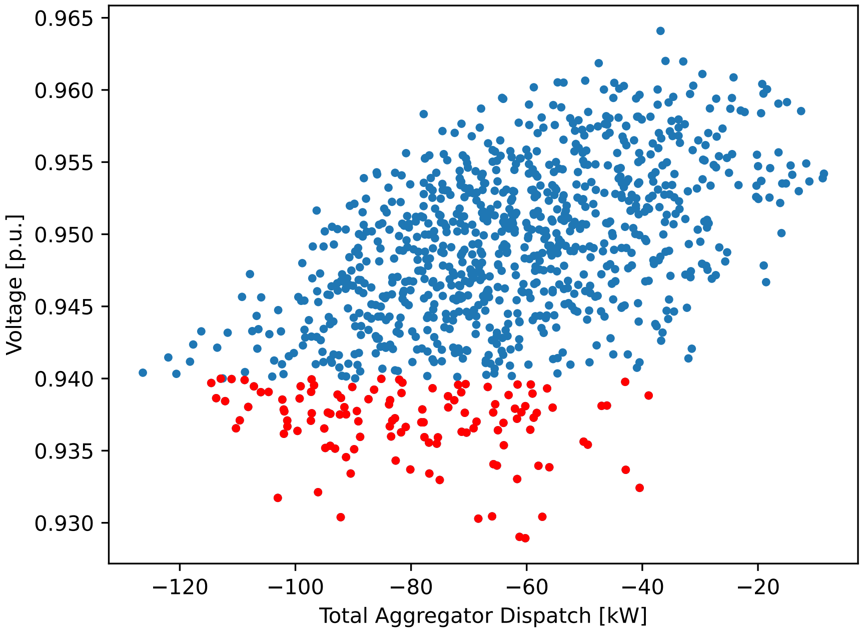

FIGURE 6.3: Minimum recorded voltage magnitudes at customer locations as a function of total aggregator dispatch assuming *randomised disaggregation*

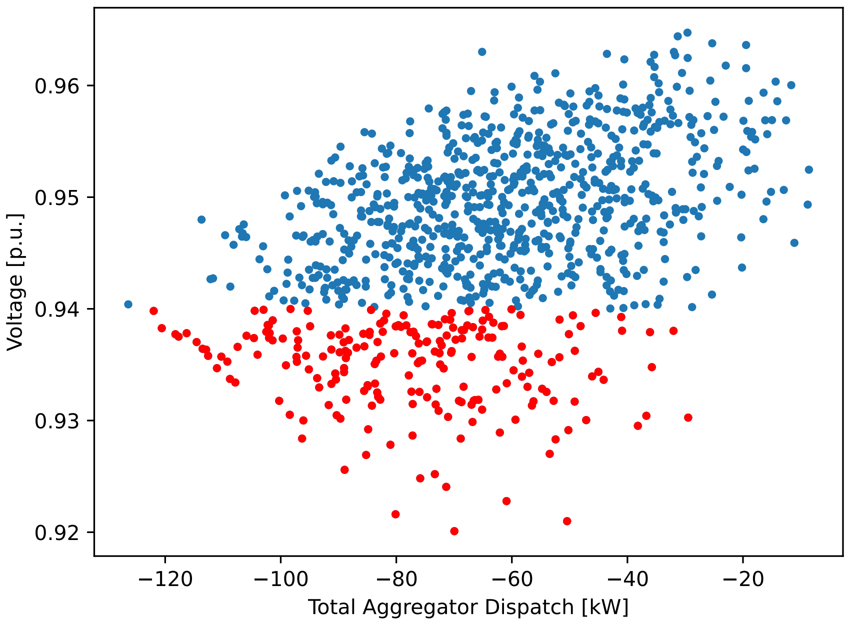

FIGURE 6.4: Minimum recorded voltage magnitudes at customer locations as a function of total aggregator dispatch assuming disaggregation according to merit order

magnitude was recorded as 0.9200 p.u. This occurred in a scenario when overall aggregator dispatch was only 70 kW (only 55% of the 126 kW made available to the wholesale market).

Further analysis revealed that voltage constraint violations generally occur under the more unbalanced loading conditions between phases, and this is consistent with our expectations given the results of Chapter 5.

These results demonstrate there remains a material risk of voltage constraint violations in unbalanced three-phase distribution networks, as demonstrated in [133] and discussed in Chapter 5, in the event of unbalanced loading across phases, if DSOs assign operating envelopes by only checking two operating points *and aggregators disaggregate market dispatch outcomes amongst DER in plausible ways*, particularly in the context of unbalanced background loads.

Robust approaches discussed and developed in Chapter 5 represent one solution to achieving robustness, however we have previously demonstrated that these methods ensure robustness with respect to extreme dispatch scenarios that aggregators collectively are well-placed to prevent from occurring. This motivates our development of a new approach.

6.1.2 Overview of Approach

In this chapter we propose Robust Aggregator operating Regions with flexible Dispatch Envelopes (RAR-DE). The primary distinction of our work compared to the literature is that we leverage aggregators' ability to coordinate their customer dispatch in groups. This coordination allows the DSO to provide structured allocations of network capacity that better span the underlying feasible operating region of unbalanced distribution networks. As a result, aggregators can provide a wider range of capacity to wholesale markets without risking voltage constraint violations in unbalanced distribution networks.

Previously under the RDOE approach (including with our proposed unbalance constraints), the requirement for collective DER *operating regions* (envelopes defined at DER-scale allowing independent operation) to take the form of hyper-rectangular regions aligned with the axes of the space describing each DER's dispatch (see footnote 3 in Chapter 3) had a restrictive effect on total network capacity available for allocation. To provide a geometric interpretation, this is because non-zero mutual impedances between phases have the effect of distorting an unbalanced network's underlying *feasible region* (often defined primarily by voltage constraints) into a slight parallelepiped shape. Network-feasible DER setpoints that result in high feeder-scale imports and exports, generally found in the extreme corners of this parallelepiped, become inaccessible to the hyper-rectangular DER *operating regions*.

Instead, we will derive Robust Aggregator operating Regions (RAR) through robust polytopic projection of the network's feasible region onto aggregator-specific subspaces, within which aggregators can play a coordination role. We note that adherence to complex projected polytopic regions represents additional complexity for aggregator operations. To facilitate aggregator adherence to their robust assigned regions, we propose market-responsive flexible *dispatch envelopes* (DE) at the DER-level, that aggregators can compute with trivial complexity when the market clears using simple scalar functions already derived by the DSO.

To summarise, our key contributions are:

- Robust Aggregator operating Regions (RAR), a flexible framework for allocating network capacity to aggregators in a network-safe manner in unbalanced networks. We leverage opportunities for coordination between customer groups to expand feeder-scale capacity allocations when compared to existing robust approaches in unbalanced systems.
- Market-responsive Dispatch Envelopes (DE) for DER, a simple framework for aggregators to adhere to complex robust aggregator regions when satisfying feeder-scale market dispatch outcomes. These DER-level envelopes adjust to market outcomes according to scalar affine functions defined by the DSO. When the market clears, aggregators can compute envelopes immediately through trivial computations, ultimately producing envelopes of the same structure as obtained by conventional dynamic operating envelope approaches.

6.2 Robust Aggregator Operating Regions (RAR) Ensuring Network-Security

In this section, we first derive the network-feasible operating region for DER in an unbalanced distribution network, as if all DER were hypothetically centrally controlled. We then calculate robust operating regions for each aggregator by applying a robust polytopic projection of the network's feasible region on a collection of subspaces representing the control domain of each individual aggregator, and demonstrate how this process can be optimised to maximise total aggregator capacity that can be traded in wholesale markets.

6.2.1 Power Flow Model and Network Feasible Region

We apply the linearised power flow model for multi-phase radial networks proposed in [42] to obtain expressions for network state variables as a function of DER setpoints[3]. Let $N^d \in \mathbb{N}$ represent the total number of DER customers in the network, and let $\boldsymbol{p} \in \mathbb{R}^{N^d}$ represent real-power setpoints of all DER in the network.

Our operational constraints consist of upper and lower bounds applied to voltage magnitudes at customer locations (at node-phase granularity). Let $N^c \geq N^d \in \mathbb{N}$ represent the total number of customers (DER and non-DER), resulting in $2N^c$ total scalar network constraints. We apply fixed background loads across network customers, then express power flow equations. We compile these scalar constraints in matrix form, then isolate variables representing squared voltage magnitudes. This allows us to express squared voltage magnitudes in the form

$$\boldsymbol{v} = \boldsymbol{V}\boldsymbol{p} + \boldsymbol{v^0} \tag{6.1}$$

where $\boldsymbol{V} \in \mathbb{R}^{N^c \times N^d}$ is a coefficient matrix, and $\boldsymbol{v^0} \in \mathbb{R}^{N^c}$ represents the squared voltage magnitudes at each customer location under the background-only scenario when dispatchable DER are idle. We impose network operational constraints in the form of the system

$$\boldsymbol{A^v}\boldsymbol{v} + \boldsymbol{b^v} \leq \boldsymbol{0} \tag{6.2}$$

where $\boldsymbol{A^v} \in \mathbb{R}^{2N^c \times N^c}, \boldsymbol{b^v} \in \mathbb{R}^{2N^c}$. Substituting the expression for squared voltage magnitudes, we obtain

$$(\boldsymbol{A^v}\boldsymbol{V})\boldsymbol{p} + (\boldsymbol{A^v}\boldsymbol{v^0} + \boldsymbol{b^v}) \leq \boldsymbol{0} \tag{6.3}$$

$$\boldsymbol{A}\boldsymbol{p} + \boldsymbol{b} \leq \boldsymbol{0} \tag{6.4}$$

where $\boldsymbol{A} \in \mathbb{R}^{2N^c \times N^d}, \boldsymbol{b} \in \mathbb{R}^{2N^c}$. This linear expression defines the network's underlying feasible operating region for DER with respect to voltage con-

[3]The linearised power flow model in [42] introduces small linearisation errors. We evaluate our approach using Monte Carlo simulations in Section IV using a non-convex power flow model. We will show that linearisation errors are small, and can be compensated by applying small buffers to voltage bounds (in our case only ~ 0.002p.u.). Linearisation effects are small compared to the effects of mutual impedances observed in our results

straints under a linear model, which we denote $\mathcal{F} \subset \mathbb{R}^{N^d}$. The process above is also described in more detail in [133].

6.2.2 Robust Polytopic Projection of the Network Feasible Region onto Aggregator Sub-Domains

We now demonstrate how this region can be partitioned favourably between aggregators. Let $N^a \in \mathbb{N}$ represent the number of aggregators in the network, each operating $N^d_a \in \mathbb{N}$ DER customers. We assume that all DER are operated by aggregators, even if $N^d_a = 1$ for some aggregators a. We group DER according to their aggregators, and re-express $\boldsymbol{p}$ as a concatenation of aggregator-specific DER real power dispatch vectors

$$\boldsymbol{p}^\top = \left[\boldsymbol{p}^{\boldsymbol{1}^\top} \dots \boldsymbol{p}^{\boldsymbol{N^a}^\top}\right] \tag{6.5}$$

with $\boldsymbol{p^a} \in \mathbb{R}^{N^d_a}$ for $a \leq N^a$. We aim to derive aggregator regions $\boldsymbol{\mathcal{R}^a} \subset \mathbb{R}^{N^d_a}$ for each aggregator's collective DER setpoint $\boldsymbol{p}^a$ such that

$$\forall a \leq N^a : \boldsymbol{p^a} \in \boldsymbol{\mathcal{R}^a} \implies \boldsymbol{p} \in \boldsymbol{\mathcal{F}} \tag{6.6}$$

or equivalently

$$\boldsymbol{\mathcal{R}^1} \times \boldsymbol{\mathcal{R}^2} \times \cdots \times \boldsymbol{\mathcal{R}^{N^d_a}} \subseteq \boldsymbol{\mathcal{F}} \tag{6.7}$$

Network capacity allocation among aggregators would ideally achieve equality in (6.7). In practice, partitioning the network's feasible region between increasing numbers of aggregators may produce latent space within the feasible region $\boldsymbol{\mathcal{F}}$ that becomes inaccessible to DER under robust frameworks.

Begin by defining sub-matrices of $\boldsymbol{A}$ following a similar approach as in (6.5)

$$\boldsymbol{A} = \left[\boldsymbol{A^1} \dots \boldsymbol{A^{N_a}}\right] \tag{6.8}$$

where $\boldsymbol{A}^a \in \mathbb{R}^{2N^c \times N^d_a}$ for aggregators $a \leq N^a$. It follows that

$$\boldsymbol{A}\boldsymbol{p} = \sum_{a=1}^{N^a} \boldsymbol{A}^a \boldsymbol{p}^a \tag{6.9}$$

Each row in (6.4) represents a network constraint, meaning that rows $\boldsymbol{A}^a_{i,:}$ capture the impacts of aggregator a's DER on each constrained network state variable. Conceptually, we wish to limit each aggregator's contribution to raising the value of each scalar constraint function bounded above in (6.4). To achieve this, we introduce vectors $\boldsymbol{s^a} \in \mathbb{R}^{2N^c}$ for $a \leq N^a$, and require that

$$\forall a \leq N_a : \boldsymbol{A}^a \boldsymbol{p}^a \leq \boldsymbol{s^a} \tag{6.10}$$

and additionally require that

$$\sum_{a=1}^{N^a} \boldsymbol{s^a} \leq -\boldsymbol{b} \tag{6.11}$$

By constraining the cumulative impacts of each aggregator on each scalar constraint function, it then follows that

$$\begin{aligned} \boldsymbol{A}\boldsymbol{p} + \boldsymbol{b} &= \sum_{a=1}^{N^a} (\boldsymbol{A}^a \boldsymbol{p}^a) + \boldsymbol{b} && (6.12)\\ &\leq \sum_{a=1}^{N^a} (\boldsymbol{s^a}) + \boldsymbol{b} && (6.13)\\ &\leq -\boldsymbol{b} + \boldsymbol{b} = 0 && (6.14) \end{aligned}$$

satisfying (6.4). We are therefore able to assign network-secure operating regions to aggregators in the form of polytopes $\boldsymbol{\mathcal{R}^a}$, defined by linear systems

$$\boldsymbol{A^a}\boldsymbol{p^a} - \boldsymbol{s^a} \leq \boldsymbol{0} \tag{6.15}$$

The structure of these aggregator operating regions is inherited from the network's feasible region. Each scalar constraint in the definition of aggregator regions $\boldsymbol{\mathcal{R}}^a \subset \mathbb{R}^{N_a^d}$ is a projection of a scalar constraint defining the network's feasible region $\boldsymbol{\mathcal{F}} \subset \mathbb{R}^{N^d}$ into aggregator-specific domains in $\mathbb{R}^{N_a^d}$. Translation terms s_i^a applied to each constraint ensure robustness with respect to unknown actions of other aggregators.

6.2.3 Optimisation of Projected Polytopes

In this paper, we choose to maximise total DER network-support capacity of aggregators which can be offered to wholesale markets. Let $\underline{\boldsymbol{p^a}}, \overline{\boldsymbol{p^a}} \in \mathbb{R}^{N_a^d}$ for $a \leq N^a$ represent aggregator setpoints that satisfy regions $\boldsymbol{\mathcal{R}^a}$, meaning that

$$\boldsymbol{A^a}\underline{\boldsymbol{p^a}} - \boldsymbol{s^a} \leq \boldsymbol{0} \tag{6.16}$$

$$\boldsymbol{A^a}\overline{\boldsymbol{p^a}} - \boldsymbol{s^a} \leq \boldsymbol{0} \tag{6.17}$$

We define feeder-scale import and export capacities allocated to each aggregator as

$$p^a_{\max} = \sum_{i=1}^{N^d_a} \left(\overline{p^a_i}\right) \qquad \text{and} \qquad p^a_{\min} = \sum_{i=1}^{N^d_a} \left(\underline{p^a_i}\right) \tag{6.18}$$

We maximise aggregator participation in wholesale markets by maximising instantaneously-available import and export capacity of aggregators. This is achieved by solving the following optimisation problem

$$\begin{aligned} \max_{s^1,\dots,s^{N^a}} \quad & \sum_{a=1}^{N^a} \left(p^a_{\max} - p^a_{\min}\right) && (6.19)\\ \text{s.t.} \quad & (6.16), (6.17) && \forall a \leq N^a \\ & (6.11) \end{aligned}$$

Although our simulations in Section IV apply this objective, our framework is ultimately agnostic to a DSO's chosen objective. The DSO may also choose to maximise a fairness-inspired metric such as proportional fairness, or may choose to maximise the sum of expected market outcomes for aggregators. Each case requires modelling the total generation and load capacity of each aggregator at the feeder-scale.

6.3 Calculating Market-Responsive Dispatch Envelopes (DE) for DER

We now propose a simple process for aggregators to calculate DER-level dynamic operating envelopes $[\underline{\epsilon^a_i}(m^a), \overline{\epsilon^a_i}(m^a)] \subset \mathbb{R}$, in response to wholesale market dispatch outcomes $m^a \in \mathbb{R}$, that ensure aggregators satisfy regions $\boldsymbol{\mathcal{R}}^a$. These allow aggregators to benefit from the flexible shape of aggregator regions obtained in Section 6.2, without the complexity of explicitly modelling them in their dispatch operations. Our concept is illustrated in Figure 6.5, and we make further reference to its elements throughout Subsection 6.3.2.

6.3.1 Motivation to reduce complexity for aggregators

In Section 6.2.2 we explained that each aggregator's region $\boldsymbol{\mathcal{R}}^a$ inherits the same number of scalar constraints as the network's feasible region. In our case study in Section IV, an aggregator representing 9 DER customers in an

LV feeder of only 55 customers is assigned a region $\mathcal{R}^a$ defined by 110 scalar inequality constraints. In larger feeders, with hundreds or potentially thousands of connection points, satisfying high-dimensional polytopic aggregator regions may be cumbersome for aggregators.

To facilitate aggregators' adherence to these complex regions, our framework instead provides aggregators scalar affine formulae to directly compute DER-level market-responsive operating envelopes $[\underline{\epsilon_i^a}(m^a), \overline{\epsilon_i^a}(m^a)] \subset \mathbb{R}$ for each DER customer i.

6.3.2 Market-responsive envelopes through homothetic transformation

In order to calculate functional envelopes at the DER level, we begin by observing that within each network-secure operating polytope $\mathcal{R}^a$ (grey area, Fig. 6.5) there exists a hyper-cube $\mathcal{C}^a \subseteq \mathcal{R}^a \subset \mathbb{R}^{N_a^d}$ (blue area, Fig. 1) with edges of length $l^a \geq 0$. This hyper-cube $\mathcal{C}^a$ represents a collection of DER-level operating envelopes for aggregator a, that independently guarantee network-feasibility such as in the robust dynamic operating envelope framework [133], and may also include the voltage unbalance constraints derived in Chapter 5.

We also know that extreme points $\underline{\boldsymbol{p}^a}, \overline{\boldsymbol{p}^a} \in \mathcal{R}^a$, and $\mathcal{C}^a \subseteq \mathcal{R}^a$, and that $\mathcal{R}^a$ is a convex polytope. It follows that all hyper-cubes obtained by continuous affine contractions of $\mathcal{C}^a$ towards homothetic centres $\underline{\boldsymbol{p}^a}, \overline{\boldsymbol{p}^a}$ (red area, Fig. 1) are also subsets of $\mathcal{R}^a$. These represent our DER-level market-responsive dispatch envelopes, and can be tailored for specific market outcomes (red line, Fig. 1).

To calculate $\mathcal{C}^a$, define matrices $\underline{\boldsymbol{A}^a}, \overline{\boldsymbol{A}^a} \in \mathbb{R}^{2N^c \times N_a^d}$ containing negative and positive elements of $\boldsymbol{A}^a$ respectively. Entry-wise definitions are given by

$$\underline{A^a}_{ij} = \min({A^a}_{ij}, 0) \tag{6.20}$$
$$\overline{A^a}_{ij} = \max({A^a}_{ij}, 0) \tag{6.21}$$

such that

$$\underline{\boldsymbol{A}^a} + \overline{\boldsymbol{A}^a} = \boldsymbol{A}^a \tag{6.22}$$

We calculate these hyper-cubes $\mathcal{C}^a = \prod_{i=1}^{N_a^d} [\underline{c_i^a}, \overline{c_i^a}]$ for all aggregators in a second-stage optimisation problem, maximising length l^a. This is because

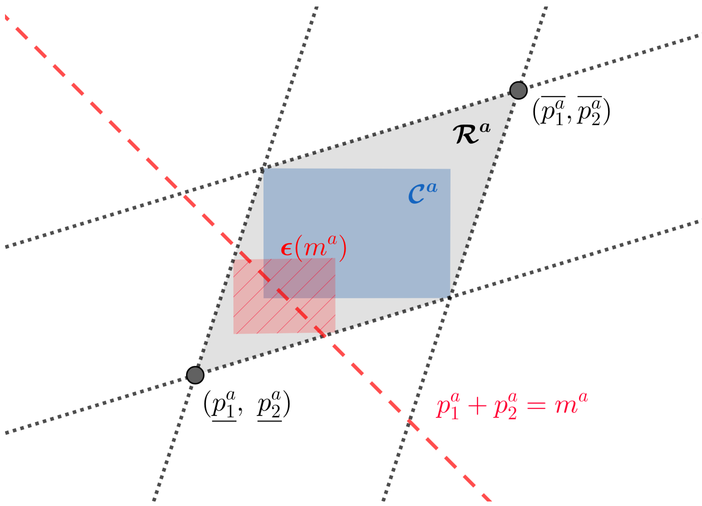

FIGURE 6.5: Illustration of DER-level dispatch envelopes (DE) in response to market dispatch outcome m^a for an aggregator a comprising two DER customers (x-axis representing p_1^a dispatch, y-axis representing p_2^a dispatch)

we seek to maximise the flexibility with which aggregators can disaggregate their wholesale market dispatch outcomes between DER devices. Calculate $\boldsymbol{\mathcal{C}^a}$ using values of $\boldsymbol{s^a}$ solving

$$\begin{aligned} \max \quad & \sum_{a=1}^{N^a} (l^a) && && (6.23) \\ \text{s.t.} \quad & \overline{\boldsymbol{A^a}}\ \overline{\boldsymbol{c^a}} + \underline{\boldsymbol{A^a}}\ \underline{\boldsymbol{c^a}} - \boldsymbol{s^a} \leq \boldsymbol{0} && \forall a \leq N^a \\ & \overline{c_i^a} - \underline{c_i^a} = l^a && \forall i \leq N_a^d, \forall a \leq N^a \\ & \underline{c_i^a} \leq 0 \leq \overline{c_i^a} && \forall i \leq N_a^d, \forall a \leq N^a \end{aligned}$$

We calculate hyper-cubic operating regions $\boldsymbol{\epsilon_1^a}(k), \boldsymbol{\epsilon_2^a}(k) \subset \boldsymbol{\mathcal{R}^a}$, representing sets of DER-level operating envelopes, by applying homothetic transformations to $\boldsymbol{\mathcal{C}^a}$ towards focal points $\underline{\boldsymbol{p^a}}$ and $\overline{\boldsymbol{p^a}}$ respectively. Applying scaling factor $k \in [0, 1]$, we either transform $\boldsymbol{\mathcal{C}^a}$ towards $\overline{\boldsymbol{p^a}}$ by calculating

$$\boldsymbol{\epsilon_1^a}(k) = k\boldsymbol{\mathcal{C}^a} + (1-k)\overline{\boldsymbol{p^a}} \tag{6.24}$$

$$= \prod_{i=1}^{N_a^d} \left[k\underline{c_i^a} + (1-k)\overline{p_i^a},\ k\overline{c_i^a} + (1-k)\overline{p_i^a} \right] \tag{6.25}$$

$$\subset \boldsymbol{\mathcal{R}^a} \tag{6.26}$$

or we transform $\boldsymbol{\mathcal{C}^a}$ towards $\underline{\boldsymbol{p^a}}$ by calculating

$$\boldsymbol{\epsilon_2^a}(k) = k\boldsymbol{\mathcal{C}^a} + (1-k)\underline{\boldsymbol{p^a}} \tag{6.27}$$

$$= \prod_{i=1}^{N_a^d} \left[k\underline{c_i^a} + (1-k)\underline{p_i^a},\, k\overline{c_i^a} + (1-k)\underline{p_i^a} \right] \tag{6.28}$$

$$\subset \boldsymbol{\mathcal{R}}^{\boldsymbol{a}} \tag{6.29}$$

For a given market dispatch outcome m^a, an aggregator must determine whether to apply transformation (6.24) or (6.27), and the value of coefficient k. We aim to provide market-responsive dispatch envelopes at the DER level such that the aggregator's wholesale market dispatch requirement is satisfied when DER operate at the centre of envelopes $[\underline{\epsilon_i^a}(m^a), \overline{\epsilon_i^a}(m^a)]$. This affords aggregators the greatest flexibility to change individual DER setpoints while still satisfying wholesale market obligations.

To achieve this, we first calculate the total aggregator dispatch at the centre-point of the aggregator's central hyper-cubic region $\boldsymbol{\mathcal{C}}^{\boldsymbol{a}}$

$$\widehat{c^a} = \sum_{i=1}^{N_a^d} \frac{\underline{c_i^a} + \overline{c_i^a}}{2}$$

Aggregators can then compute regions $\boldsymbol{\epsilon}^{\boldsymbol{a}}(m^a)$ such that

- if $m^a \geq \widehat{c^a}$, then

$$\boldsymbol{\epsilon}^{\boldsymbol{a}}(m^a) = \boldsymbol{\epsilon}_{\boldsymbol{1}}^{\boldsymbol{a}}(k) \quad \text{for} \quad k = \frac{p_{\max}^a - m^a}{p_{\max}^a - \widehat{c^a}} \tag{6.30}$$

- if $m^a < \widehat{c^a}$, then

$$\boldsymbol{\epsilon}^{\boldsymbol{a}}(m^a) = \boldsymbol{\epsilon}_{\boldsymbol{2}}^{\boldsymbol{a}}(k) \quad \text{for} \quad k = \frac{m^a - p_{\min}^a}{\widehat{c^a} - p_{\min}^a} \tag{6.31}$$

The DSO is able to directly compute $\widehat{c^a}$, and two pairs of scalars for each DER representing parameters for affine functions defining upper and lower envelope bounds as functions of m^a. Values for $p_{\max}^a$ and $p_{\min}^a$ and envelope function parameters are communicated to aggregators before they submit bids to wholesale markets. After the market clears, aggregators can directly compute market-responsive envelopes $[\underline{\epsilon_i^a}, \overline{\epsilon_i^a}]$ in the event that either $m^a \geq \widehat{c^a}$ or $m^a \leq \widehat{c^a}$. As a result, the total computational complexity for aggregators is limited to evaluating two scalar affine expressions of the form $\alpha_i^a m^a + \beta_i^a$ for each of its DER customers i. This final calculation is trivial, and aggregators obtain DER-level envelopes with the same structure as existing envelope approaches.

6.4 Simulations

We demonstrate our proposed approach by repeating the protocol outlined in the Case Study from the beginning of this Chapter. As outlined in the Case Study, we have previously modelled:

- **Dynamic Operating Envelopes (DOE e.g. [147]):** Calculated per DER-customer, satisfying network-security constraints in scenarios of 1) maximum DER imports and 2) maximum DER exports. We model the following policies for aggregators to disaggregate their dispatch:
  (a) **Randomised:** Aggregators disaggregate their wholesale market dispatch outcomes randomly between DER customers, ensuring each satisfies individual envelopes. Under this policy aggregators may only deploy a subset of their DER if their wholesale market dispatch result is small.
  (b) **Merit order:** Aggregators privately compute DER-specific dispatch costs (capturing projected needs of customers with self-consumption preferences, or distribution of battery cycling). These variable costs produce a dynamic merit order hidden from the DSO. Aggregators minimise their dispatch costs by maximising dispatch of their cheapest DER first.

We now compare these results to the RDOE approach (as introduced in Chapter 5) and our proposed RAR-DE approach (Chapter 6). Specifically,

- **Robust Dynamic Operating Envelopes (RDOE [133]):** Envelopes are calculated at the DER-level such that network voltage magnitude[4] constraints are satisfied under all potential disaggregation scenarios. We apply network-security criteria for envelopes as in [133], and seek to maximise total operating envelope size. We model the same dispatch

[4]In Chapter 5 we demonstrated that the inclusion of voltage unbalance constraints did assist in rectifying pre-existing levels of voltage unbalance in the network, however extensive simulations revealed that if top-of-feeder adjustments were not made to induce voltage unbalance at the substation, it was difficult to construct scenarios that resulted in voltage unbalance exceeding 2% in the three-wire Kron-reduced 906-bus feeder. For this reason, and to give appropriate comparison to literature, in this Chapter we do not apply voltage unbalance constraints when applying the RDOE method. We will however study the impacts of including voltage unbalance constraints derived in Chapter 5 when applying the RAR-DE method below.

disaggregation approaches as under **DOE**.

- **Robust Aggregator Regions with flexible Dispatch Envelopes (RAR-DE), with and without voltage unbalance constraints (Chapter 5) in the definition of inner hyper-cubes $\mathcal{C}^{\dashv}$:** Capacity is allocated at the aggregator-level according to method in Section 6.2, and market-responsive DER-level envelopes are calculated according to method in Section 6.3. To provide a robust comparison, we will model disaggregation of wholesale market dispatch outcomes according to the merit-order approach, as this was observed to pose the greatest risk of constraint violation in results. We also investigate the impacts of including voltage unbalance constraints, as derived in Chapter 5, on the total capacity made available to aggregators, as well as the overall flexibility afforded to aggregators through interior hypercubes $\mathcal{C}^a$

We apply the COIN-OR solver (default solver for linear programming using PuLP) on an Intel®Core™ i7-9700 3.00 GHz processor with 16 GB RAM. The average solver time required to generate aggregator feasible regions (Section 6.2) was 0.109 seconds for each market period, and deriving parameters for DER-level operating envelopes (Section 6.3) required an additional 0.037 seconds per aggregator.

6.4.1 Network-security outcomes of Monte-Carlo simulations

For each capacity allocation approach, and for each disaggregation policy considered, repeat the following Monte Carlo simulation protocol:

1. Every half-hour (48 time instants), allocate capacity to aggregators in the form of DER-level operating envelopes or aggregator-level operating regions. We apply the same load traces to each household as outlined in Section 6.1.1 (Monte Carlo analysis is only conducted to assess the impact on the manner of disaggregation, not to the level of unbalance studied in the case study. Validate that voltage constraints are satisfied in cases of maximum DER imports/exports using a non-convex power flow model.

2. Generate 1000 scenarios of wholesale market dispatch outcomes in which aggregators export power to higher voltage networks through the top-of-feeder, i.e. $0 \leq m^a \leq p^a_{\max}$ for each aggregator.

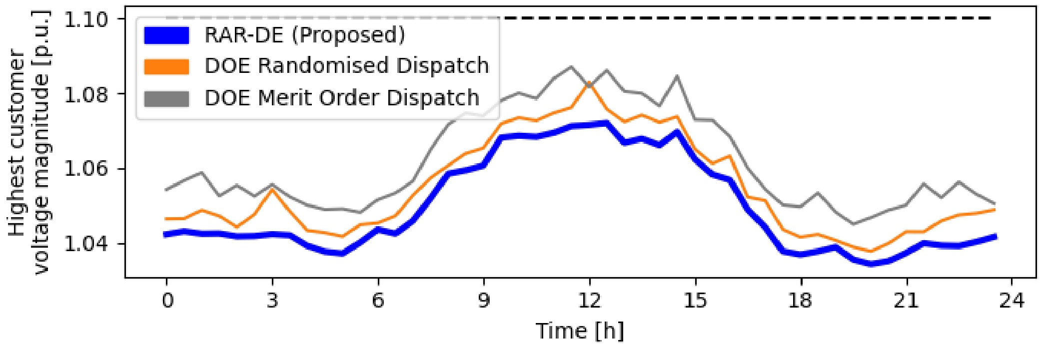

FIGURE 6.6: Maximum customer voltages observed for each time instant

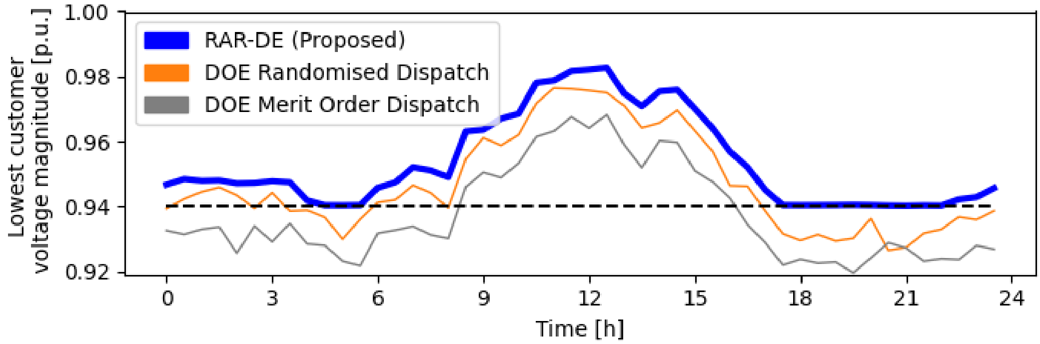

FIGURE 6.7: Minimum customer voltages observed for each time instant

3. For each scenario, disaggregate wholesale dispatch outcomes to individual DER customers according to a specified disaggregation policy, and evaluate the network state using a non-convex power flow model.

4. Repeat points 2) to 4) modelling wholesale market outcomes in which aggregators import from higher voltage networks through the substation, i.e $p^a_{\text{min}} \leq m^a \leq 0$.

Results demonstrate that our **RAR-DE** approach ensures network constraints are satisfied in all randomised market outcome scenarios[5]. In contrast, the conventional **DOE** method fails to provide this robustness in unbalanced networks.

Maximum and minimum voltage magnitudes observed across customer locations are plotted in Figures 6.6 and 6.7. Using the **DOE** approach, customers

[5]The **RDOE** approach also ensured network constraints are satisfied in all scenarios. This was an expected result due to inherent robustness in the method. For brevity, we reserve comparisons to **RDOE** until Subsection 6.4.2.

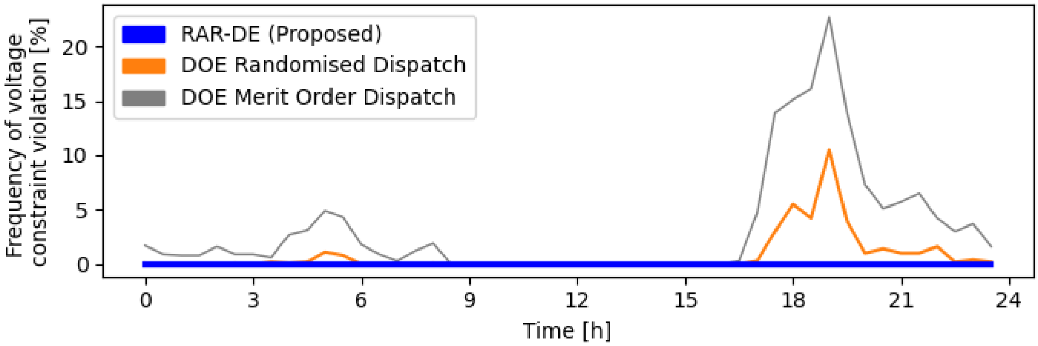

FIGURE 6.8: Frequency of voltage constraint violation in Monte Carlo analysis

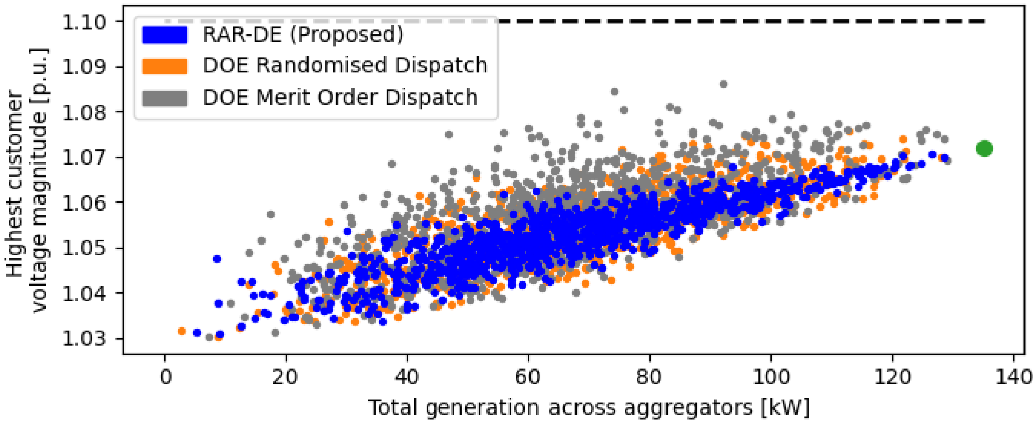

FIGURE 6.9: Highest voltage magnitudes in simulations at 12:30pm

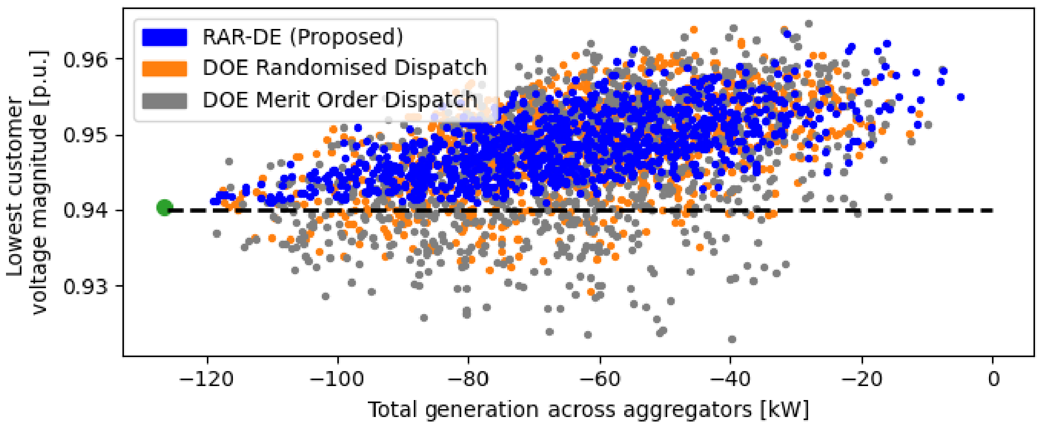

FIGURE 6.10: Lowest voltage magnitudes in simulations at 7:00pm

experience voltage magnitudes as low as 0.926p.u. under randomised disaggregation, and as low as 0.919p.u. under merit-order disaggregation. Figure 6.8 shows voltage constraint violations were observed in morning and evening using the **DOE** approach, with frequency of constraint violation in simulations at 7:00pm reaching 10.5% under randomised disaggregation, and 22.7% under merit-order disaggregation. While these do not strictly represent probabilities due to our randomised modelling of market dispatch outcomes, these results demonstrate the potential for voltage constraint violation without deliberate mitigation. In contrast, voltage constraints are satisfied in all scenarios when applying the **RAR-DE** approach, demonstrating its robustness with respect to uncertain utilisation of network capacity allocated to DER aggregators in unbalanced networks.

Figures 6.9 and 6.10 present the distribution of highest and lowest customer voltage magnitudes as a function of total DER dispatch in the network, studying cases of aggregators providing feeder-scale exports at 12:30pm (studying highest voltages) and feeder-scale imports at 7:00pm (studying lowest voltages). Both **RAR-DE** and **DOE** approaches produce similar distributions of extreme customer voltages when overall feeder dispatch is low. As feeder-level dispatch increases towards aggregators' maximum capacities (green dots, common to all approaches as discussed in the sequel), the spread of extreme voltages remains large under **DOE**, resulting in voltage constraint violations. These violations are avoided under **RAR-DE**, and we observe that extreme voltages are bounded by the case of full capacity utilisation (green dot), demonstrating the robustness of our approach.[6]

6.4.2 Total market participation outcomes for aggregators

Figure 6.11 compares total capacity allocations $p^a_{\min}$, $p^a_{\max}$ for aggregators under our proposed **RAR-DE** approach and under **RDOE**[7] throughout the day (48 time instants). Our **RAR-DE** approach achieves 29% greater total capacity allocations than **RDOE** on average in this case study, and in general is limited by assumed 5 kW DER inverter limits. The **RAR-DE** approach

[6]We note that upper bound voltage magnitude constraints are not binding for the dispatch outcome represented by the green datapoint in Figure 6.9, as there is insufficient DER export capacity in the modelled network. However, the presence of grey and orange points in Figure 6.9 where maximum voltage magnitudes exceed the green point demonstrates the need for our approach in networks with greater DER export capacity.

[7]We compare our approach to the instance of **RDOE** in [133] that does not assume knowledge of the operational status of individual DER. This is because DER may be dispatched as imports or exports, depending on the wholesale market outcomes for aggregators.

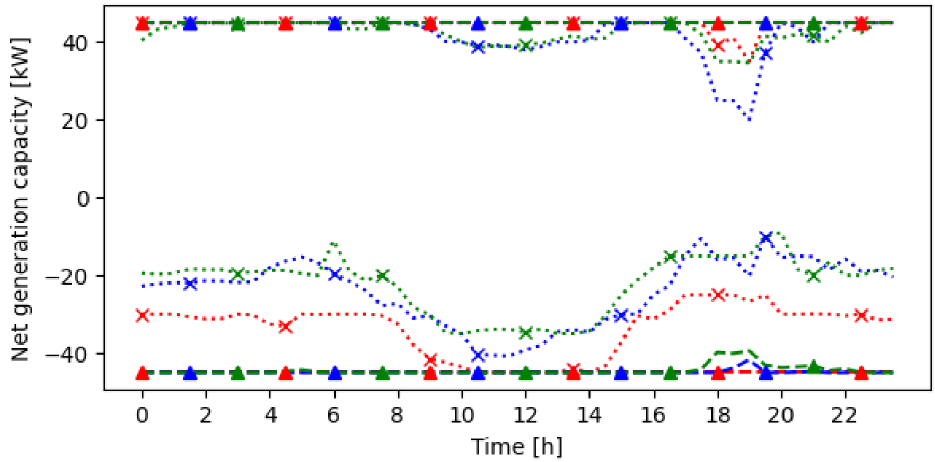

FIGURE 6.11: Total capacity $p^a_{\min}$, $p^a_{\max}$ allocated to aggregators (identified by colour) under **RAR-DE** and **DOE** (dashed, triangles) and **RDOE** (dotted, crosses) approaches.

achieved exactly the same capacity allocation outcomes as under the **DOE** approach throughout the day, and this included when voltage unbalance constraints were included in the formulation.

This demonstrates our approach successfully combines the favourable feeder-scale capacity allocations of the **DOE** approach with network-feasibility assurances of the **RDOE** approach in unbalanced networks, and this is achieved by leveraging the coordination abilities of aggregators.

6.4.3 Inner hyper-cubic regions

We briefly illustrate hyper-cubic inner regions $\mathcal{C}^a$ used to calculate flexible market-responsive dispatch envelopes $\epsilon^a(m^a)$ in Figure 6.12a. In this example, Aggregator 3 (green) will be afforded larger market-responsive envelopes due its larger inner-region $\mathcal{C}^3$. In contrast, Aggregator 2 (blue) will be constrained to rather proportional dispatch. While this may suggest an unfair allocation of capacity between aggregators, it indicates that Aggregator 2 would be more likely to experience curtailment without our flexible framework.

In principle, we are motivated to create areas $\mathcal{C}^a$ as large as possible so as to provide aggregators with as much flexibility in how they wish to dispatch their assets. As our initial goal is to maximise the lengths of the edges of $\mathcal{C}^a$, we performed simulations in which we removed as many optimisation constraints as possible. As such, we initially do not require centring of envelopes around the idle point. It was often found that the optimal inner hypercubes $\mathcal{C}^a$ had

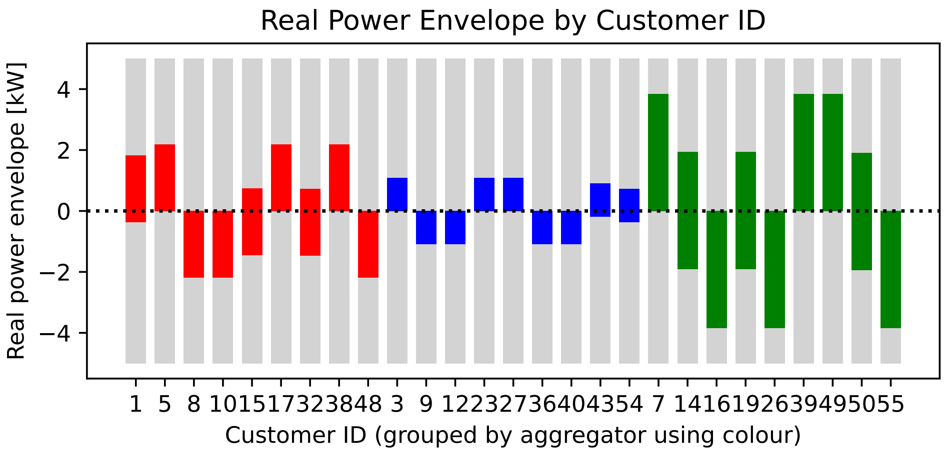

(A) The case where $\mathcal{C}^a$ is not required to be centred around the idle position.

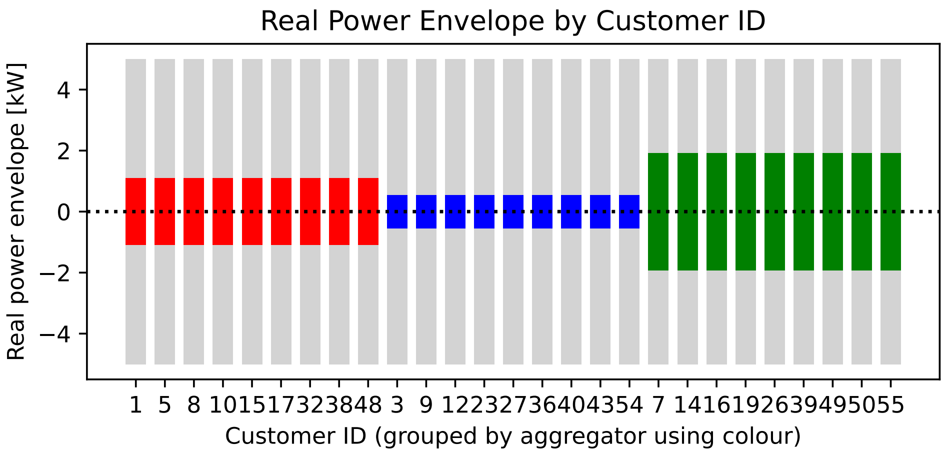

(B) The case where $\mathcal{C}^a$ is required to be centred around the idle position for each aggregator.

FIGURE 6.12: Example of total capacity $\underline{p_i^a}, \overline{p_i^a}$ which can be made available under **RAR-DE** approaches at the DER-level (grey), and inner hyper-cubic regions $\mathcal{C}^a$ (coloured) used as the basis for calculating flexible DER-level dispatch envelopes ϵ^a. This corresponds to 3pm in study outlined above, in the case $\mathcal{C}^a$ was not required to be centred around the idle position for each aggregator.

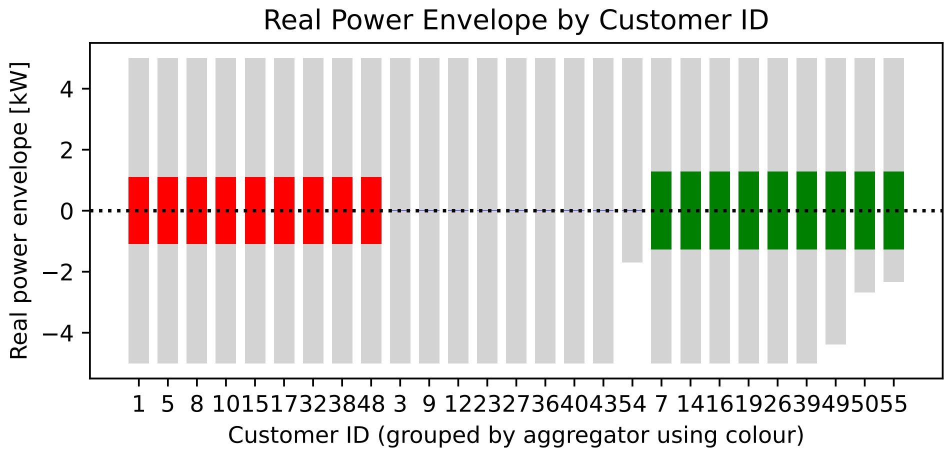

FIGURE 6.13: Example of total capacity allocations $\underline{p_i^a}, \overline{p_i^a}$ under **RDOE** and **RAR-DE** approaches at the DER-level (grey), and inner hyper-cubic regions $\mathcal{C}^a$ (coloured), as illustrated in Figure 6.12a, at 7pm when lower voltage magnitude constraints are binding.

some DER assigned an import limit of zero, and other DER assigned an export limit of zero. This has an interesting interpretation - this indicates that aggregators can gain flexibility in their disaggregation overall if some assets commit to importing or exporting more than others. When compared to the case of proportional dispatch, this deviation represents a superimposed set of exchanges between assets within the aggregator's portfolio that enable a wider range of network-feasible disaggregation outcomes. However, while this may represent an opportunity for greater disaggregation flexibility, there are several reasons this may be undesirable in practice. Some locations may consistently find themselves exporting more than others, and importing less than others, and this may not be practical given batteries only contain a limited state of charge.

We then considered the scenario of requiring envelopes to be centred around the zero point. Results are presented in Figure 6.12b. In the case study above the penalty imposed on $\mathcal{C}^a$ for requiring centered operating envelopes was only very small (difference to the sum of side lengths of $\mathcal{C}^a$ is less than 1%). However, this setting corresponds to 3pm, at a time when the RAR-DE approach was able to find a solution that enabled each aggregator's entire capacity to be made available through operating envelopes.

We repeated this experiment at 7pm, a time when lower voltage magnitude constraints were binding, and the results were significantly different. Results are present in Figure 6.13. Most notably, the second aggregator's internal regions $\mathcal{C}^a$ were reduced to almost zero volume, indicating that the overall aggregator allocations indicated in grey are only possible of the aggregator commits to disaggregating almost exactly proportionately. This demonstrates that where our approach does successfully open up more capacity to be allocated in a robust manner, this is sometimes only possible if aggregators are able to dispatch with exactitude. Affording a robust aggregator region with greater volume may come at the cost of the objective, namely network capacity made available overall to the aggregator.

Some preliminary studies were performed in which a control buffer of e.g. +/-1 kW was applied in all instances that variables p appear in constraint equations, achieved by duplicating all constraint equations and ensuring they hold in both the cases of $p + 1$kW and $p - 1$kW. Early results indicated this approach would produce fairly conservative results, for reasons very similar to those outlined in the discussion of Chapter 5. Ensuring robustness with respect to the case that potentially all DER on a given phase dispatch at 1 kW over the control signal, and all assets on another phase dispatch at 1 kW under the control signal, is very unlikely but is included in the set of scenarios that a robust approach will protect against. We identify that a probabilistic approach may be well suited to achieve this goal in future work.

6.4.4 Incorporating Voltage Unbalance Factor constraints (derived in Chapter 5) in RAR-DE framework

Finally, we consider the impact of voltage unbalance constraints when applied in our RAR-DE framework. Noting that voltage unbalance constraints appeared to induce a degree of conservatism when studied in Chapter 5[8], we are intrigued to see what impact they have when introduced as network feasibility constraints in the RAR-DE approach.

We performed a similar study to Figure 6.12, this time considering the time of 12pm. We introduced the voltage unbalance constraints derived in Chapter 5 in the definition of the network feasible region, and also introduced a multiplying factor γ taking values of 1, 5 and 10, applied as follows

$$\text{linLVUR} \leq \gamma\mu'$$

[8] In the sense that when voltage unbalance was introduced at the top of the feeder, voltage unbalance constraints resulted in significantly less capacity allocated through RDOE and Monte Carlo simulations generally resulted in voltage unbalance outcomes well below the limit applied in envelope calculation

TABLE 6.3: Aggregator DER Customers

	Agg. 1	Agg. 2	Agg. 3	
Phase A	1, 5, 48	3, 9, 54	14, 49, 55	(9 of 21 customers)
Phase B	10, 15, 38	23, 36, 40	7, 26, 50	(9 of 19 customers)
Phase C	8, 17, 32	12, 27, 43	16, 19, 39	(9 of 15 customers)

The purpose of this form of parametric analysis was to gradually introduce the impact of voltage unbalance constraints - for high values of γ, the constraints will not be binding, and will become increasingly binding as γ decreases to 1. Inner hypercube regions $\mathcal{C}^a$ (requiring equal cube side length across all DER operated by the same aggregator) obtained using our approach for various values of γ are plotted in Figure 6.14. Aggregator-level capacity allocations, indicated by grey bars, were found to be uncurtailed, however as the severity of voltage unbalance restrictions was increased the volume of network-feasible inner-hypercubes $\mathcal{C}^a$ was found to decrease until it effectively reduced to an empty set[9].

We note that simulations in Chapter 6 model a network with 49% uptake of DER (27 dwellings), instead of only 35% (19 dwellings) as in Chapter 5, where results were already demonstrating conservatism. These results in this chapter further demonstrate the conservatism incurred by ensuring that voltage unbalance constraints remain satisfied purely through envelope construction, as it restricts voltage unbalance for worst-case combinations of each aggregator's potential method of disaggregating their dispatch according to the proposed framework. These results suggest that management of voltage unbalance levels likely warrants some alternative approach involving measurement and recourse actions in real time.

The introduction of voltage unbalance constraints did not prevent the RAR-DE method from unlocking points of collectively high DER exports and imports - this is expected as high collective imports and high collective exports generally result in fairly balanced resource utilisation across all 3 phases. However, these results provide a further example that where our formulation attains greater capacity allocations than robust dynamic operating envelope approach at the aggregator-scale, the level of freedom aggregators have to dispatch assets in a network-robust manner is often sacrificed, meaning that aggregators would have to adhere to relatively strict rules if they are to attain the valuable collective DER setpoints of high collective imports and high collective exports.

[9] We remind the reader of the aggregator and phase breakdown for each DER customer in Table 6.3

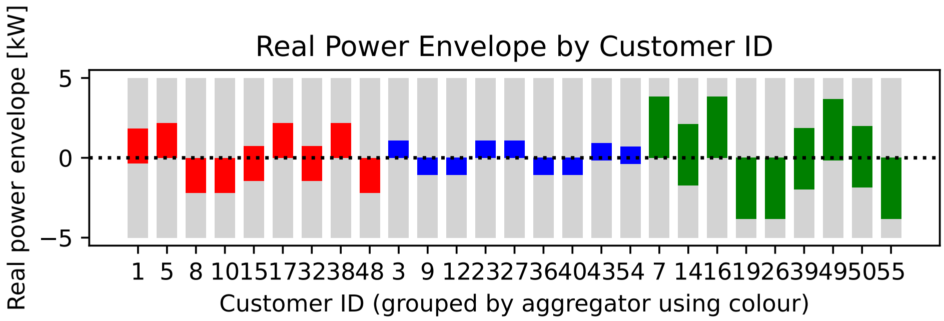

(A) Without applying voltage unbalance factor constraints

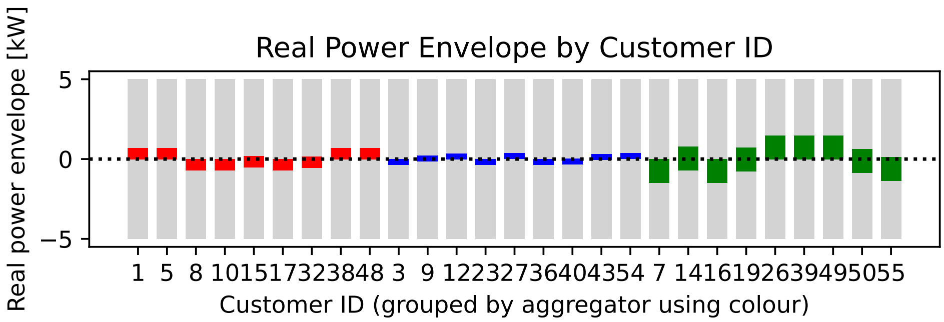

(B) Applying voltage unbalance factor constraints with $\gamma = 10$

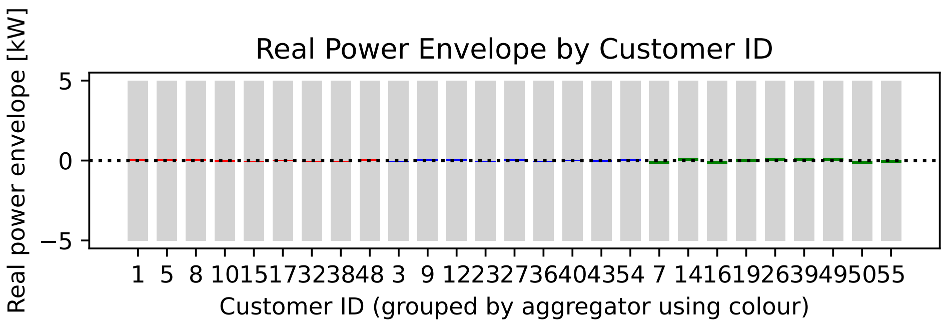

(C) Applying voltage unbalance factor constraints with $\gamma = 5$

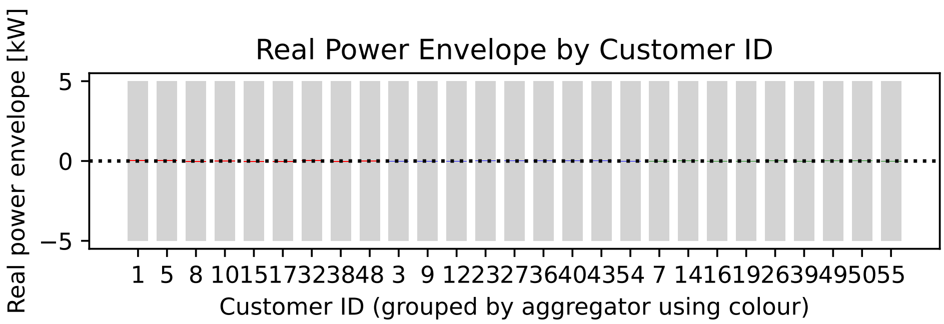

(D) Applying voltage unbalance factor constraints with $\gamma = 1$

FIGURE 6.14: Impact of voltage unbalance factor constraints on internal hyper-cubic regions $\mathcal{C}^a$ at 12pm as a function of γ coefficients

In the case of applying voltage unbalance constraints we derived previously, this is further exacerbated by the sources of conservatism in the derivations of linLVUR as discussed in Chapter 5.

6.5 Conclusion

We have proposed a flexible approach to allocate constrained distribution network capacity to aggregators in unbalanced systems. Results demonstrate that our **RAR-DE** approach combines the benefits of **DOE** and **RDOE** approaches, achieving favourable market participation outcomes for aggregators while also ensuring satisfaction of network voltage constraints in unbalanced networks. This is achieved by leveraging aggregators' ability to coordinate the dispatch of their customers in response to outcomes in wholesale markets. This enables the DSO to assign aggregators more complex operating regions, collectively achieving greater coverage of the network's underlying feasible region than existing robust approaches. Our proposed market-responsive dispatch envelopes defined at the DER-level eliminate the need for aggregators to model these complex versatile regions in their operations, instead requiring only trivial computation after markets clear to generate conventionally-structured operating envelopes. When introducing voltage unbalance constraints into RAR-DE calculation, we observed that inner hypercubic regions $\mathcal{C}^a$ become very restrictive, and this may be due to some of the sources of inherent conservatism in the derivations of linLVUF as discussed in Chapter 5. In future work we will investigate the effects of requiring minimum dispatch envelope sizes for aggregators, explore the potential for real-reactive power co-optimisation and incorporate uncertainty of background load.

Chapter 7

Conclusion

The contributions in this thesis aim to facilitate DER integration in distribution networks, enabling efficient outcomes while ensuring robust operation of networks.

7.1 Key Learnings

Our first contribution demonstrated that incorporating both bid prices and wholesale market prices into the optimisation objective when calculating operating envelopes can significantly improve the economic efficiency of DER participation in wholesale markets. We achieved an 8% improvement in aggregator benefit compared to approaches that prioritise fairness or minimise the sum of square of curtailments measure in kilowatts. Our proposed approach effectively implements a novel form of TSO-DSO coordination, where the TSO communicates the value of services being offered by DER can when allocating constrained distribution network capacity, helping the DSO to evaluate what capacity allocations will result in the greatest creation of value given cost-reflective bid prices from aggregators.

Our stochastic programming extension further enhanced this approach by accounting for price uncertainty. By generating scenarios that capture the probability distribution of market prices, we were able to achieve outcomes within 1% of the perfect information case in our simulations. This demonstrates that even with imperfect price forecasts, DSOs can allocate network capacity in a manner that maximises the expected market value of DER services.

Our second contribution addressed the challenge of ensuring secure network operation in unbalanced three-phase distribution networks when voltage magnitude constraints must be respected. Inspired by the framework in [133], we developed a method to incorporate voltage unbalance constraints into operating envelope calculations, ensuring that voltage unbalance factor remains within operational limits for any combination of DER actions within their assigned envelopes. Simulations modelling a network with an inherited level of voltage unbalance at the substation demonstrate that our approach prevented voltage unbalance constraint violations, whereas the same framework applied without our proposed VUF constraints resulted in voltage unbalance constraints being violated. This demonstrated that our constraints can achieve their intended purpose, and we demonstrated how the envelopes obtained differed between scenarios of inherited unbalance caused by differences in either (a) voltage magnitude or (b) phase angle between phases.

However, our simulations demonstrated that applying voltage unbalance constraints resulted in significant reductions in allocated capacity, whereas Monte Carlo simulations demonstrated a network outcomes generally resulted in voltage unbalance levels that were significantly below the thresholds set when deriving constraints. This underscored a limitation of applying robust optimisation in this setting, due to the fact that (a) our approach involved making approximations and therefore included a safety factor of $\approx 15\%$, and that robustness was achieved with respect to highly improbable scenarios of all DER exporting on one phase and all DER importing on another phase - a highly unlikely scenario. This finding motivated our third contribution, which leveraged aggregators' ability to coordinate their customers to expand network-secure capacity allocations.

Our third contribution introduced Robust Aggregator Operating Regions with Flexible Dispatch Envelopes (RAR-DE), a framework that assigns more complex operating regions to aggregators rather than simple rectangular envelopes to individual DER. By recognising that aggregators can coordinate the dispatch of their DER fleets, and therefore deliberately avoid scenarios that cause robust approaches to become unreasonably conservative, we were able to achieve 29% greater total capacity allocations compared to robust approaches that assume independent operation of all DER. Our market-responsive dispatch envelopes provide a simple mechanism for aggregators to adhere to these complex regions, requiring only trivial computation after markets clear. We believe further work is necessary to understand how voltage unbalance constraints can best be introduced in this approach, and we also note that our proposed framework can craft larger DER-scale flexible dispatch envelopes as a function of what constraints are applied to these (e.g. all equal, or all centred at the idle point in the event of zero top-of-feeder dispatch).

Together, these contributions add to the body of knowledge required to enable safe and efficient integration of DER into wholesale markets through operating envelopes. Our work demonstrates that by considering market efficiency, network security in unbalanced systems, and the coordination capabilities of aggregators, DSOs can significantly expand the capacity available for DER to provide valuable services to the grid.

7.2 Future Research

While this thesis has made a number of contributions, several areas warrant further investigation.

In Chapter 4 we studied how price and bid data could be used to enable greater efficiency in transactions between DER and the wholesale market. Our approach did not consider the impact of distribution network charges, and as such, our model does not factor how how the DSO recovers costs of operating the distribution network. We also model our bidding on grid-scale battery storage assets, as a means to avoid performing an optimisation of bidding practices according to prices, however these assets may operate differently to DER-scale assets. In particular, solar PV represents a cheap source of generation for charging distributed battery systems, however our modelling excluded solar PV of households from the operating envelopes themselves, instead modelling in a simlar manner to background loads. More appropriate modelling of these DER assets could cast light on whether our approach would continue to deliver benefits, factoring network demand charges and therefore the comparative advantage of charging from co-located solar systems.

In Chapter 5, we studied how voltage unbalance constraints can be derived to complete the set of voltage constraint guarantees afforded by the robust dynamic operating envelope framework. We note that our approach employed the multi-phase radial LinDistflow model. One challenge with this linearisation is that currents are not modelled - they are instead assumed to be nil in order to omit the impacts of quadratic losses and therefore obtain a linear approximation. In doing so, we lose the ability to directly apply thermal constraints in our model. The work of Liu and Braslavsky in [133] applies a different linearisation technique, resulting in a power flow model that models voltages instead of squared voltage magnitudes as in the Distflow relaxation. In turn, they are able to apply thermal constraints in their model in a way that is somewhat inaccessible to the LinDistflow model, due to the fact currents are not modelled (they are assumed to be zero). While our framework is equally applicable to either linearised power flow model, we have not at this stage applied our method to a linearised power flow model that includes current values, and we are therefore yet to apply our constraints in a problem that also enforces thermal constraint satisfaction. This is left to future work.

In Chapter 6, we demonstrate that a more flexible allocation of distribution network capacity to aggregators can help to mitigate the level of conservatism that may be encountered when seeking a robust solution in the unbalanced three-phase case. The flexible dispatch envelopes derived in our approach can appear restrictive, but the level of restrictiveness also reflects where only our approach is able to unlock greater overall capacity allocations. For instance, if internal orthogonal regions $\mathcal{C}$ within aggregator operating regions are large, it can be shown that envelopes obtained using the robust dynamic operating envelopes approach from [133] would likely be large as well, indicating the RAR-DE approach does not carry significant benefit in that context. However, it may be beneficial to set a minimum envelope size for DER for any market dispatch outcomes, in order to mitigate uncertainty in DER actions from the aggregator perspective. In preliminary studies, we found that employing a robust approach for this purpose resulted in significantly reduced envelopes, again due to the relatively unlikelihood that all deviation of DER control actions from reference signals be directly correlated to the phase of the DER, resulting in protecting against unlikely scenarios. However, a probabilistic approach may be suitable to factor potential deviations of DER actions from their reference signals.

Additionally, our simulations in Chapters 5 and 6 did not explore utilisation of reactive power. We did perform preliminary studies which sought to define reactive power envelopes and real power envelopes simultaneously. Without a sequential solving process, or established functional relationship between real and reactive power, our approach yielded reactive power envelopes constrained to [0], and this can be understood in the context of a robust model. Our robust approach determine that it was better to constrain reactive power to zero, otherwise real power envelopes may have to be reduced in order to protect against the improbable but technically possible unfavourable combinations of real and reactive power dispatch. However, Liu and Braslavsky have demonstrated that a sequential process can be well-suited to deriving real power operating envelopes, then expanding these through a considered utilisation of reactive power. We may also consider the potential for an optimisation to derive a functional relationship between real and reactive power, although we should be aware of the risks of introducing bilinearities in such approaches.

Finally, we note that studies at the distribution network scale are often performed on a small sample of networks, and that network topology can vary significantly from network to network. While the aim of this thesis was to demonstrate that novel conceptual approaches to coordinating DER can achieve effective outcomes, the applicability of methods should be tested on a broader range of networks. This would also allow us to establish whether methods designed on a European test feeder may offer similar levels of benefit when applied in different contexts such as in the United States where the MV components of networks carry power much closer to individual homes.

7.3 Summary

This thesis has studied the challenge of coordinating DER in unbalanced distribution networks through operating envelopes. We have proposed approaches that factor , ensuring robustness in unbalanced systems, and leveraging aggregator coordination, DSOs can safely unlock the full potential of DER to provide valuable services to wholesale markets.

Together, these contributions provide a blueprint for the safe and efficient integration of DER into electricity markets, supporting the transition to cleaner, more decentralized energy systems. As DER continue to proliferate, the frameworks developed in this thesis will become increasingly valuable for ensuring that these resources can contribute effectively to system operation while respecting the physical constraints of distribution networks.

Bibliography

[1] J. S. Russell, P. Scott and A. Attarha, "Stochastic shaping of aggregator energy and reserve bids to ensure network security," *Electric Power Systems Research*, vol. 212, p. 108 418, 2022.

[2] J. S. Russell, P. Scott and J. Iria, "Robust operating envelopes with phase unbalance constraints in unbalanced three-phase networks," in *2023 IEEE PES Innovative Smart Grid Technologies-Asia (ISGT Asia)*, IEEE, 2023, pp. 1–5.

[3] J. S. Russell, P. Scott and J. Iria, "Network-secure aggregator operating regions with flexible dispatch envelopes in unbalanced systems," *Electric Power Systems Research*, vol. 123, p. 123 456, 2024.

[4] V. Foster and D. Bedrosyan, "Understanding co2 emissions from the global energy sector," 2014.

[5] IREA, *Renewable power generation costs in 2023*, 2024.

[6] Australian Energy Market Operator, "2024 integrated system plan," AEMO, Tech. Rep., 2024.

[7] S. Agnew and P. Dargusch, "Effect of residential solar and storage on centralized electricity supply systems," *Nature Climate Change*, vol. 5, no. 4, pp. 315–318, 2015.

[8] Energy Networks Australia and Commonwealth Scientific and Industrial Research Organisation, "Electricity Network Transformation Roadmap Final Report," *Energy Networks Australia*, 2017.

[9] K. Say, M. John and R. Dargaville, "Power to the people: Evolutionary market pressures from residential pv battery investments in australia," *Energy Policy*, vol. 134, p. 110 977, 2019.

[10] A. Hirsch, Y. Parag and J. Guerrero, "Microgrids: A review of technologies, key drivers, and outstanding issues," *Renewable and sustainable Energy reviews*, vol. 90, pp. 402–411, 2018.

[11] Australian Energy Market Operator, "Technical integration of distributed energy resources," *Report, Apr*, 2019.

[12] G. Pepermans, J. Driesen, D. Haeseldonckx, R. Belmans and W. D'haeseleer, "Distributed generation: Definition, benefits and issues," *Energy policy*, vol. 33, no. 6, pp. 787–798, 2005.

[13] W. Tushar et al., "Peer-to-peer energy systems for connected communities: A review of recent advances and emerging challenges," *Applied energy*, vol. 282, p. 116 131, 2021.

[14] R. Walling, R. Saint, R. C. Dugan, J. Burke and L. A. Kojovic, "Summary of distributed resources impact on power delivery systems," *IEEE Transactions on power delivery*, vol. 23, no. 3, pp. 1636–1644, 2008.

[15] R. Tonkoski, L. A. Lopes and T. H. El-Fouly, "Coordinated active power curtailment of grid connected pv inverters for overvoltage prevention," *IEEE Transactions on sustainable energy*, vol. 2, no. 2, pp. 139–147, 2010.

[16] T. A. Short, *Electric power distribution handbook*. CRC press, 2003.

[17] M. H. Bollen and F. Hassan, *Integration of distributed generation in the power system*. John wiley & sons, 2011.

[18] ARPA-E, *NODES — ARPA-E*, https://arpa-e.energy.gov/programs-and-initiatives/view-all-programs/nodes, Advanced Research Projects Agency–Energy (ARPA-E), U.S. Department of Energy, 2019.

[19] S. P. Burger, J. D. Jenkins, C. Batlle and I. J. Perez-Arriaga, "Restructuring revisited part 2: Coordination in electricity distribution systems," *The Energy Journal*, vol. 40, no. 3, pp. 55–76, 2019.

[20] L. Blackhall, "On the calculation and use of dynamic operating envelopes," Tech. Rep., 2020. [Online]. Available: https://arena.gov.au/assets/2020/09/on-the-calculation-and-use-of-dynamic-operating-envelopes.pdf.

[21] M. Z. Liu, L. Ochoa, T. Ting and J. Theunissen, "Bottom-up services & network integrity: The need for operating envelopes," in *IET Conference Proceedings CP785*, IET, vol. 2021, 2021, pp. 1944–1948.

[22] Distributed Energy Integration Program, "Dynamic operating envelopes working group outcomes report," Distributed Energy Integration Program, Tech. Rep., 2022. [Online]. Available: https://arena.gov.au/assets/2022/03/dynamic-operating-envelope-working-group-outcomes-report.pdf.

[23] Endeavour Energy. "Distributed Energy Resources (DER). "[Online]. Available: https://www.endeavourenergy.com.au/modern-grid/creating-the-modern-grid/distributed-energy-resources-der.

[24] CleanEnergyReviews. "Guide to designing off-grid and hybrid solar systems," Accessed: 28 Aug. 2024. [Online]. Available: https://www.cleanenergyreviews.info/blog/designing-off-grid-hybrid-solar-systems.

[25] M. H. Anowar and P. Roy, "A modified incremental conductance based photovoltaic mppt charge controller," in *2019 International Conference on Electrical, Computer and Communication Engineering (ECCE)*, IEEE, 2019, pp. 1–5.

[26] myElectricalEngineering. "How D.C. to A.C. Inverters Work," Accessed: 28 Aug. 2024. [Online]. Available: https://myelectrical.com/notes/entryid/250/how-d-c-to-a-c-inverters-work.

[27] S. Avram, V. Plotenco and L.-N. Paven, "Design and development of an electricity meter test equipment," in *2017 International Conference on Optimization of Electrical and Electronic Equipment (OPTIM) & 2017 Intl Aegean Conference on Electrical Machines and Power Electronics (ACEMP)*, IEEE, 2017, pp. 96–101.

[28] J. Webb, H. N. de Silva and C. Wilson, "The future of coal and renewable power generation in australia: A review of market trends," *Economic Analysis and Policy*, vol. 68, pp. 363–378, 2020.

[29] Australian Energy Market Commission (AEMC), *National Electricity Rules: Clause S5.1a.7 Voltage Unbalance*, National Electricity Rules (NER), Chapter 5, Schedule 5.1a System standards, 2025. [Online]. Available: https://energy-rules.aemc.gov.au/ner/468/253886.

[30] M. E. Baran and F. F. Wu, "Optimal capacitor placement on radial distribution systems," *IEEE Transactions on power Delivery*, vol. 4, no. 1, pp. 725–734, 2002.

[31] A. S. Abbas, A. A. Abou El-Ela and R. A. El-Sehiemy, "Maximization approach of hosting capacity based on uncertain renewable energy resources using network reconfiguration and soft open points," *International Transactions on Electrical Energy Systems*, vol. 2022, no. 1, p. 2 947 965, 2022.

[32] *IEEE PES Test Feeder &x2013; IEEE PES AMPS DSAS Test Feeder Working Group — cmte.ieee.org*, https://cmte.ieee.org/pes-testfeeders/, [Accessed 23-02-2025].

[33] A. Visakh and M. P. Selvan, "Feasibility assessment of utilizing electric vehicles for energy arbitrage in smart grids considering battery degradation cost," *Energy Sources, Part A: Recovery, Utilization, and Environmental Effects*, vol. 44, no. 2, pp. 4664–4678, 2022.

[34] Australian Energy Market Operator (AEMO), "Learnings from industry implementation of emergency backstop mechanisms for distributed resources: Insights from industry implementation experiences in australia to date," Australian Energy Market Operator (AEMO), Technical Report, Q2 2025, Date specified as Q2 2025 in the document cover. References made to May 2025 data in the Important Notice section.

[35] Energy Networks Australia and Australian Energy Market Operator, "Open energy networks project: Energy networks australia position paper," Energy Networks Australia, Melbourne, VIC, Tech. Rep., 2020.

[36] AEMO, "Fcas model in nemde: Scaling, enablement, and co-optimisation of fcas offers in central dispatch," Oct. 2023. [Online]. Available: https://aemo.com.au/-/media/files/electricity/nem/security_and_reliability/dispatch/policy_and_process/fcas-model-in-nemde.pdf.

[37] B. Subhonmesh, S. H. Low and K. M. Chandy, "Equivalence of branch flow and bus injection models," in *2012 50th Annual Allerton Conference on Communication, Control, and Computing (Allerton)*, IEEE, 2012, pp. 1893–1899.

[38] C. Coffrin, H. L. Hijazi and P. Van Hentenryck, "Distflow extensions for ac transmission systems," *arXiv preprint arXiv:1506.04773*, 2015.

[39] F. Geth and B. Liu, "Notes on bim and bfm optimal power flow with parallel lines and total current limits," in *2022 IEEE Power & Energy Society General Meeting (PESGM)*, IEEE, 2022, pp. 01–05.

[40] M. Farivar and S. H. Low, "Branch flow model: Relaxations and convexification—part i," *IEEE Transactions on Power Systems*, vol. 28, no. 3, pp. 2554–2564, 2013.

[41] Q. Peng and S. H. Low, "Distributed optimal power flow algorithm for radial networks, i: Balanced single phase case," *IEEE Transactions on Smart Grid*, vol. 9, no. 1, pp. 111–121, 2016.

[42] L. Gan and S. H. Low, "Convex relaxations and linear approximation for optimal power flow in multiphase radial networks," in *2014 Power Systems Computation Conference*, IEEE, 2014, pp. 1–9.

[43] S. P. Boyd and L. Vandenberghe, *Convex optimization*. Cambridge university press, 2004.

[44] C. Coffrin and L. Roald, "Convex relaxations in power system optimization: A brief introduction," *arXiv preprint arXiv:1807.07227*, 2018.

[45] *HSL - Archive Catalogue — hsl.rl.ac.uk*, [Accessed 04-09-2024]. [Online]. Available: https://www.hsl.rl.ac.uk/archive/.

[46] J. R. Birge and F. Louveaux, *Introduction to stochastic programming*. Springer Science & Business Media, 2011.

[47] L. A. Roald, D. Pozo, A. Papavasiliou, D. K. Molzahn, J. Kazempour and A. Conejo, "Power systems optimization under uncertainty: A review of methods and applications," *Electric Power Systems Research*, vol. 214, p. 108 725, 2023.

[48] S. I. Nanou, G. N. Psarros and S. A. Papathanassiou, "Network-constrained unit commitment with piecewise linear ac power flow constraints," *Electric Power Systems Research*, vol. 195, p. 107 125, 2021.

[49] C. Byers and G. Hug, "Long-run optimal pricing in electricity markets with non-convex costs," *European Journal of Operational Research*, vol. 307, no. 1, pp. 351–363, 2023.

[50] S. Makkonen and R. Lahdelma, "Non-convex power plant modelling in energy optimisation," *European Journal of Operational Research*, vol. 171, no. 3, pp. 1113–1126, 2006.

[51] S. Takriti, J. R. Birge and E. Long, "A stochastic model for the unit commitment problem," *IEEE Transactions on Power Systems*, vol. 11, no. 3, pp. 1497–1508, 1996.

[52] P. Carpentier, G. Gohen, J.-C. Culioli and A. Renaud, "Stochastic optimization of unit commitment: A new decomposition framework," *IEEE Transactions on Power Systems*, vol. 11, no. 2, pp. 1067–1073, 1996.

[53] A. Tuohy, P. Meibom, E. Denny and M. O'Malley, "Unit commitment for systems with significant wind penetration," *IEEE Transactions on power systems*, vol. 24, no. 2, pp. 592–601, 2009.

[54] P. Meibom, R. Barth, B. Hasche, H. Brand, C. Weber and M. O'Malley, "Stochastic optimization model to study the operational impacts of high wind penetrations in ireland," *IEEE Transactions on Power Systems*, vol. 26, no. 3, pp. 1367–1379, 2010.

[55] M. Bucksteeg, L. Niesen and C. Weber, "Impacts of dynamic probabilistic reserve sizing techniques on reserve requirements and system costs," *IEEE Transactions on Sustainable Energy*, vol. 7, no. 4, pp. 1408–1420, 2016.

[56] K. De Vos, N. Stevens, O. Devolder, A. Papavasiliou, B. Hebb and J. Matthys-Donnadieu, "Dynamic dimensioning approach for operating reserves: Proof of concept in belgium," *Energy policy*, vol. 124, pp. 272–285, 2019.

[57] M. Vrakopoulou, K. Margellos, J. Lygeros and G. Andersson, "A probabilistic framework for reserve scheduling and n-1 security assessment of systems with high wind power penetration," *IEEE Transactions on Power Systems*, vol. 28, no. 4, pp. 3885–3896, 2013.

[58] A. Papavasiliou, A. Bouso, S. Apelfröjd, E. Wik, T. Gueuning and Y. Langer, "Multi-area reserve dimensioning using chance-constrained optimization," *IEEE Transactions on Power Systems*, vol. 37, no. 5, pp. 3982–3994, 2021.

[59] N. Rhodes, L. Ntaimo and L. Roald, "Balancing wildfire risk and power outages through optimized power shut-offs," *IEEE Transactions on Power Systems*, vol. 36, no. 4, pp. 3118–3128, 2020.

[60] N. Rhodes, C. Coffrin and L. Roald, "Recursive restoration refinement: A fast heuristic for near-optimal restoration prioritization in power systems," *Electric Power Systems Research*, vol. 212, p. 108 454, 2022.

[61] M. V. Pereira and L. M. Pinto, "Multi-stage stochastic optimization applied to energy planning," *Mathematical programming*, vol. 52, pp. 359–375, 1991.

[62] M. Carrión, A. B. Philpott, A. J. Conejo and J. M. Arroyo, "A stochastic programming approach to electric energy procurement for large consumers," *IEEE Transactions on Power Systems*, vol. 22, no. 2, pp. 744–754, 2007.

[63] Q. Zhang, A. M. Bremen, I. E. Grossmann and J. M. Pinto, "Long-term electricity procurement for large industrial consumers under uncertainty," *Industrial & Engineering Chemistry Research*, vol. 57, no. 9, pp. 3333–3347, 2018.

[64] M. V. Pereira, "Optimal stochastic operations scheduling of large hydroelectric systems," *International Journal of Electrical Power & Energy Systems*, vol. 11, no. 3, pp. 161–169, 1989.

[65] N. Löhndorf and D. Wozabal, "Gas storage valuation in incomplete markets," *European Journal of Operational Research*, vol. 288, no. 1, pp. 318–330, 2021.

[66] M. G. Morgan and S. N. Talukdar, "Electric power load management: Some technical, economic, regulatory and social issues," *Proceedings of the IEEE*, vol. 67, no. 2, pp. 241–312, 1979.

[67] F. C. Schweppe, R. D. Tabors, J. L. Kirtley, H. R. Outhred, F. H. Pickel and A. J. Cox, "Homeostatic utility control," *IEEE Transactions on Power Apparatus and Systems*, no. 3, pp. 1151–1163, 1980.

[68] J. Aghaei and M.-I. Alizadeh, "Demand response in smart electricity grids equipped with renewable energy sources: A review," *Renewable and Sustainable Energy Reviews*, vol. 18, pp. 64–72, 2013.

[69] M. H. Albadi and E. F. El-Saadany, "A summary of demand response in electricity markets," *Electric power systems research*, vol. 78, no. 11, pp. 1989–1996, 2008.

[70] M. H. Albadi and E. F. El-Saadany, "Demand response in electricity markets: An overview," in *2007 IEEE power engineering society general meeting*, IEEE, 2007, pp. 1–5.

[71] F. Pallonetto, S. Oxizidis, F. Milano and D. Finn, "The effect of time-of-use tariffs on the demand response flexibility of an all-electric smart-grid-ready dwelling," *Energy and Buildings*, vol. 128, pp. 56–67, 2016.

[72] D. T. Nguyen, H. T. Nguyen and L. B. Le, "Dynamic pricing design for demand response integration in power distribution networks," *IEEE Transactions on power systems*, vol. 31, no. 5, pp. 3457–3472, 2016.

[73] K. Petrou and L. F. Ochoa, "Customer-led operation of residential storage for the provision of energy services," in *2019 IEEE PES Innovative Smart Grid Technologies Conference-Latin America (ISGT Latin America)*, IEEE, 2019, pp. 1–6.

[74] M. Di Somma, G. Graditi, E. Heydarian-Forushani, M. Shafie-khah and P. Siano, "Stochastic optimal scheduling of distributed energy resources with renewables considering economic and environmental aspects," *Renewable energy*, vol. 116, pp. 272–287, 2018.

[75] M. A. A. Pedrasa, T. D. Spooner and I. F. MacGill, "Coordinated scheduling of residential distributed energy resources to optimize smart home energy services," *IEEE Transactions on Smart Grid*, vol. 1, no. 2, pp. 134–143, 2010.

[76] P. Scott, S. Thiébaux, M. Van Den Briel and P. Van Hentenryck, "Residential demand response under uncertainty," in *Principles and Practice of Constraint Programming: 19th International Conference, CP 2013, Uppsala, Sweden, September 16-20, 2013. Proceedings 19*, Springer, 2013, pp. 645–660.

[77] J. L. Mathieu et al., "A new definition and research agenda for demand response in the distributed energy resource era," *IEEE Transactions on Energy Markets, Policy and Regulation*, 2025.

[78] S. Burger, J. P. Chaves-Ávila, C. Batlle and I. J. Pérez-Arriaga, "A review of the value of aggregators in electricity systems," *Renewable and Sustainable Energy Reviews*, vol. 77, pp. 395–405, 2017.

[79] L. Šikšnys, E. Valsomatzis, K. Hose and T. B. Pedersen, "Aggregating and disaggregating flexibility objects," *IEEE Transactions on Knowledge and Data Engineering*, vol. 27, no. 11, pp. 2893–2906, 2015.

[80] L. Zhao, H. Hao and W. Zhang, "Extracting flexibility of heterogeneous deferrable loads via polytopic projection approximation," in *2016 IEEE 55th Conference on Decision and Control (CDC)*, IEEE, 2016, pp. 6651–6656.

[81] M. Zhang, Y. Xu, X. Shi and Q. Guo, "A fast polytope-based approach for aggregating large-scale electric vehicles in the joint market under uncertainty," *IEEE Transactions on Smart Grid*, vol. 15, no. 1, pp. 701–713, 2023.

[82] F. L. Müller, J. Szabó, O. Sundström and J. Lygeros, "Aggregation and disaggregation of energetic flexibility from distributed energy resources," *IEEE Transactions on Smart Grid*, vol. 10, no. 2, pp. 1205–1214, 2017.

[83] Y. Wen, Z. Hu, S. You and X. Duan, "Aggregate feasible region of ders: Exact formulation and approximate models," *IEEE Transactions on Smart Grid*, vol. 13, no. 6, pp. 4405–4423, 2022.

[84] C. Li, V. R. Disfani, Z. K. Pecenak, S. Mohajeryami and J. Kleissl, "Optimal oltc voltage control scheme to enable high solar penetrations," *Electric Power Systems Research*, vol. 160, pp. 318–326, 2018.

[85] C. R. Sarimuthu, V. K. Ramachandaramurthy, K. Agileswari and H. Mokhlis, "A review on voltage control methods using on-load tap changer transformers for networks with renewable energy sources," *Renewable and Sustainable Energy Reviews*, vol. 62, pp. 1154–1161, 2016.

[86] P. Mallet, P.-O. Granstrom, P. Hallberg, G. Lorenz and P. Mandatova, "Power to the people!: European perspectives on the future of electric distribution," *IEEE Power and Energy magazine*, vol. 12, no. 2, pp. 51–64, 2014.

[87] W. van Westering, A. Zondervan, A. Bakkeren, F. Mijnhardt and J. Van Der Els, "Assessing and mitigating the impact of the energy demand in 2030 on the dutch regional power distribution grid," in *2016 IEEE 13th International Conference on Networking, Sensing, and Control (ICNSC)*, IEEE, 2016, pp. 1–6.

[88] E. Veldman, M. Gibescu, H. J. Slootweg and W. L. Kling, "Scenario-based modelling of future residential electricity demands and assessing their impact on distribution grids," *Energy policy*, vol. 56, pp. 233–247, 2013.

[89] A. H. Etemadi, E. J. Davison and R. Iravani, "A decentralized robust control strategy for multi-der microgrids—part i: Fundamental concepts," *IEEE Transactions on Power Delivery*, vol. 27, no. 4, pp. 1843–1853, 2012.

[90] T. Morstyn, B. Hredzak and V. G. Agelidis, "Control strategies for microgrids with distributed energy storage systems: An overview," *IEEE Transactions on Smart Grid*, vol. 9, no. 4, pp. 3652–3666, 2016.

[91] M. Juamperez, G. Yang and S. B. Kjær, "Voltage regulation in LV grids by coordinated volt-var control strategies," *Journal of Modern Power Systems and Clean Energy*, vol. 2, no. 4, pp. 319–328, 2014.

[92] J. M. Guerrero, J. C. Vasquez, J. Matas, M. Castilla and L. G. de Vicuña, "Control strategy for flexible microgrid based on parallel line-interactive ups systems," *IEEE Transactions on industrial Electronics*, vol. 56, no. 3, pp. 726–736, 2008.

[93] C. Li, T. Dragicevic, N. L. Diaz, J. C. Vasquez and J. M. Guerrero, "Voltage scheduling droop control for state-of-charge balance of distributed energy storage in dc microgrids," in *2014 IEEE international energy conference (ENERGYCON)*, IEEE, 2014, pp. 1310–1314.

[94] M. Savaghebi, A. Jalilian, J. C. Vasquez and J. M. Guerrero, "Secondary control scheme for voltage unbalance compensation in an islanded droop-controlled microgrid," *IEEE transactions on Smart Grid*, vol. 3, no. 2, pp. 797–807, 2012.

[95] T. Morstyn, B. Hredzak and V. G. Agelidis, "Distributed cooperative control of microgrid storage," *IEEE transactions on power systems*, vol. 30, no. 5, pp. 2780–2789, 2014.

[96] C. Li, E. A. A. Coelho, T. Dragicevic, J. M. Guerrero and J. C. Vasquez, "Multiagent-based distributed state of charge balancing control for distributed energy storage units in ac microgrids," *IEEE Transactions on Industry Applications*, vol. 53, no. 3, pp. 2369–2381, 2016.

[97] B. Zhang, A. Y. Lam, A. D. Domínguez-García and D. Tse, "An optimal and distributed method for voltage regulation in power distribution systems," *IEEE Transactions on Power Systems*, vol. 30, no. 4, pp. 1714–1726, 2014.

[98] W. van Westering and H. Hellendoorn, "Low voltage power grid congestion reduction using a community battery: Design principles, control and experimental validation," *International Journal of Electrical Power & Energy Systems*, vol. 114, p. 105 349, 2020.

[99] K. Anuradha, C. P. Mediwaththe and M. Mahmoodi, "A multi-objective planning and scheduling framework for community energy storage systems in low voltage distribution networks," in *2023 13th International Conference on Power, Energy and Electrical Engineering (CPEEE)*, IEEE, 2023, pp. 379–385.

[100] K. Anuradha, J. Iria and C. P. Mediwaththe, "Multi-objective planning of community energy storage systems under uncertainty," *Electric Power Systems Research*, vol. 230, p. 110 286, 2024.

[101] S. A. El-Batawy and W. G. Morsi, "Optimal design of community battery energy storage systems with prosumers owning electric vehicles," *IEEE Transactions on Industrial Informatics*, vol. 14, no. 5, pp. 1920–1931, 2017.

[102] P. Wolfs and G. S. Reddy, "A receding predictive horizon approach to the periodic optimization of community battery energy storage systems," in *2012 22nd Australasian Universities Power Engineering Conference (AUPEC)*, IEEE, 2012, pp. 1–6.

[103] Energy Networks Australia, "Unlocking the value of community batteries: Response to AER ring-fencing class waiver initiation notice," Technical Report, Jan. 2023.

[104] K. Bell and S. Gill, "Delivering a highly distributed electricity system: Technical, regulatory and policy challenges," *Energy policy*, vol. 113, pp. 765–777, 2018.

[105] J. Silva et al., "Estimating the active and reactive power flexibility area at the tso-dso interface," *IEEE Transactions on Power Systems*, vol. 33, no. 5, pp. 4741–4750, 2018.

[106] S. Riaz and P. Mancarella, "Modelling and characterisation of flexibility from distributed energy resources," *IEEE transactions on power systems*, vol. 37, no. 1, pp. 38–50, 2021.

[107] F. Capitanescu, "Tso–dso interaction: Active distribution network power chart for tso ancillary services provision," *Electric Power Systems Research*, vol. 163, pp. 226–230, 2018.

[108] H. Gerard, E. I. R. Puente and D. Six, "Coordination between transmission and distribution system operators in the electricity sector: A conceptual framework," *Utilities Policy*, vol. 50, pp. 40–48, 2018.

[109] A. G. Givisiez, K. Petrou and L. F. Ochoa, "A review on tso-dso coordination models and solution techniques," *Electric Power Systems Research*, vol. 189, p. 106 659, 2020.

[110] N. Etherden and M. H. Bollen, "Increasing the hosting capacity of distribution networks by curtailment of renewable energy resources," in *2011 IEEE Trondheim PowerTech*, IEEE, 2011, pp. 1–7.

[111] N. Etherden, "Increasing the hosting capacity of distributed energy resources using storage and communication," Ph.D. dissertation, Luleå tekniska universitet, 2014.

[112] D. E. I. Program, "DER Market Integration Trials Summary Report," Tech. Rep., Dec. 2023.

[113] M. Z. Liu, A. Simonovska, L. F. Ochoa, P. K. Wong, K. Chew and J. Theunissen, "Validating real LV feeder models using smart meter data: a practical experience from project EDGE," 2023.

[114] T. Fernando, O. Rubasinghe, T. Zhang, P. Howe and A. Rajander, "Project Symphony: Distribution Constraints Optimization Algorithm Report," Tech. Rep., Mar. 2022.

[115] L. Jones, P. Watson, S. Wilson, B. Martin and D. Gordon, "KSR 12 Converge Project Final Knowledge Sharing Report," Tech. Rep., 2023.

[116] P. F. Flora Strauli Eglantine Mansion, "Project Edith - Knowledge Share Report," Blunomy, Tech. Rep., 2023.

[117] Y. Z. Gerdroodbari, M. Khorasany and R. Razzaghi, "Dynamic pq operating envelopes for prosumers in distribution networks," *Applied Energy*, vol. 325, p. 119 757, 2022.

[118] M. Mahmoodi, L. Blackhall, S. M. N. Rahim Abadi, A. Attarha, B. Weise and A. Bhardwaj, "Der capacity assessment of active distribution systems using dynamic operating envelopes," *IEEE Transactions on Smart Grid*, 2023.

[119] M. Z. Liu, L. F. Ochoa, P. K. Wong and J. Theunissen, "Using opf-based operating envelopes to facilitate residential der services," *IEEE Transactions on Smart Grid*, vol. 13, no. 6, pp. 4494–4504, 2022.

[120] Y. Yi and G. Verbič, "Fair operating envelopes under uncertainty using chance constrained optimal power flow," *Electric Power Systems Research*, vol. 213, p. 108 465, 2022.

[121] S. Boyd, N. Parikh, E. Chu, B. Peleato, J. Eckstein et al., "Distributed optimization and statistical learning via the alternating direction method of multipliers," *Foundations and Trends® in Machine learning*, vol. 3, no. 1, pp. 1–122, 2011.

[122] A. Attarha, S. M. N. Rahim Abadi, P. Scott and S. Thiébaux, "Network-secure envelopes enabling reliable der bidding in energy and reserve markets," *IEEE Transactions on Smart Grid*, vol. 13, no. 3, pp. 2050–2062, 2021.

[123] A. Attarha, P. Scott, J. Iria and S. Thiébaux, "Network-secure and price-elastic aggregator bidding in energy and reserve markets," *IEEE Transactions on Smart Grid*, vol. 12, no. 3, pp. 2284–2294, 2021.

[124] M. R. Alam, P. T. Nguyen, L. Naranpanawe, T. K. Saha and G. Lankeshwara, "Allocation of dynamic operating envelopes in distribution networks: Technical and equitable perspectives," *IEEE Transactions on Sustainable Energy*, 2023.

[125] EDGE, "Fairness in dynamic operating envelope objective functions," University of Melbourne, Tech. Rep., 2023. [Online]. Available: https://aemo.com.au/-/media/files/initiatives/%20der/2023/the-fairness-in-dynamic-operating-envelope-objectives-report.pdf?la=en.

[126] T. Milford and O. Krause, "Managing der in distribution networks using state estimation & dynamic operating envelopes," in *2021 IEEE PES Innovative Smart Grid Technologies-Asia (ISGT Asia)*, IEEE, 2021, pp. 1–5.

[127] B. Liu and J. Ma, "Feasible region for ders in unbalanced distribution networks with uncertain line impedances," in *2023 IEEE Power & Energy Society General Meeting (PESGM)*, IEEE, 2023, pp. 1–5.

[128] S. Jang, N. Ozay and J. L. Mathieu, "Data-driven estimation of probabilistic constraints for network-safe distributed energy resource control," in *2022 58th Annual Allerton Conference on Communication, Control, and Computing (Allerton)*, IEEE, 2022, pp. 1–8.

[129] H. Moring, S. Jang, N. Ozay and J. L. Mathieu, "Nodal operating envelopes vs. network-wide constraints: What is better for network-safe coordination of ders?" *Electric Power Systems Research*, vol. 234, p. 110 702, 2024.

[130] S. H. Low, "Convex relaxation of optimal power flow—part i: Formulations and equivalence," *IEEE Transactions on Control of Network Systems*, vol. 1, no. 1, pp. 15–27, 2014.

[131] N. Nazir and M. Almassalkhi, "Convex inner approximation of the feeder hosting capacity limits on dispatchable demand," in *2019 IEEE 58th Conference on Decision and Control (CDC)*, IEEE, 2019, pp. 4858–4864.

[132] B. Liu and J. H. Braslavsky, "Sensitivity and robustness issues of operating envelopes in unbalanced distribution networks," *IEEE Access*, vol. 10, pp. 92 789–92 798, 2022.

[133] B. Liu and J. H. Braslavsky, "Robust dynamic operating envelopes for der integration in unbalanced distribution networks," *IEEE Transactions on Power Systems*, pp. 1–15, 2023.

[134] T. Antić, F. Geth and T. Capuder, "The importance of technical distribution network limits in dynamic operating envelopes," in *2023 IEEE Belgrade PowerTech*, IEEE, 2023, pp. 1–6.

[135] A. Koirala, F. Geth and T. Van Acker, "Day-ahead dynamic operating envelopes using stochastic unbalanced optimal power flow," *Sustainable Energy, Grids and Networks*, vol. 40, p. 101 528, 2024.

[136] K. Petrou et al., "Ensuring distribution network integrity using dynamic operating limits for prosumers," *IEEE Transactions on Smart Grid*, vol. 12, pp. 3877–3888, Sep. 2021.

[137] J. Savier and D. Das, "Impact of network reconfiguration on loss allocation of radial distribution systems," *Power Delivery, IEEE Transactions on*, vol. 22, pp. 2473–2480, Nov. 2007.

[138] P. Scott, D. Gordon, E. Franklin, L. Jones and S. Thiébaux, "Network-aware coordination of residential distributed energy resources," *IEEE Transactions on Smart Grid*, vol. 10, no. 6, pp. 6528–6537, 2019.

[139] P. Scott and S. Thiébaux, "Identification of manipulation in receding horizon electricity markets," *IEEE Transactions on Smart Grid*, vol. 10, no. 1, pp. 1046–1057, 2017.

[140] J. Iria, P. Scott, D. Gordon, A. Attarha and S. M. N. RA, "Trial of shaped operating envelopes," 2024.

[141] P. Pillay and M. Manyage, "Definitions of voltage unbalance," *IEEE Power Engineering Review*, vol. 21, no. 5, pp. 50–51, 2001.

[142] K. Girigoudar, D. K. Molzahn and L. A. Roald, "On the relationships among different voltage unbalance definitions," in *2019 North American Power Symposium (NAPS)*, 2019, pp. 1–6.

[143] J. Chen and L. A. Roald, "A data-driven linearization approach to analyze the three-phase unbalance in active distribution systems," *Electric Power Systems Research*, vol. 211, p. 108 573, 2022.

[144] P. Arboleya, "State estimation in low voltage networks using smart meters: Statistical analysis of the errors," in *2018 IEEE Power & Energy Society General Meeting (PESGM)*, IEEE, 2018, pp. 1–5.

[145] R. Razzaghi, B. Bahrani, A. Kumarawadu, A. Asbafkan, P. Blackburn and V. Moreno, "Assessing the impact of network exchanger (nex) on power quality in distribution networks: Final report," RACE for 2030 (Cooperative Research Centre), Tech. Rep. 24.NT5.R.0838, Oct. 2025, ISBN: 978-1-922746-78-8. [Online]. Available: https://www.racefor2030.com.au/content/uploads/0838_Assessing-the-impact-of-NEx_final-report_FINAL.pdf.

[146] K. Ma, L. Fang and W. Kong, "Review of distribution network phase unbalance: Scale, causes, consequences, solutions, and future research directions," *CSEE Journal of Power and Energy systems*, vol. 6, no. 3, pp. 479–488, 2020.

[147] M. Z. Liu, L. F. Ochoa, P. K. C. Wong and J. Theunissen, "Using opf-based operating envelopes to facilitate residential der services," *IEEE Transactions on Smart Grid*, vol. 13, no. 6, pp. 4494–4504, 2022.